



2810377749



**A TOOL-KIT FOR IN-PROCESS DETERMINATION AND  
CONTROL OF STRUCTURAL AND CONFORMATIONAL  
AUTHENTICITY OF COMPLEX BIOPHARMACEUTICALS**

A thesis submitted to University College London for the degree of  
DOCTOR OF PHILOSOPHY

by

Elin Cecilia Therese Qvist Reid

The Advanced Centre for Biochemical Engineering  
Department of Biochemical Engineering  
UCL  
Torrington Place  
WC1E 7JE  
United Kingdom

UMI Number: U592746

All rights reserved

INFORMATION TO ALL USERS

The quality of this reproduction is dependent upon the quality of the copy submitted.

In the unlikely event that the author did not send a complete manuscript and there are missing pages, these will be noted. Also, if material had to be removed, a note will indicate the deletion.



UMI U592746

Published by ProQuest LLC 2013. Copyright in the Dissertation held by the Author.  
Microform Edition © ProQuest LLC.

All rights reserved. This work is protected against  
unauthorized copying under Title 17, United States Code.



ProQuest LLC  
789 East Eisenhower Parkway  
P.O. Box 1346  
Ann Arbor, MI 48106-1346

I, Elin Cecilia Therese Qvist Reid, confirm that the work presented in this thesis is my own. Where information has been derived from other sources, I confirm that this has been indicated in the thesis.

Cecilia Reid

**“The beginning of wisdom is found in doubting;  
by doubting we come to the question,  
and by seeking we may come upon the truth.”**

- Pierre Abelard

## **Abstract**

The work presented here focuses on a Chinese hamster ovary cell line producing monoclonal IgG. A key challenge in the production of mAbs is to produce a consistent glycoform profile between batches, since glycosylation can impact efficacy. This work examines the effect of time of harvest and means of cell removal on the molecular structure of recombinant IgG. The glycosylation status of IgG was compared at different stages of fermentation through analysis of intact mAb using liquid-chromatography-electrospray-time-of-flight-mass-spectrometry. Heterogeneity in glycosylation patterns, as well as C-terminal lysine and N-terminal glutamine residues, could be seen in all samples and an increase in the proportion of shorter glycans was observed over time of culture, indicating time of harvest could impact upon the efficacy of the product. A shear device mimicking the feed zone of a large-scale disc stack centrifuge was used to allow better prediction of the effects of early stage cell recovery on the structural authenticity of the protein. The composition of the intracellular material, in terms of H<sub>2</sub>L<sub>2</sub> tetramers, HL dimers and H and L single chains, is clearly different to the extracellular intact mAb, however, their relatively low concentration gives little change to the overall profile when released into the product stream. Shear rate and time seem to have little effect on the molecular structure of the mAb. The effect of holding time and temperature before cell removal was also examined. While neither seems to have an effect on the glycosylation pattern of the mAb, there was an increase in “half-antibodies” with holding time, from 0 h to 24 h, when holding at either +4°C or +37°C. This work highlights the importance of looking at the interaction between stages and the bioprocessing units as a whole rather than single steps.

## **Acknowledgements**

I would like to thank everyone who in one way or another assisted and supported me during my PhD. First of all I would like to thank my supervisor Professor Mike Hoare for his guidance, advice and patience. I would also like to thank my advisor Dr. Mark Smales at University of Kent for guidance through different analytical techniques as well as advice on antibody structure and cell functions.

I am very grateful to Dr. Andy Tait whose input and encouragement has been invaluable. My thanks also go to Dr. Helen Baldascini who helped me get started and find my way during my first year.

A big thank you to Lonza Biologics and especially Atul Mohindra for the provision of material as well as interesting discussions. Also a big thank you to Agilent Technologies and especially Shaun Bilsborough, who has truly helped me in my journey towards mastering mass spectrometry.

A special thank you goes to my parents who have encouraged and supported me in every way throughout my studies, it would not have been possible without you. Also thanks to my husband for his patience and for always managing to cheer me up when feeling low.

I would like to thank Brenda without whom I might not have reached the end. Thank you for our stress relieving chats, lunches and tea breaks and for being a real friend.

Finally thank you to all of my friends and to everyone in the Department of Biochemical Engineering at UCL, as well as the Department of Biosciences at University of Kent, for being supportive and making everyday work fun.

This work was supported by the Engineering and Physical Sciences Research Council (EPSRC).

# Table of contents

<b>ABSTRACT</b>	<b>4</b>
<b>ACKNOWLEDGEMENTS</b>	<b>5</b>
<b>LIST OF FIGURES</b>	<b>9</b>
<b>LIST OF TABLES</b>	<b>11</b>
<b>LIST OF ABBREVIATIONS</b>	<b>12</b>
<b>1 INTRODUCTION</b>	<b>14</b>
<b>1.1 Cell culture</b>	<b>14</b>
1.1.1 Mammalian cell lines	14
1.1.2 Selection method	14
1.1.3 Media	15
1.1.4 Culture conditions	16
1.1.5 Culture method	16
1.1.5.1 Adherent	16
1.1.5.2 Suspension	17
1.1.5.3 Batch/Fed-batch	17
1.1.5.4 Perfusion	17
1.1.6 Type of reactor	18
1.1.6.1 Stirred tank reactor	18
1.1.6.2 Airlift fermenter	18
1.1.6.3 Hollow-fibre reactor	19
1.1.6.4 Wave bioreactor	19
<b>1.2 Downstream processing</b>	<b>22</b>
<b>1.3 Scales and dosages</b>	<b>23</b>
<b>1.4 Challenges and trends in cell culture</b>	<b>24</b>
<b>1.5 Centrifugation</b>	<b>25</b>
1.5.1 Sigma theory	27
1.5.2 Shear	30
1.5.3 Ultra scale-down	31
1.5.4 Shear device	33
<b>1.6 Antibodies</b>	<b>35</b>
1.6.1 Commercial production of antibodies	35
1.6.2 Basic structure	36
1.6.3 Formation in the cell	38
1.6.4 Half-antibodies	40
1.6.5 Modifications of IgG	41
<b>1.7 Glycosylation</b>	<b>44</b>
1.7.1 Glycan structures	44
1.7.2 Glycan synthesis	44
1.7.3 Glycosylation of IgG	49
1.7.4 Effects of glycosylation	51

1.7.5	Factors affecting glycosylation	52
1.7.6	Glycoengineering and current trends	53
<b>1.8</b>	<b>Protein analysis</b>	<b>55</b>
1.8.1	Electrophoresis	56
1.8.1.1	SDS-PAGE	56
1.8.1.2	Isoelectric focusing	56
1.8.1.3	2D-gels	57
1.8.2	ELISA	57
1.8.3	Chromatography	58
1.8.3.1	Protein A/G affinity chromatography	58
1.8.3.2	Lectin affinity chromatography	58
1.8.3.3	Size Exclusion Chromatography	59
1.8.3.4	HPLC	59
1.8.4	Mass spectrometry	60
1.8.4.1	LC/ESI-MS	60
1.8.4.2	MALDI-TOF	61
1.8.4.3	SELDI-MS	62
1.8.4.4	ESI-TOF	62
<b>1.9</b>	<b>Aim</b>	<b>63</b>
<b>1.10</b>	<b>Objectives</b>	<b>63</b>
<b>2</b>	<b>MATERIALS AND METHODS</b>	<b>65</b>
<b>2.1</b>	<b>Cell culture</b>	<b>65</b>
<b>2.2</b>	<b>Centrifugation for clarification</b>	<b>65</b>
<b>2.3</b>	<b>Shear</b>	<b>65</b>
<b>2.4</b>	<b>Holding</b>	<b>66</b>
<b>2.5</b>	<b>Disruption of cells for purification of intracellular material</b>	<b>66</b>
<b>2.6</b>	<b>Protein A affinity chromatography for purification</b>	<b>66</b>
<b>2.7</b>	<b>Sample modification</b>	<b>68</b>
2.7.1	Deglycosylation	68
<b>2.8</b>	<b>Antibody profiling by gel electrophoresis</b>	<b>68</b>
2.8.1	Lab-on-a-chip	68
<b>2.9</b>	<b>Mass spectrometry</b>	<b>68</b>
2.9.1	LC/MSD-TOF	69
<b>3</b>	<b>STRUCTURAL ANALYSIS OF IGG</b>	<b>70</b>
<b>3.1</b>	<b>Basic structure and sequence</b>	<b>70</b>
<b>3.2</b>	<b>Modifications</b>	<b>70</b>
<b>3.3</b>	<b>HL complexes</b>	<b>76</b>
<b>3.4</b>	<b>Analysis of mass spectra</b>	<b>76</b>

<b>4</b>	<b>EFFECT OF HARVEST TIME ON THE MOLECULAR STRUCTURE AND CONFORMATION OF A MAB</b>	<b>95</b>
4.1	Growth profiles	95
4.2	Glycosylation profiles	100
4.3	Glycoform production	101
4.4	Half antibodies	111
4.5	Lysine and glycoform levels	116
4.6	Discussion	120
<b>5</b>	<b>EFFECT OF HARVEST ON THE MOLECULAR STRUCTURE AND OVERALL CONFORMATION OF A MAB</b>	<b>125</b>
5.1	Effect of shear on the glycosylation profile of a mAb	125
5.1.1	Sampling overview	125
5.1.2	Structural analysis	125
5.2	Effect of shear rate and time	129
5.2.1	Sampling overview	129
5.2.2	Structural analysis	131
5.3	Comparison of intra- and extracellular mAb	138
5.3.1	Sampling overview	138
5.3.2	Structural analysis	138
5.4	Discussion	142
<b>6</b>	<b>EFFECT OF HOLDING TIME AND CONDITIONS IN BETWEEN STAGES</b>	<b>144</b>
6.1	Effect of holding on molecular structure and glycosylation	144
6.2	Effect of holding on mAb conformation	150
6.3	Discussion	155
<b>7</b>	<b>OVERALL DISCUSSION</b>	<b>157</b>
<b>8</b>	<b>CONCLUSIONS</b>	<b>158</b>
<b>9</b>	<b>FUTURE WORK</b>	<b>160</b>
	<b>BIBLIOGRAPHY</b>	<b>162</b>

## List of figures

<i>Figure 1.1 Schematic of an airlift fermenter</i>	20
<i>Figure 1.2 Schematic of the hollow fibre system</i>	21
<i>Figure 1.3 Schematic of a disc stack centrifuge</i>	29
<i>Figure 1.4 Schematic of the shear device</i>	34
<i>Figure 1.5 Schematic of an IgG</i>	39
<i>Figure 1.6 C-terminal lysine cleavage</i>	43
<i>Figure 1.7 Cyclization of N-terminal glutamine</i>	43
<i>Figure 1.8 Different subgroups of N-linked oligosaccharide structures</i>	46
<i>Figure 1.9 Schematic of N-linked glycosylation</i>	47
<i>Figure 1.10 Glycosylation of IgG</i>	50
<i>Figure 1.11 Variations in glycosylation of IgG</i>	50
<i>Figure 1.12 Basic schematic of ESI-TOF</i>	64
<i>Figure 3.1 Nucleotide sequence of the cB72.3 heavy chain</i>	71
<i>Figure 3.2 Nucleotide sequence of the cB72.3 light chain</i>	72
<i>Figure 3.3 Amino acid sequence of the heavy chain</i>	72
<i>Figure 3.4 Amino acid sequence of the light chain.</i>	72
<i>Figure 3.5 Glycosylation structures in IgG</i>	73
<i>Figure 3.6 Sample total ion chromatogram of an intact mAb</i>	80
<i>Figure 3.7 Mass spectrum; sample raw data before deconvolution</i>	81
<i>Figure 3.8 Deconvoluted mass spectrum of the whole mass range</i>	82
<i>Figure 3.9 Deconvoluted mass spectrum of the intact mAb.</i>	83
<i>Figure 3.10 Mass spectrum with assigned peaks</i>	84
<i>Figure 3.11 Interpretation of mass spectra, main peaks</i>	87
<i>Figure 3.12 Interpretation of mass spectra, glutamine not converted</i>	89
<i>Figure 3.13 Interpretation of mass spectra, one intact lysine</i>	91
<i>Figure 3.14 Interpretation of mass spectra, two intact lysines</i>	93
<i>Figure 4.1 Growth profile of cell culture, 1<sup>st</sup> fermentation</i>	96
<i>Figure 4.2 Logarithmic growth curve, 1<sup>st</sup> fermentation</i>	97
<i>Figure 4.3 Growth profile of cell culture, 2<sup>nd</sup> fermentation</i>	98
<i>Figure 4.4 Logarithmic growth curve, 2<sup>nd</sup> fermentation</i>	99
<i>Figure 4.5 Effect of harvest time on the glycosylation pattern of an IgG, 1<sup>st</sup> fermentation.</i>	102
<i>Figure 4.6 Effect of harvest time on the glycosylation pattern of an IgG, 2<sup>nd</sup> fermentation</i>	104
<i>Figure 4.7 Product formation, 1<sup>st</sup> fermentation</i>	107
<i>Figure 4.8 Formation of different glycoforms per viable cell per day, 1<sup>st</sup> fermentation</i>	108
<i>Figure 4.9 Product formation, 2<sup>nd</sup> fermentation</i>	109
<i>Figure 4.10 Formation of different glycoforms per viable cell per day, 2<sup>nd</sup> fermentation</i>	110
<i>Figure 4.11 Effect of harvest time on the overall mAb composition, 1<sup>st</sup> fermentation.</i>	112
<i>Figure 4.12 Effect of harvest time on the overall mAb composition, 2<sup>nd</sup> fermentation</i>	114
<i>Figure 4.13 Lysine levels over time, 2<sup>nd</sup> fermentation</i>	117

<i>Figure 4.14 Deglycosylated mAb</i>	118
<i>Figure 4.15 Glycoform levels over time, 2<sup>nd</sup> fermentation</i>	119
<i>Figure 5.1 Sampling overview</i>	126
<i>Figure 5.2 Effect of shear on mAb conformation</i>	127
<i>Figure 5.3 Effect of shear on the glycosylation profile of a mAb</i>	128
<i>Figure 5.4 Sampling overview of shear investigation</i>	130
<i>Figure 5.5 Effect of shear rate on the glycosylation profile of a mAb</i>	132
<i>Figure 5.6 Effect of shearing time on the glycosylation profile of a mAb</i>	133
<i>Figure 5.7 Effect of shear rate on the conformation of a mAb</i>	134
<i>Figure 5.8 Effect of shearing time on the conformation of a mAb</i>	136
<i>Figure 5.9 Sampling overview</i>	139
<i>Figure 5.10 Comparison of intra- and extracellular mAb</i>	140
<i>Figure 6.1 Sampling overview</i>	145
<i>Figure 6.2 Sample treatment</i>	145
<i>Figure 6.3 Effect of holding at +4°C on the molecular structure of a mAb</i>	146
<i>Figure 6.4 Comparison of the two most extreme samples from Figure 6.3</i>	147
<i>Figure 6.5 Effect of holding at +37°C on the molecular structure of a mAb</i>	148
<i>Figure 6.6 Comparison of the two most extreme samples from Figure 6.5</i>	149
<i>Figure 6.7 Effect of holding at +4°C on the proportion of HL dimers</i>	151
<i>Figure 6.8 Effect of holding at +37°C on the proportion of HL dimers</i>	153
<i>Figure 8.1 Schematic of the tool-kit</i>	159

## List of tables

<i>Table 2.1 Maximum energy dissipation rates of large-scale centrifuges</i>	67
<i>Table 3.1 Average masses of the glycan building blocks</i>	73
<i>Table 3.2 Calculation of theoretical masses of the IgG used in the study</i>	75
<i>Table 3.3 Interpretation of the mass spectrum in Figure 3.10</i>	85
<i>Table 3.4 Peak assignation from Figure 3.11</i>	88
<i>Table 3.5 Peak assignation from Figure 3.12</i>	90
<i>Table 3.6 Peak assignation from Figure 3.13</i>	92
<i>Table 3.7 Peak assignation from Figure 3.14</i>	94
<i>Table 4.1 Growth characteristics, 1<sup>st</sup> fermentation</i>	97
<i>Table 4.2 Growth characteristics, 2<sup>nd</sup> fermentation</i>	99
<i>Table 4.3 Effect of harvest time on the proportion of HL dimers, 2<sup>nd</sup> fermentation</i>	115
<i>Table 5.1 Proportion of HL dimers after shearing at different rates</i>	135
<i>Table 5.2 Proportion of HL dimers after shearing for different times</i>	137
<i>Table 5.3 Compositions of the intra- and extracellular material</i>	141
<i>Table 6.1 Proportion of HL dimers after holding at +4°C</i>	152
<i>Table 6.2 Proportion of HL dimers after holding at +37°C</i>	154

## List of abbreviations

<i>ADCC</i>	<i>antibody-dependent cell-mediated cytotoxicity</i>
<i>ADH</i>	<i>alcohol dehydrogenase</i>
<i>Asn</i>	<i>asparagine</i>
<i>BHK</i>	<i>baby hamster kidney</i>
<i>BSA</i>	<i>bovine serum albumin</i>
<i>C<sub>H</sub></i>	<i>constant heavy chain</i>
<i>C<sub>L</sub></i>	<i>constant light chain</i>
<i>CDC</i>	<i>complement-dependent cytotoxicity</i>
<i>CDR</i>	<i>complementarity-determining region</i>
<i>CFD</i>	<i>computational fluid dynamics</i>
<i>CHO</i>	<i>Chinese hamster ovary</i>
<i>DHFR</i>	<i>dihydrofolate reductase</i>
<i>DO</i>	<i>dissolved oxygen</i>
<i>DNA</i>	<i>deoxyribonucleic acid</i>
<i>EC</i>	<i>extracapillary circuit</i>
<i>ELISA</i>	<i>enzyme-linked immunosorbent assay</i>
<i>ER</i>	<i>endoplasmic reticulum</i>
<i>ESI</i>	<i>electrospray ionisation</i>
<i>Fab</i>	<i>antibody binding fragment</i>
<i>Fc</i>	<i>crystallisable fragment</i>
<i>Q</i>	<i>glutamine</i>
<i>GA</i>	<i>Golgi Apparatus</i>
<i>GS</i>	<i>glutamine synthetase</i>
<i>H</i>	<i>heavy (chain)</i>
<i>HPLC</i>	<i>high pressure liquid chromatography</i>
<i>IEF</i>	<i>isoelectric focusing</i>
<i>IFN</i>	<i>interferon</i>
<i>Ig</i>	<i>Immunoglobulin</i>
<i>IC</i>	<i>intracapillary circuit</i>
<i>IMAC</i>	<i>immobilized metal affinity capture</i>
<i>K</i>	<i>lysine</i>
<i>L</i>	<i>light (chain)</i>
<i>LC</i>	<i>liquid chromatography</i>
<i>LD</i>	<i>laser desorption</i>
<i>MALDI</i>	<i>matrix-assisted laser desorption ionisation</i>
<i>MS</i>	<i>mass spectrometry</i>

<i>mAb</i>	<i>monoclonal antibody</i>
<i>MSD</i>	<i>mass selective detector</i>
<i>m/z</i>	<i>mass-to-charge ratio</i>
<i>NK</i>	<i>natural killer</i>
<i>NS0</i>	<i>mouse myeloma</i>
<i>PAGE</i>	<i>polyacrylamide gel electrophoresis</i>
<i>PBS</i>	<i>phosphate-buffered saline</i>
<i>PCD</i>	<i>picograms per cell per day</i>
<i>pE</i>	<i>pyroglutamic acid</i>
<i>PNGase</i>	<i>N-glycosidase F</i>
<i>RNA</i>	<i>ribonucleic acid</i>
<i>RP</i>	<i>reversed phase</i>
<i>rpm</i>	<i>rotations per minute</i>
<i>scFv</i>	<i>single chain antibody fragment</i>
<i>SDS</i>	<i>sodium dodecyl sulphate</i>
<i>SEC</i>	<i>size exclusion chromatography</i>
<i>SELDI</i>	<i>surface-enhanced laser desorption ionisation</i>
<i>SpA</i>	<i>staphylococcal protein A</i>
<i>SpG</i>	<i>streptococcal protein G</i>
<i>SPR</i>	<i>surface plasmon resonance</i>
<i>TCA</i>	<i>trichloro acetic acid</i>
<i>TIC</i>	<i>total ion chromatogram</i>
<i>TOF</i>	<i>time-of-flight</i>
<i>USD</i>	<i>ultra scale-down</i>
<i>V<sub>H</sub></i>	<i>variable heavy chain</i>
<i>V<sub>L</sub></i>	<i>variable light chain</i>

# **1 Introduction**

## ***1.1 Cell culture***

The following is a brief overview of mammalian cell culture; culture methods and types of reactors, to help set the project in context. More detailed reviews are available elsewhere Birch and Racher, 2006; Wurm, 2004. Issues that are of concern in the work presented here are process performance related; cell concentration, cell viability and lysis, antibody formation and titre, culture and processing environment etc.

### **1.1.1 Mammalian cell lines**

Of all approved recombinant proteins on the market, about 60-70% are produced in mammalian cell lines (Wurm, 2004). This is due to the ability of the cells to produce correctly folded and assembled proteins with the right post-translational modifications, glycosylation being one of the most important ones. Most commonly used are Chinese hamster ovary (CHO) cell lines (Schlatter et al, 2005; Sethuraman and Stadheim, 2006) and mouse myeloma (NS0) (Beck et al, 2005). To a smaller extent baby hamster kidney (BHK) cell lines are also used. CHO cell lines are currently the most widely used due to the knowledge and experience that exist and is constantly growing in the industry.

### **1.1.2 Selection method**

In order to cultivate the cells containing the product of interest a selection step is needed. In the case of monoclonal antibody (mAb) production the selection step is required to select the successfully fused hybridomas that produce the desired antibodies. This is done prior to fusion by introducing an additional gene into the B-cell that will then translate into a protein that the cells can be selected for. In mammalian cell culture the most commonly used genes are those for glutamine synthetase (GS) and dihydrofolate reductase (DHFR). Selection is then carried out in media lacking the relevant metabolite (hypoxanthine and thymidine for DHFR and glutamine for GS), preventing cells that have not been transformed from

growing and providing a way of removing the myeloma cells that lack the gene coding for the selected protein. The cells are then further cultivated and analysed in order to obtain the clone with the most efficient antibody production for large scale cultivation.

### 1.1.3 Media

The medium is usually made up of the following components; carbohydrates, amino acids, salts, bicarbonate, vitamins, hormones and supplements. Glucose is the most commonly used carbon and energy source and it also serves as a precursor for biosynthesis, such as ribose, which is needed for nucleic acid synthesis. Amino acids are added as precursors for protein synthesis. Salts are added to keep the solution isotonic in order to prevent imbalances with the intracellular content. Bicarbonate is added to serve as a buffer system together with gaseous carbon dioxide to keep the pH stable around 7 as in the natural environment of the cells inside the body. Vitamins and hormones work as metabolic cofactors, while supplements are added to aid cell growth. The traditional supplement is serum, e.g. foetal calf or bovine. However this contains undefined materials that can cause inconsistency between batches, the proteins it contains can cause problems during purification and it is also prone to contamination with viruses and prions. These are the main reasons the industry has been working towards serum free media, which is not as complex, easier to define and to ensure purity after downstream processes for validation purposes. Instead of serum, bovine serum albumin (BSA) or similar can be added to the media. However, this still introduces problems such as contaminating host cell proteins. The result can be a product that contains unacceptable levels of bovine IgG (Rasmussen et al, 2005). The levels of bovine IgG could be reduced by using protein A affinity chromatography and not protein G when purifying the protein, if the product has affinity for both staphylococcal protein A (SpA) and streptococcal protein G (SpG) (see section 1.2). Instead of serum or BSA, other nutrients can be added, creating a protein free (animal component free) or chemically defined media, which is the subject for constant ongoing research in order to develop a highly productive cell culture. Standard media is available from

suppliers, but most companies invest time and money in optimising the contents to suit their own processes and to obtain maximal productivity.

#### **1.1.4 Culture conditions**

Mammalian cells are most stable around neutral pH and at 37°C for obvious reasons. Cells can handle a lower temperature than the optimum, but the growth rate will decrease. If the temperature increases slightly however, the cells are not as tolerant and this would lead to cell death. Temperature is usually controlled through coiled pipes in large scale reactors or through a jacket for lab-scale fermenters. A bicarbonate-CO<sub>2</sub> buffering system can keep pH in the range of 6.9-7.4, but it is also common to add a buffer to aid the buffering capacity. pH is controlled by direct addition of acid or alkali, normally only alkali due to the formation of lactic acid, which brings the pH of the broth down.

#### **1.1.5 Culture method**

There are two main methods of cultivating mammalian cells; adherent and suspension culture, the latter one being the most widely used.

##### ***1.1.5.1 Adherent***

In adherent culture, media is added to roller bottles to a level of 10-30% of the total volume. Cells are then seeded into the bottles that are slowly rotated, allowing cells to adhere and to be wetted while the large head space supplies them with oxygen. The roller bottle system is easily scaled up by increasing the number of bottles; however, the titres obtained are lower than that for suspension cultures due to the lower cell/reactor volume ratio (Wurm, 2004), causing limitations in the use of the system. Adherent culture can also be carried out in bioreactors with the use of microcarriers, cultivated in stirred tank reactors. This allows the use of cells not capable of growth in suspension to make use of the scale-up efficiency of the stirred tanks.

### ***1.1.5.2 Suspension***

Suspension culture is the most commonly used method due to the wide knowledge available about the stirred tank system. It is also easy to scale up in order for large scale production to be carried out once the culture conditions have been determined.

### ***1.1.5.3 Batch/Fed-batch***

The most basic mode of operation for cell culture is the batch mode. Here the medium and the inoculum are placed in the reactor before the start of the culture. The culture is then run for as many days as required and the contents then harvested. The disadvantage of batch mode is that the cells are using the same media the entire time and there is therefore a risk of exhausting vital nutrients or energy sources. It also results in the build up of metabolites that can be growth inhibiting. A modification to this method is the fed-batch process. This involves the addition of fresh media at one or more time points between beginning and end of culture. The addition supplies the cells with fresh nutrients and energy sources aiding cell growth and protein production. On the downside it could also be an extra source for contamination, so care must be taken in order to prevent this. Fed-batch is today the most commonly used mode of operation in large scale mAb production and allows for high cell densities to be achieved.

### ***1.1.5.4 Perfusion***

The perfusion culture was introduced in order to further aid cell growth and culture performance. This involves the constant addition of fresh media while harvesting is carried out so that the volume stays constant. The additions of fresh media keep the nutrient levels up and metabolite levels down. At the same time it protects the product from possible degradation that can occur if kept for too long in the vessel (e.g. from the release of proteolytic enzymes). The feeding aids in keeping a high cell viability and in reaching higher cell densities. Over the last few years, high cell densities have been the focus of a lot of research in order to improve process economics, so perfusion culture is becoming a more popular mode of operation. At the moment there are a few different retention devices used at large-scale in industry, including the spin-filter system, the inclined settling

device and the ultra-sound retention device (Merten, 2006).

### **1.1.6 Type of reactor**

There are many different types of reactors on the market at the moment, but there are some that are more commonly used than others, like the stirred tank reactor, airlift fermenter and the hollow-fibre reactor. There have also been disposable systems emerging over the past decade, one of the most popular being the Wave bioreactor (Wave Biotech, GE Healthcare, Somerset, NJ).

#### ***1.1.6.1 Stirred tank reactor***

The stirred tank reactor is the basic design that has been used for years in bacterial fermentations and there is therefore an extensive know-how about this system and scale-up is well understood. Since mammalian cells are different to bacterial ones, stirred tanks for animal cells have a slightly different design and operation, but the basics are still the same. Stirred tank reactors at lab-scale are usually made of glass, while large scale vessels are made of stainless steel. Agitation is provided by impellers that are usually top-driven. Since mammalian cells are more fragile than bacterial, the impellers are normally operated at lower stirring speeds. If microcarriers are used, the stirrer speeds used are even lower. The bottom of the vessel is round in order to aid mixing. Suitable impellers are the marine and pitched blade types that provide both vertical and horizontal mixing. At lab-scale enough oxygen is supplied through surface aeration. At larger scale sparging is required for oxygen supply. The disadvantage of this is the damage it can cause to the cells through bubble breakage at the surface and the excessive foaming which may occur.

#### ***1.1.6.2 Airlift fermenter***

An airlift fermenter has a higher aspect ratio (height:width) than a regular stirred tank reactor. It has a draught tube inside the vessel, at the bottom of which air is sparged providing fluid circulation in an upward movement inside the tube (Figure 1.1). This provides aeration and agitation at the same time, without any mechanical input, creating a system with lower energy consumption, hence lower

operating costs. It also provides milder conditions for the cells and so reduces cell damage.

### ***1.1.6.3 Hollow-fibre reactor***

The hollow-fibre reactor (Figure 1.2), based on the kidney dialysis system, consists of synthetic, semi permeable hollow fibres. The media is pumped into the intracapillary circuit (IC) inside the fibres where nutrients and gases are exchanged, through the capillary wall, with the extracapillary circuit (EC), which contains the growing cells. The molecular weight cut-off of the fibre is such that the cells and large molecular weight products are kept in the EC, while the pressure inside the fibres pushes the nutrients from the media through the wall. The system allows for product and dead cells to be removed from the EC throughout the culture and can therefore be run for months at a time. It is however not suitable for scale-up due to nutrient gradients and uneven cell growth.

### ***1.1.6.4 Wave bioreactor***

As a solution to the costly and time consuming cleaning, sterilisation and validation procedures connected with reusable equipment, the Wave bioreactor was created. This is a sterile disposable bag, partially filled with media, placed on a rocking table that creates a wave-like motion and provides agitation and aids gas transfer. The head space in the bag is filled with air to provide oxygen and with CO<sub>2</sub> to lower the pH accordingly. The system is commonly used at lab-scale, providing a mean of increasing the speed of production towards early stages of development for evaluation, but can be used for volumes up to 1000 L. The system has been shown to exhibit good batch-to-batch reproducibility as well as comparable biomass and recombinant protein titres to the stirred tank system, for an NS0, a CHO and an insect cell line (Fries et al, 2005). It can be used for suspension culture and with the help of microcarriers and is also a good alternative for virus production due to the ease of containment (Singh, 1999).

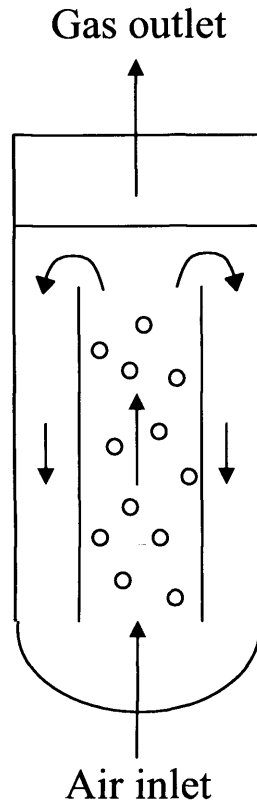


**Figure 1.1 Schematic of an airlift fermenter**

*The vessel contains a draught tube through which air is sparged in an upward motion. This provides oxygen to the broth aiding cell growth. It also provides agitation that is less harsh as compared to mechanical impellers. The liquid flow is circulated back down on the outside of the draught tube, mixing with the air inlet at the bottom and pushed upwards again. Any waste gases are removed through the top of the vessel.*

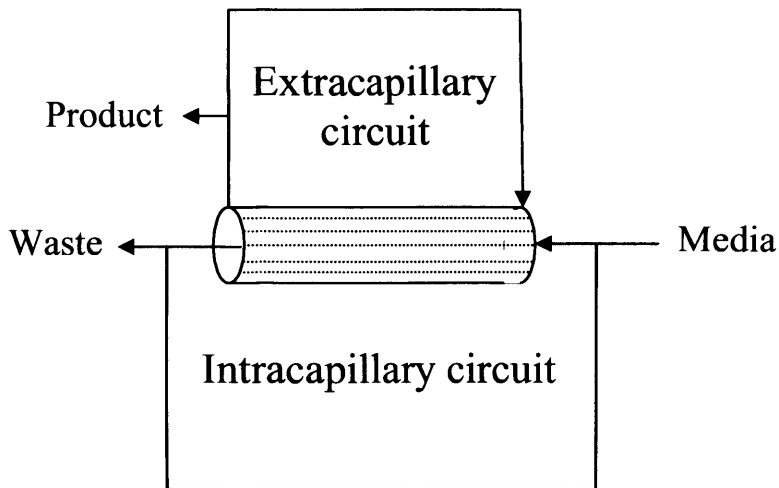


**Figure 1.2 Schematic of the hollow fibre system**

*Media is pumped through the inside of the fibres – the intracapillary circuit (IC) – providing the cells with fresh nutrients. The media is pushed through the fibres creating a higher pressure, which will aid the exchange of nutrients and gases with the extracapillary circuit (EC). The cells are kept in the EC together with the large molecular weight products by the cut-off of the fibre and can make use of fresh nutrients and energy sources throughout the culture thanks to this recycling system. Waste containing low molecular weight compounds can be removed and disposed of from the IC, while product is extracted from the EC allowing for higher cell densities.*

## ***1.2 Downstream processing***

The following is a brief introduction to the downstream processing related to mAb production, which is followed by more detailed reviews on issues that are of concern in the work presented here, such as harvest, processing conditions and antibody structure to mention a few. Further details on antibody purification can be found elsewhere (Gottschalk, 2005; Gottschalk, 2008; Jagschies et al, 2006; Shukla et al, 2007).

The standard purification sequence for monoclonal and polyclonal antibodies is centrifugation, microfiltration, protein A/G chromatography and finally ion exchange chromatography. This is in order to achieve the high degree of purity required for use as therapeutic agents.

Centrifugation clarifies the broth so that only the antibody-containing supernatant can be further processed. This technique involves high shear forces that could have a deteriorating effect on the product and could also lead to aggregation. Therefore it is of particular importance to confirm the structural integrity and general quality of the product after this step.

The absence of debris in the broth is of great importance due to the high cost of the protein A matrix (see below). It is therefore crucial to remove solid material that can cause column fouling. Microfiltration is often used after centrifugation to further minimise the level of particulates and achieve the required purity needed for the chromatography steps.

Protein A/G matrices are rather expensive and it is therefore of importance to keep the number of runs per column high by introducing a clear feed stream. The matrices are developed from staphylococcal protein A (SpA) and streptococcal protein G (SpG) respectively. Both proteins bind to immunoglobulin providing a highly specific affinity chromatography technique. Protein A is obtained from *Staphylococcus aureus*, while protein G is produced by species of *Streptococcus* (Bjorck and Kronvall, 1984). It has been commonly accepted that SpA and SpG

bind to the Fc part of the Ig molecule. However, more recent publications show several binding sites on the antibody. For example one study used papain digested IgG (resulting in Fab and two Fc, distinguished as a high and a low molecular weight fragment) fragments and it was observed that SpA bound only to the high molecular weight Fc fragment, while SpG bound to Fab and also the low molecular weight Fc fragment (Aybay, 2003). Protein A/G affinity chromatography is a highly specific purification method where excellent yields and purities can be obtained. One study reported yields of up to 100% and purities over 99% (Fahrner et al, 1999). A problem with protein A chromatography is the leakage of ligand into the eluted material. This has to be removed together with other contaminants such as host cell proteins by cation and/or anion chromatography in order to obtain a product of the required purity.

### ***1.3 Scales and dosages***

The doses required for *in vivo* usages of mAbs are relatively large. Common dosages for intravenous infusions are similar to that of Herceptin (Genentech, San Francisco, CA, USA) at 4 mg/kg bodyweight as a first injection, followed by 2 mg/kg weekly. For intramuscular injections the dosages are even higher, as for Synagis (MedImmune, Gaithersburg, MD, USA), which requires 15 mg/kg. This puts pressure on companies to meet the high demand and there is therefore a constant search for ways to increase the productivity. Over the past decades there has been a great increase in product titres, now a common titre is 2 g/L for mAbs in cell culture (Wurm, 2004). This has been achieved by extensive research in areas of genetic engineering and optimisation of media, cell culture format and important cultivation parameters such as temperature, pH, and harvest time. Lately there have even been reports of mAb titres of 5 g/L and above (Jagschies et al, 2006). The scale of operation has also increased rapidly over the past decades. Lonza (Portsmouth, NH, USA) is now operating a 20,000 L process for the production of recombinant mAb and perfusion processes are run elsewhere (Centocor Inc., Horsham, PA, USA) up to a scale of 500 L for mAb production (Merten, 2006).

### ***1.4 Challenges and trends in cell culture***

Over the past decades, research has improved and made economically feasible the production of therapeutic proteins using mammalian cell lines. This research has focused on the understanding of the mammalian cell system and has provided knowledge about cell physiology and growth characteristics. Improvements have been made through host cell and metabolic engineering, medium development and screening methods. This has resulted in better productivity including higher cell densities and product titres. An example comparing a stirred-tank process in 1986 and one in 2004 claims an increase in cell density from  $2 \times 10^6$  cells/mL to  $10 \times 10^6$  cells/mL, an increase in specific productivity from 10 pg/cell/day (PCD) to 90 PCD, and a close to 100-fold increase in mAb titre from 50 mg/L to 4.7 g/L (Wurm, 2004). The cell densities now achieved in mammalian cell culture are nowhere near what can be achieved in microbial cultures, so this is still a very important area for further research to improve productivity.

So far most research has focused on cell engineering and optimisation as well as the cell culture process in order to achieve higher cell densities and product titres. What will naturally then be needed is more research into downstream processes to cope with these high cell densities. There are processes in place to deal with high microbial cell densities, but due to the more fragile nature of the mammalian cells, these may not be suitable for this purpose. Even more importantly, the product quality must be carefully monitored to keep a consistency and to assure the product safety. This calls for standard procedures and protocols to be established for the analysis of the protein products.

Another issue that has been in focus over the last few years is the choice between reusable and disposable equipment. Disposable equipment may seem like a more expensive option, but reusable equipment is subject to extensive, time consuming and costly cleaning, sterilisation and validation procedures in order to prevent any cross-contamination between batches. Disposable equipment is therefore a very much up-and-coming alternative in mammalian cell culture.

## 1.5 Centrifugation

The first harvest step following fermentation in the production process of biopharmaceuticals is perhaps the most important one, since any losses of, or modifications to the product here will have a great impact on all subsequent purification steps. Centrifugation is the most commonly used harvest method for different types of cell culture, including mammalian, due to the relatively short processing times and the effectiveness in clarification. The main purpose of the harvest step is to separate the cells from the liquid broth, whether the product is in the supernatant or inside the cells or if the cells are the actual product. Any lack of performance will have a knock-on effect on any further purification steps, for example the commonly used subsequent filtration step, that will be prone to clogging and larger filtration areas will be needed. If the filtration step does not perform to the required standard, this will then cause expensive chromatography matrices to foul, causing increases in processing costs and decreases in product yield and purity. Centrifugation is an established separation method that is based on the principles of sedimentation, utilizing density differences between the cells and the liquid broth. The sedimentation properties for gravity settling are represented by Stoke's law, which if assuming the cells are spherical takes the form:

$$u_g = \frac{\rho_p - \rho_f}{18\mu} D_p^2 g \quad (1.1)$$

where  $u_g$  is the terminal sedimentation velocity,  $\rho_p$  is the density of the particle,  $\rho_f$  is the density of the liquid,  $\mu$  is the viscosity of the liquid,  $D_p$  is the particle diameter and  $g$  is the gravitational acceleration. The terminal velocity can similarly be represented for a particle in a centrifuge:

$$u_c = \frac{\rho_p - \rho_f}{18\mu} D_p^2 \omega^2 r \quad (1.2)$$

where  $u_c$  is the particle velocity in the centrifuge,  $\omega$  is the angular velocity of the bowl ( $\text{rad s}^{-1}$ ) and  $r$  is the radius of the centrifuge.

Equations 1.1 and 1.2 can be related using the centrifuge effect ( $Z$ ):

$$Z = \frac{\omega^2 r}{g} \quad (1.3)$$

The centrifugal field experienced in a centrifuge is commonly expressed as multiples of the gravitational acceleration and is then called the relative centrifugal force.

From equation 1.2 it becomes obvious that the rate of sedimentation in a certain centrifuge at a certain speed depends on a few important properties; the size and density of the particles and the density and viscosity of the liquid broth. One important aspect to note here is that the smaller the particle, the lower the rate of sedimentation, i.e. the less efficient will the centrifugation process be and so for batch processes higher angular velocities are needed exposing the product stream to higher shear rates (see section 1.5.2), or longer processing times are required. For a continuous operation the residence time within the centrifuge is increased by decreasing the flow rate.

There are different types of large-scale centrifuges that are used in industry for clarification of cell culture broths. Some are capable of continuous flow, while others work as a batch operation requiring manual solids discharge.

The tubular bowl centrifuge is a simple semi-continuous model that has been used in industry for many years. It is operated vertically and consists of a long cylinder that rotates inside a stationary casing so that when the broth is fed up through the cylinder the solids are forced outwards and stick to the walls, while the liquid flows up towards the top of the tube. The way the system is set up prevents continuous operation due to solids build-up and requires stopping, dismantling and manual removal of the cell debris.

The chamber bowl is a batch operated centrifuge that consists of one big bowl containing several tubular bowls with increasing diameter, where the broth is

introduced from the bottom centre and is fed through the cylinders. The solids stick to the walls of the chambers while the liquid proceeds through the whole system and can be collected at the outlet. This set-up requires a batch-operated process where the centrifuge has to be stopped and the solids manually removed.

An example of a continuously operating centrifuge is the disc stack. It consists of a rotating bowl filled with stacked plates at a downward angle (Figure 1.3), which provides an increased settling area, allowing for a faster process. When the bowl rotates the solids are forced outwards against the wall of the bowl, as well as the discs, while the clarified liquid continues to flow up along the axis and towards the outlet at the top of the bowl. The solid paste can be removed continuously, intermittently or manually, depending on the complexity of the system.

### 1.5.1 Sigma theory

Sigma theory is a concept used in centrifuge scale-up. It describes the characteristics of the centrifuge related to that of an equivalent sedimentation process without any force applied, i.e. from gravity alone. The characteristic this is described by is the equivalent settling area, sigma ( $\Sigma$ ,  $m^2$ ) and for a continuous centrifuge the sigma factor can be related to the feed rate through the following equation:

$$\Sigma = \frac{Q}{2u_g} \quad (1.4)$$

where  $Q$  is the volumetric feed rate. The sigma concept allows comparison of different types of centrifuges, as well as centrifuges of different scale, through the following equation.

$$\frac{Q_1}{\Sigma_1 E_1} = \frac{Q_2}{\Sigma_2 E_2} \quad (1.5)$$

where  $Q_1$  and  $Q_2$  are the volumetric flow rates of centrifuge 1 and 2 respectively,

$\Sigma_1$  and  $\Sigma_2$  are the sigma factors of centrifuge 1 and 2 respectively and  $E_1$  and  $E_2$  are the correction factors of centrifuge 1 and 2 respectively.

When using sigma theory to compare centrifuges of different types or scale, one of them is set as base case and its correction factor is set to 1. The correction factor for the centrifuge it is being compared to can then be looked up in literature.

The type of lab-scale centrifuge used in this work was a bottle swing out rotor type. The equivalent settling area for this type is defined as (Maybury et al, 2000):

$$\Sigma_{lab} = \frac{\omega^2(3-2x-2y)V_{lab}}{\ln\left(\frac{2r_2}{r_2+r_1}\right)6g} \quad (1.6)$$

where  $x$  and  $y$  are the fractions of total time required for acceleration and deceleration respectively,  $V_{lab}$  is the volume of the sample,  $r_1$  and  $r_2$  are the radii of the surface of the centrifuge liquor and the base of the centrifuge tube respectively. For a disc stack centrifuge, the equivalent settling area is expressed by:

$$\Sigma = \frac{2\pi\omega^2(N-1)}{3g \tan \theta} (r_o^3 - r_i^3) \quad (1.7)$$

where  $N$  is the number of discs,  $r_o$  is the outer radius of the disc,  $r_i$  is the inner radius of the disc and  $\theta$  is the half-cone angle of the disc. When comparing a batch type small scale centrifuge, such as the bottle swing out rotor, to a large scale continuous type, such as the disc stack, equation 1.5 becomes:

$$\frac{V_{lab}}{\Sigma_{lab}E_{lab}t_{lab}} = \frac{Q_{ds}}{\Sigma_{ds}E_{ds}} \quad (1.8)$$

where  $t_{lab}$  is the residence time of the small scale batch centrifuge.

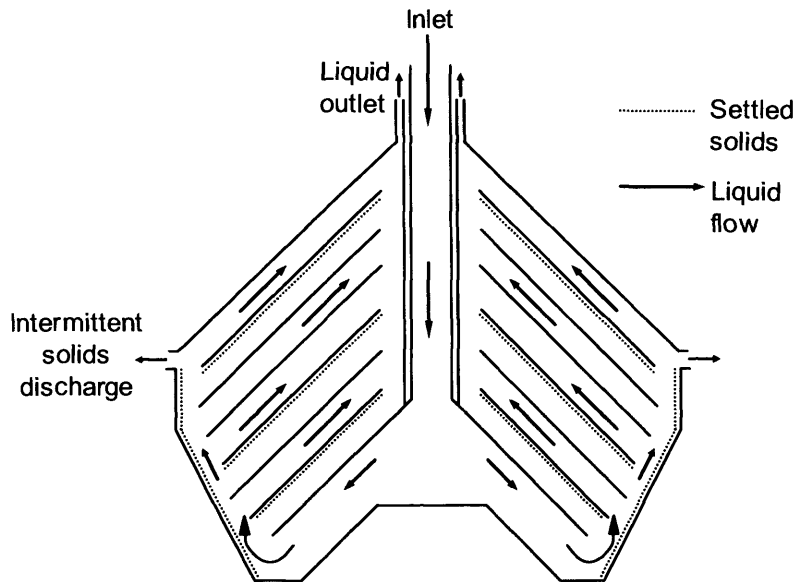


**Figure 1.3 Schematic of a disc stack centrifuge**

*The fermentation broth is fed in through the top and travels down the middle and when the centrifuge spins around its own axis the broth is forced out towards the sides of the chamber and up through the spacing of the disc stacks. The solids settle on the disc stacks and the walls of the chamber and can be removed intermittently or manually.*

### 1.5.2 Shear

During production and purification of biologic materials, such as therapeutic proteins, the product stream is exposed to possibly damaging hydrodynamic as well as mechanical forces. Although there are many causes of damage to cells, the main physical causes relate to shear and elongational flow stresses (Yim and Shamlou, 2000). Some of the main concerns are the shear forces experienced during centrifugation. Shear is not only experienced during centrifugation, but also in other unit operations, such as bioreactors, but to a much lesser extent. Shear can also be experienced during transport of the material through pumping. The damaging forces are generally expressed as a function of the energy dissipation rate ( $\text{Wkg}^{-1}$ ) and the magnitude can vary widely between different types of centrifuges, but can be in the range of  $10^5$ - $10^7 \text{ Wkg}^{-1}$ , which is nearly as high as the energy dissipation rate in a homogeniser ( $10^7$ - $10^9 \text{ Wkg}^{-1}$ ) (Yim and Shamlou, 2000).

In order to be able to design suitable processes and to produce consistent and safe therapeutics, the effects of shear forces have to be investigated and understood. Several studies have been carried out looking at the effects of shear on various biomaterials and shear in combination with other possibly damaging factors, such as temperature and air-liquid interfaces. A lot of these studies were carried out using various enzymes but not all of them report major damage due to shear. One study looked at the effects of shear, temperature and adverse pH conditions on yeast alcohol dehydrogenase (ADH) (Thomas et al, 1979). They found that shearing made the solutions turbid without causing large activity losses (only ~2%). Experiments at a higher temperature caused precipitation, but this was assigned to temperature rather than shear, while adverse pH conditions did not seem to contribute to shear damage. Supporting these findings are studies where shearing by a concentric-cylinder device did not cause losses in activity of ADH (Virkar et al, 1981). These studies also looked at the effect of shear experienced in pumps, with negligible damage to ADH in a single pass, but with excessive numbers of passes they saw a decrease in enzyme activity. Further studies (Thomas and Dunnill, 1979) on bovine liver catalase and jack bean urease saw no losses in activity due to shear. When reproducing previous experiments by other

groups, they noted much lower losses than reported previously. This led to repeating the experiments with enzymes from different suppliers where no losses of activity was noted for the enzyme from one supplier, while a 27% decrease was noted from the other supplier. This is strong evidence of the complexity of biologic material and hydrodynamic forces and highlights the importance of looking at different materials in order to draw conclusions regarding shear damage. One study used a stirred vessel to investigate the effect of shear in the presence of air-liquid interfaces on recombinant single chain antibody fragments (scFv) produced in *E.coli* (Harrison et al, 1998). Activity losses of up to 80% were recorded for stirred scFv in buffer, while stirred scFv in fermentation broth showed no losses. The antifoam was thought to have provided the protected environment in the latter case. It is obvious that even though shear might not be a major cause of concern to some biologic materials, it will have a great impact on others. It is also not only the active product that can be affected by shear. Hutchinson et al. (2006) showed that shearing of mammalian cell culture caused a decrease in particle sizes, which in turn heavily affected the clarification performance and would then affect all following purification stages and the overall process economics.

### **1.5.3 Ultra scale-down**

In the pharmaceutical industry there are many factors affecting the process from research to commercial production of the completed product. In contrast to other areas, cost is not necessarily always the major determinant. Instead, other factors play an important role. The degree of purity, for example, that is required for injection is extremely high and has to be obtained at all cost, otherwise the product will never reach the market. One of the most important factors in this fast-moving industry is time. It is a highly competitive market, with many companies working on similar products. It is therefore of vital importance for a company to secure patents and have its product reach market first. This calls for quick decisions and a need to often start the next stage in the development process even before the previous one is complete. During the development of new products there are usually only very limited amounts of material available and this material is often also very expensive. This means that process development needs to be

carried out at a small scale before long and expensive trials at large scale can be carried out. The results obtained from the small-scale experiments have to be possible to correlate to the large scale so that predictions can be made. Many rules for scale-up have been determined over the years and for some unit operations good correlations have been achieved. There are, however, further challenges even where these procedures have been established; not only microbial and yeast cultures are being used, but also shear-sensitive mammalian cultures for example, that have different properties and require other variables to be taken into consideration.

On the other hand, there is also a need for large-scale processes already in use to be mimicked at small scale for further investigations, analysis, and possible process changes. This could significantly decrease the time and cost of future developments.

The problems experienced in scale-down/scale-up of centrifuges mainly relate to differences in the fluid flow. The lab-scale equipment that is available is geometrically very different to the industrial-scale centrifuges and flow of material will therefore be very different, which in turn causes differences in forces acting upon the broth. To be able to predict the performance of the large-scale equipment, these forces need to be modelled if a true mimic is to be created.

Several attempts to scale down centrifugation have been carried out. One of these managed to scale down an industrial-size disc stack centrifuge 10-fold by reduction of the separation area (Mannweiler and Hoare, 1992). The scale-down model successfully predicted the recovery of polyvinyl particles. This model however still requires fairly large process volumes. A similar approach was taken where inserts were used to reduce the separation area by 76% and the bowl volume by 70% (Maybury et al, 1998). In a later study (Maybury et al, 2000) a bench-top centrifuge was instead used to mimic the performance of a large-scale continuous disc stack centrifuge. To carry out the study sigma theory was utilized, but the important acceleration/deceleration times for the small-scale centrifuge were taken into account and incorporated into the sigma factor. The study found that the recovery of shear-insensitive material, such as polyvinyl acetate particles

and yeast cell debris, was well predicted, while for shear sensitive material, such as protein precipitates, the recovery was over-predicted due to solids break-up.

#### **1.5.4 Shear device**

Work carried out at University College London has resulted in a miniature shear device being constructed (Levy et al, 1999), mimicking the high shear forces experienced in large scale centrifuges. This system is using an ultra scale-down (USD) approach to perform experiments on the millilitre scale. The device was developed by application of computational fluid dynamics (CFD) in order to predict the energy dissipation rates in the feed zone of an industrial disc stack centrifuge. A rotating disc device was then constructed mimicking the same rates. This device can be used as a time saving and cost efficient research tool for investigations of effects of centrifugation in bioprocessing and the potential damage to proteins caused by the shear experienced (Boulding et al, 2002; Boychyn et al, 2001; Boychyn et al, 2004; Levy et al, 1999; Neal et al, 2003). It can be valuable in the early development stages of biological products, such as therapeutic proteins, when often only a small amount of material is available. Another useful aspect lies in predicting the large-scale process and for developing process solutions in a very rapid manner allowing for a quicker route to the market. It can also be of use when changes are to be made for an already existing process in order to evaluate any effects these changes could have on the product. The device used in these studies was a modified version of that described by Levy et al. (1999). It was made of stainless steel with a 1 mm thick rotating disc, 40 mm diameter, inside a chamber of 50 mm diameter and 12 mm height (see Figure 1.4). The speed of the disc is correlated to the shear experienced in the feed zone of a centrifuge by CFD, which has been done previously (Boychyn et al, 2001; Boychyn et al, 2004). The work carried out here was building upon results from studies carried out by Hutchinson et al. (2006), successfully correlating the shear rates of the disc device to that of various large-scale centrifuges, and similar energy dissipation rates were therefore used.

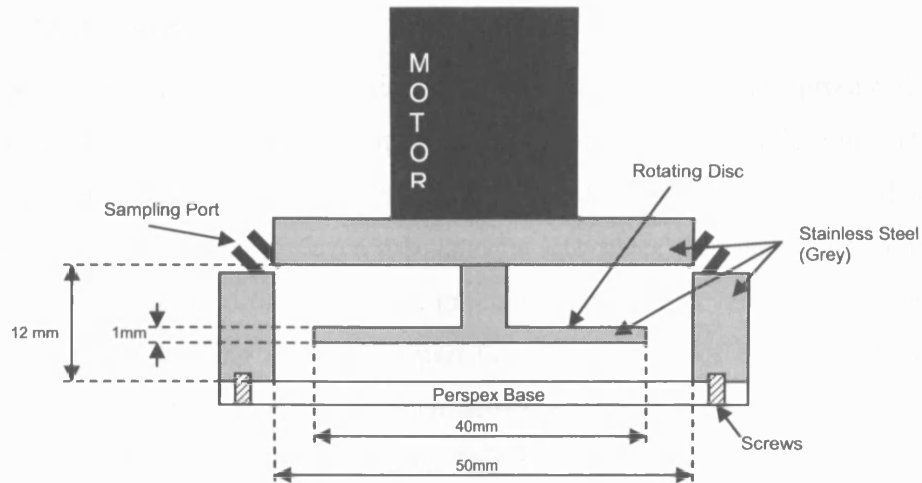


**Figure 1.4 Schematic of the shear device**

The shear device used in the studies was a cylinder made of stainless steel with a rotating disc inside it, mimicking the shear experienced at the inlet of a large-scale centrifuge. The disc was 1 mm thick, 40 mm diameter, while the chamber had an inner diameter of 50 mm and 12 mm height (schematic from McCoy, 2009).

## **1.6 Antibodies**

Antibodies are vital parts of the human immune system. They are produced by B lymphocytes and are distributed throughout the body in the biologic fluids. During the immune defence, antibodies that are secreted from the B cells bind to the foreign antigen and puts defence mechanisms into place that leads to elimination of the antigen. Antibodies work in the immune defence in several ways that are all initiated by the binding of the Fab part (see Figure 1.5) of the antibody to the antigen on the infected cell. This then activates response mechanisms in the Fc part in order to destroy the antigen. These mechanisms are interactions with specific ligands, e.g. the C1 component of the complement cascade and the cellular receptors, FcγRs (Abbas et al, 2000). The FcγRs are part of the antibody-dependent cell-mediated cytotoxicity (ADCC) mechanism. This is where the Fc receptors on natural killer (NK) cells recognise and bind to the Fc part of the antibody. This in turn triggers a response from the NK cells that causes apoptosis of the infected cell. The Fc receptors that bind to IgG are called FcγRs. The other mechanism of action for IgG is complement-dependent cytotoxicity (CDC). This is initiated by the binding of antibodies to antigens on the infected cell and the binding of the antibody to the C1 component of the complement cascade, which in turn punctures the infected cell membrane and causes the cell to lyse and therefore die. ADCC and CDC are the two most common mechanisms by which today's approved mAbs work.

### **1.6.1 Commercial production of antibodies**

During the past decades, there have been immense advancements in the area of treating diseases with biological products, such as therapeutic proteins. Over the past few years in the late nineties and beginning of the new century, the Food and Drug Administration (FDA) has approved new drugs treating some of the most common diseases that have been difficult to treat before. A large proportion of the therapeutic proteins that have been licensed or are presently in clinical trials are mAbs. By the end of 2002, there were twelve antibodies, antibody fragments or conjugated antibodies approved by the FDA (Harris et al, 2004). To date, there are mAbs that have been approved for all sorts of cancers (non-Hodgkin lymphoma, breast cancer, leukaemia and colorectal cancer, to mention a few) and other

diseases such as multiple sclerosis. Many of these are genetically engineered mouse mAbs, which have been made to look like human mAbs, examples including trastuzumab (Herceptin<sup>®</sup> by Genentech, Inc, South San Francisco, CA) for breast cancer, cetuximab (Erbix<sup>™</sup> by ImClone Systems Inc, New York, NY) for colorectal cancer, daclizumab (Zenapax<sup>®</sup> by Hoffman-La Roche Inc, Nutley, NJ) to help prevent acute kidney transplant rejection and palivizumab (Synagis<sup>®</sup> by MedImmune, Inc, Gaithersburg, MD) to protect high-risk infants against respiratory syncytial virus disease. Another important advancement in biotechnology is the first radiopharmaceutical product that was approved in 2002; ibritumomab tiuxetan (Zevalin<sup>®</sup>) that is used together with rituximab (Rituxan<sup>®</sup>), both by Cell Therapeutics, Inc. Seattle, WA) to treat non-Hodgkin's lymphoma. All of these therapeutic proteins are produced on a large scale for commercial exploitation. Many of them have been fast-tracked for approval due to the urgency of developing drugs targeting diseases that have so far been untreatable.

### 1.6.2 Basic structure

There are five different classes of antibodies, which are all soluble proteins of globular structure with a common name of immunoglobulins (Igs). All antibodies share the same core structure of 4 polypeptide chains, two heavy (H) and two light (L), held together covalently by disulphide bonds and by non-covalent interactions between the chains. The entire core structure has a molecular weight of around 150,000 Da, the light chains of approximately 25,000 Da and the heavy of 50,000 Da each. Both heavy and light chains contain a series of repeated homologous units, creating intrachain disulphide bonds that cause the protein to fold into a number of globular domains. Light chains have 2 domains each while heavy chains have 4 or 5.

All antibodies have constant carboxy terminal regions (C), which are identical within a class, while the amino terminal regions are variable (V). The variable region is the part that binds to the epitopes. The N-terminal amino acids of both heavy and light chains contain regions of sequence variability different in antibodies produced by one clone of B cells from those produced by another. There are three short stretches of greatest variability, the hypervariable regions,

while the less variable stretches in-between are the framework regions. The hypervariable regions are also called complementarity-determining region (CDR) 1, 2 and 3, since they bind the antigen by complementarity.

The light chains are divided into two major classes, kappa ( $\kappa$ ) and lambda ( $\lambda$ ); however one immunoglobulin molecule only contains one class. The heavy chains are divided into five major classes, which provide the differentiation of the immunoglobulin classes (isotypes). The differences can be found in the constant region of the heavy chains and the different types are called alpha ( $\alpha$ ), delta ( $\delta$ ), epsilon ( $\epsilon$ ), gamma ( $\gamma$ ) and mu ( $\mu$ ), corresponding to the isotypes IgA, IgD, IgE, IgG and IgM respectively. As with the light chains, one immunoglobulin molecule only contains one class of heavy chain. The different classes contain different numbers of immunoglobulin domains in the constant region of the heavy chain, which are numbered  $C_{H1}$ ,  $C_{H2}$  etc. (Figure 1.5) from amino to carboxy terminus. Human IgA, IgD and IgG contain three domains each, while IgE and IgM contain four. IgA and IgG are further divided into two and four subclasses respectively, where minor differences occur, mainly concerning the interchain disulphide bonds. The structural variations in the different classes of immunoglobulin provide a way of producing different effector mechanisms when the antibody binds to an epitope. This is due to the heavy chain constant regions binding to, for example, proteins from the complement cascade and the structural variations causing the binding of different complement proteins.

Of the major classes of immunoglobulin, IgG is the most abundant in humans. IgG has the longest half-life of the immunoglobulins of up to 23 days, depending on the subclass, and is therefore the most suitable for passive immunization. The subclasses that exist are; IgG1, IgG2, IgG3 and IgG4, with IgG1 being the most abundant in serum and IgG4 the least. A common feature for all classes of immunoglobulins is an area containing a large number of cysteine and proline residues providing interchain disulphide bonds and preventing globular folding. This area, in certain isotypes located between  $C_{H1}$  and  $C_{H2}$ , is called the hinge region due to the flexibility it confers on the molecule. The immunoglobulin molecule can be cleaved at the hinge region by the proteolytic enzyme papain. The enzyme cleaves N-terminally to the disulphide bridge between the heavy

chains. This results in three approximately equal sized fragments; two of these carry the antigen binding sites, Fab (antigen binding fragment) while the third one provides the immunological response after antigen binding. This last fragment can be crystallised out of solution and is therefore called Fc (crystallisable fragment) (Figure 1.5). Immunoglobulins can also be cleaved by pepsin. This enzyme cleaves C-terminally to the disulfide bridge between the heavy chains at the hinge region. This results in the separation of the Fc fragment from the two Fab fragments, that are this time held together by disulfide bridges and called  $F(ab')_2$ . The Fc fragment is further cleaved along both chains into several fragments (Abbas et al, 2000; Coico et al, 2003; Tizard, 1995).

### 1.6.3 Formation in the cell

Antibodies occur in both secreted and membrane bound forms. They are produced by B lymphocytes in the bone marrow, where the membrane bound antibodies form part of the B cell antigen receptor. The secreted antibodies are found in blood plasma and other extracellular fluids such as mucosal secretions and also in the interstitial fluid of the tissues. They often attach to other cells part of the immune system, which have specific receptors for binding antibody molecules. Membrane associated and secreted antibodies differ slightly in constant region amino acid sequence. B cells are the only cells that can synthesise antibodies, where they can be found in the endoplasmic reticulum (ER) and Golgi complex. The heavy and light chains are synthesised on membrane bound ribosomes in the ER, where the formation of disulphide bonds takes place, covalently associating the chains into immunoglobulin molecules, and oligosaccharides are attached to the molecule (see section 1.7). The antibodies are then transferred into the Golgi complex, where modification of the carbohydrates takes place, and then to the plasma membrane in vesicles, where they are secreted or anchored to the cell membrane.

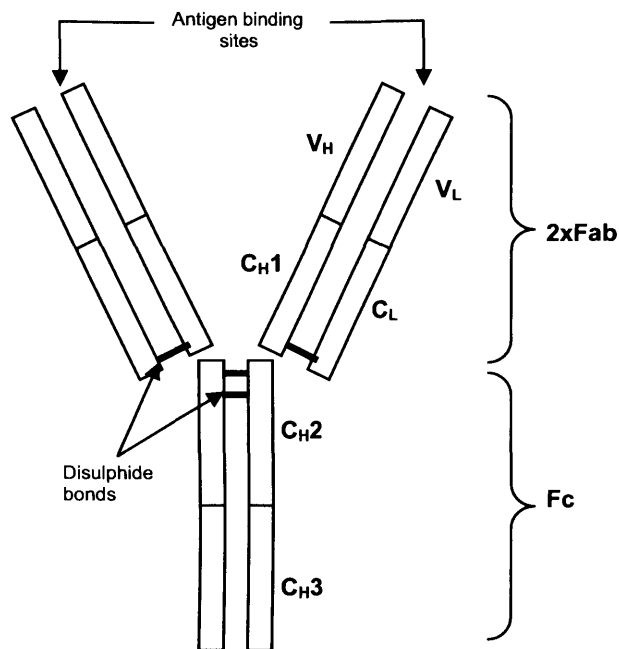


**Figure 1.5 Schematic of an IgG**

The molecule is built up of four polypeptide chains; two heavy (H) and two light (L), held together by disulphide bonds between the cystein residues on the chains, one between the heavy and light chain and two connecting the two heavy chains. The light chains contain one constant region ( $C_L$ ) and one variable ( $V_L$ ) region while the heavy chains contain three constant regions ( $C_{H1}$ ,  $C_{H2}$  and  $C_{H3}$ ) and one variable region ( $V_H$ ). The hinge region is located between  $C_{H1}$  and  $C_{H2}$  and confers flexibility on the molecule. This is where the proteolytic enzyme papain can cleave the IgG into two parts that carry the antigen binding sites, Fab, and one crystallisable fragment, the Fc part.

### 1.6.4 Half-antibodies

The IgG molecule is built up by two heavy and two light chains linked together by disulphide bonds. The heavy and light chains are synthesized separately and then assembled into the IgG tetramer structure  $H_2L_2$ . Each light chain is built up by two domains that are created through two intrachain disulphide bonds between cysteine residues, while each heavy chain is built up by four of these domains, through four intrachain disulphide bonds. One heavy and one light chain are then linked together aided by the heavy chain-binding ER chaperone of the HSP 70 family, BiP (Lee et al, 1999). Lee describes how BiP interacts with the  $C_{H1}$  domain, which remains unfolded in free heavy chains, until the light chain binds to the heavy chain and BiP is released and the  $C_{H1}$  domain folds into its correct conformation and the intact IgG molecule is obtained.

The subclasses of IgG (IgG1, IgG2, IgG3 and IgG4) mainly vary in the structure of the hinge region, where the disulphide bonds between the two heavy chains are situated. The structure of this region affects the flexibility of the molecule and this in turn has an effect on the ability of correct and stable interchain disulphide bonding. In IgG4 the covalently linked  $H_2L_2$  tetramer, which is bound by two interchain disulphide bonds between the two heavy chains in addition to the disulphide bonds linking each light chain to a heavy chain (see Figure 1.5), is secreted together with a non-covalently linked tetrameric structure, which can disassociate into HL dimers (Angal et al, 1993; Bloom et al, 1997; Deng et al, 2004; King et al, 1992; Zhang and Czupryn, 2002). These tetramers lack the interchain disulphide bonds in the hinge region between the two heavy chains and seem to be a general feature of the IgG4 subclass (King et al, 1992). The four subclasses have the same sequence CPXCP in the core hinge region, where X is proline in IgG1 and IgG2, arginine in IgG3 and serine in IgG4 (Angal et al, 1993). The difference in structure and stability of the different subclasses was shown by Angal et al. (1993) and Bloom et al. (1997), who both substituted the serine of the IgG4 hinge region with that of a proline of the IgG1/2 hinge region, which eliminated the presence of the half- mAb. The fact that the IgG1 subclass does not experience these half-antibodies is probably one of the reasons that most approved mAbs are of this subclass.

The mAb used in this research is an IgG4, serving as a model antibody, and will therefore be subject to the presence of HL dimers. These dimers may be undesirable in the production of mAbs for therapeutic purposes, unless they can stay non-covalently bound. There have been a few attempts in the literature to reduce their occurrence. The mAbs where dimers occur have been reported to contain a higher proportion of free sulphhydryl groups than those only containing covalently bound intact tetramers (Chaderjian et al, 2005; Cromwell et al, 2006; Zhang and Czupryn, 2002). The presence of free sulphhydryl groups was reduced 10-fold by Chaderjian et al. (2005) with the addition of copper sulfate, which creates an oxidative environment, facilitating the formation of disulphide bonds. Deng et al. (2004) took a more preventative approach that could be used during early product development. They developed a Western-blot based screening method that could help identify the most promising clone with regards to HL dimers when screening for which cell line to use. In the research presented here, it was not attempted to minimise the HL dimers, but rather to note their presence, evaluate their structure and investigate the effect of processing conditions on the amount present.

### **1.6.5 Modifications of IgG**

After the protein structure of the antibody has been synthesised, post-translational modifications take place. Some of these apply to a number of proteins in general, for example glycosylation (see section 1.7), while others are specific to mammalian cell culture or even to mAbs in particular. One example of a modification that is specific to proteins produced using mammalian cell culture is the proteolytic degradation of the C-terminal lysine residues (Figure 1.6). This has been observed during characterisation of numerous mAbs. To mention a few, one group showed the complete absence of the expected C-terminal lysine residue of a CD4-IgG hybrid (Harris et al, 1990), while Beck et al. (2005) detected similar data for a humanized recombinant mAb produced in NS0 cells with almost complete absence of C-terminal lysine, however in this case a more heterogeneous population was detected with 6% of the population still carrying a lysine residue on one of the two heavy chains and 2% with both lysines still intact. An even

more heterogeneous population of a mAb was recorded (Santora et al, 1999) where approximately 70% of the antibodies had both lysines removed, 23% had one intact lysine and 7% still had both lysines intact. It has not been established when or where this modification takes place or even why, but it is of common knowledge that it does take place. The reaction is enzymatic by the action of a carboxypeptidase and is evident in culture produced mAbs as well as plasma derived mAbs (as reviewed by Harris, 1995).

Another commonly observed modification of mAbs is the cyclization of *N*-terminal glutamine to pyroglutamic acid. Most IgG heavy chains have either a glutamine (Q) or a glutamic acid (E) residue at its *N*-terminal, which can be converted into pyroglutamic acid (pE) with the loss of an amino group (Figure 1.7 a and b). Studies show that this modification takes place at a high rate; a 70% conversion of Q to pE was detected during production as well as continued conversion after storage at 29°C for 3 months to almost complete conversion to pE (Rehder et al, 2006). It has been debated whether this process is enzymatic or spontaneous and whether it is a co-translational or post-translational modification, and the consensus seems to be that it could be all of these. Early studies indicated that the cyclization of glutamic acid is enzymatic rather than spontaneous (Twardzik and Peterkof, 1972). A study looked at the cyclization of glutamine on a peptide and showed that this reaction does occur spontaneously, but at a low rate under physiological conditions (Busby et al, 1987). They also identified the enzyme glutaminyl cyclase to carry out the conversion *in vivo*. In contrast to most reports, one group did not detect any pyroglutamic acid in their purified mAb, but noted conversions of up to 50% upon storage, with higher conversion rates at temperatures above 29°C and lower or higher pH (in the range pH 4-8, the minimum conversion was observed at pH 6) (Yu et al, 2006). From the mentioned studies it has become obvious that the conversion of glutamine to pyroglutamic acid takes place both during production and during storage and the final mAb product will be a heterogeneous population with one, none or two glutamine residues converted. While it seems the modification is more likely to take place than not, the effects it has on stability and bioactivity of the mAb are not entirely understood.

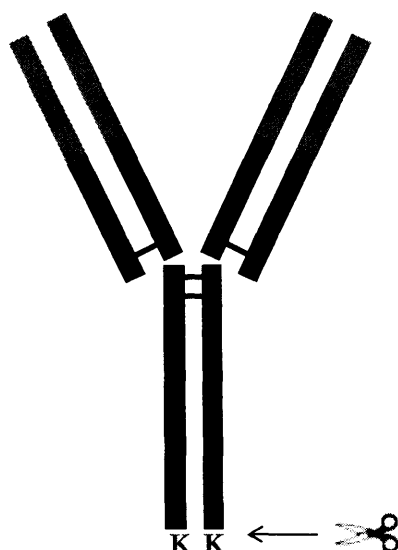


**Figure 1.6 C-terminal lysine cleavage**

This shows a schematic of an IgG. The variable regions are shown in grey while the constant regions are shown in black. The lysine residues (K) at the C-terminal of each of the heavy chains have been marked out. These are prone to being cleaved off resulting in a mass shift of  $-128$  Da per residue and a heterogeneous population where the IgG has none, one or two lysine residues.

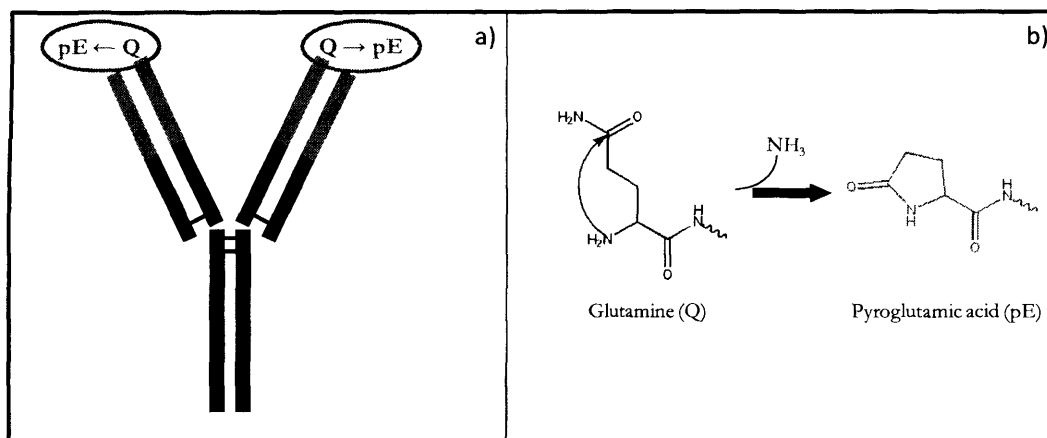


**Figure 1.7 Cyclization of N-terminal glutamine**

a) shows a schematic of an IgG with the glutamine residues (Q) at the N-terminal of each of the heavy chains have been marked out. These can be converted to pyroglutamic acid (pE) by cyclization and the loss of an amino group ( $\text{NH}_3$ ) (b), resulting in a mass shift of  $-17$  Da per amino group, a total of  $-34$  Da.

## 1.7 Glycosylation

Antibodies are glycoproteins, meaning they are proteins that have carbohydrates attached to them through the process of glycosylation. Glycoproteins can be found in cellular membranes, particularly the plasma membrane, and also in extracellular secretions such as plasma. Oligosaccharides are covalently attached to the amino acid side chains of the protein, which will have an impact on the three dimensional structure of the molecule. Glycosylation is of great importance not only to the structure, but also to the function of the protein, which is further discussed in section 1.7.4.

### 1.7.1 Glycan structures

Glycoprotein carbohydrate chains vary in structure and can therefore be divided into 2 major classes; *N*-linked and *O*-linked. *N*-linked can then be further divided into three classes; the complex type, the high-mannose type and the hybrid type. These subgroups share the common feature of linkage to the amino group of asparagine (Asn) while differing in the sugar components; the complex type consists of *N*-acetylglucosamine (GlcNAc), mannose, galactose, fucose and sialic acid, the high-mannose type consists only of *N*-acetylglucosamine and mannose and the hybrid type has features of both the two first mentioned (Figure 1.8). *N*-linked glycosylation does not take place on every asparagine residue, but only at the recognition sequence Asn-X-Ser/Thr, where X can be any amino acid except proline. *O*-linked oligosaccharides on the other hand, are linked to the hydroxyl groups of serine or threonine, the first sugar residue usually being *N*-acetylglucosamine, and do not share a recognition sequence (Ashford and Platt, 1999; Fukuda, 1994). A glycoprotein can contain both *N*- and *O*-linked oligosaccharide chains at multiple sites, which together with the different monosaccharide combinations give rise to structural heterogeneity.

### 1.7.2 Glycan synthesis

The glycosylation reactions take place in the ER and in the Golgi vesicles. However, there is a difference in the biosynthesis of *N*- and *O*-linked oligosaccharides. *N*-linked glycosylation (Figure 1.9) is commenced in the lumen

of the ER where first a lipid-linked oligosaccharide precursor is synthesised. This oligosaccharide, GlcNAc<sub>2</sub>Man<sub>9</sub>Glc<sub>3</sub>, linked to dolichol, is then transferred to an Asn residue on the nascent peptide chain. This is catalysed by oligosaccharyltransferase. From the newly synthesised glycoprotein the three glucose and one mannose residues are enzymatically cleaved off by ER  $\alpha$ -glucosidase I and II and ER  $\alpha$ -mannosidase respectively, and the folded protein is then exported from the ER. This process is aided by interactions with integral membrane proteins such as calnexin, which can bind to incompletely or incorrectly folded glycoproteins that will have a glucose residue reattached to it, preventing export, while refolding occurs.  $\alpha$ -glucosidase II then cleaves off the remaining glucose residue and the corrected glycoprotein can be released and carried by vesicular transport from the ER to the Golgi Apparatus (GA). Here the oligosaccharide chain, Man<sub>8</sub>GlcNAc<sub>2</sub>, is attacked by Golgi  $\alpha$ -mannosidase I, which cleaves off a further three mannose residues creating the precursor for oligosaccharides of the high-mannose type, which can then be further processed. This molecule also serves as a precursor for the other types of *N*-linked oligosaccharides; the enzyme *N*-acetylglucosaminyl transferase adds a GlcNAc to the structure to form the precursor for the hybrid type oligosaccharide. This molecule then also serves as a precursor for the complex type where Golgi  $\alpha$ -mannosidase II cleaves off two mannose residues to form a molecule to which other monosaccharides can be added (Ashford and Platt, 1999; Fukuda, 1994). The further processing of the oligosaccharide chains varies from species to species. This creates a problem when producing biopharmaceuticals that need to be properly glycosylated; the host cell usage is very restricted. As mentioned in section 1.1.1, this has prompted for usage of mammalian cell culture in order to achieve the correct glycosylation.

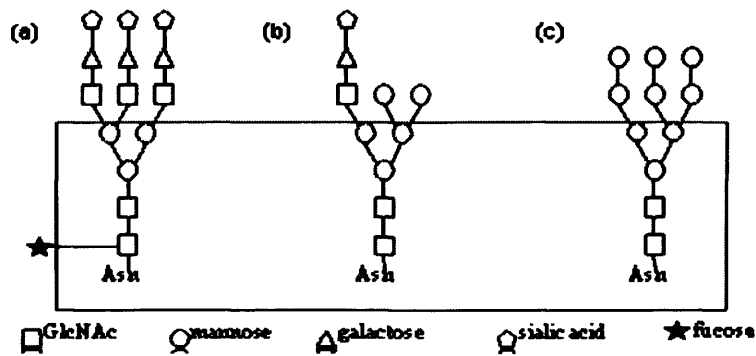


**Figure 1.8 Different subgroups of N-linked oligosaccharide structures**

(a) complex type, (b) hybrid type and (c) high-mannose type. The highlighted area shows the common pentasaccharide core of two N-acetylglucosamine and three mannose residues attached to the asparagines (Asn) in the recognition sequence Asn-X-Ser-Thr. The additions to the core structure are what separate the different types. The high-mannose type is only made up of mannose residues in addition to the core while the complex type can have GlcNAc, galactose and sialic acid added to the mannose antennae, as well as a fucose residue attached to the Asn-linked GlcNAc residue. The hybrid type is a mix of the two.

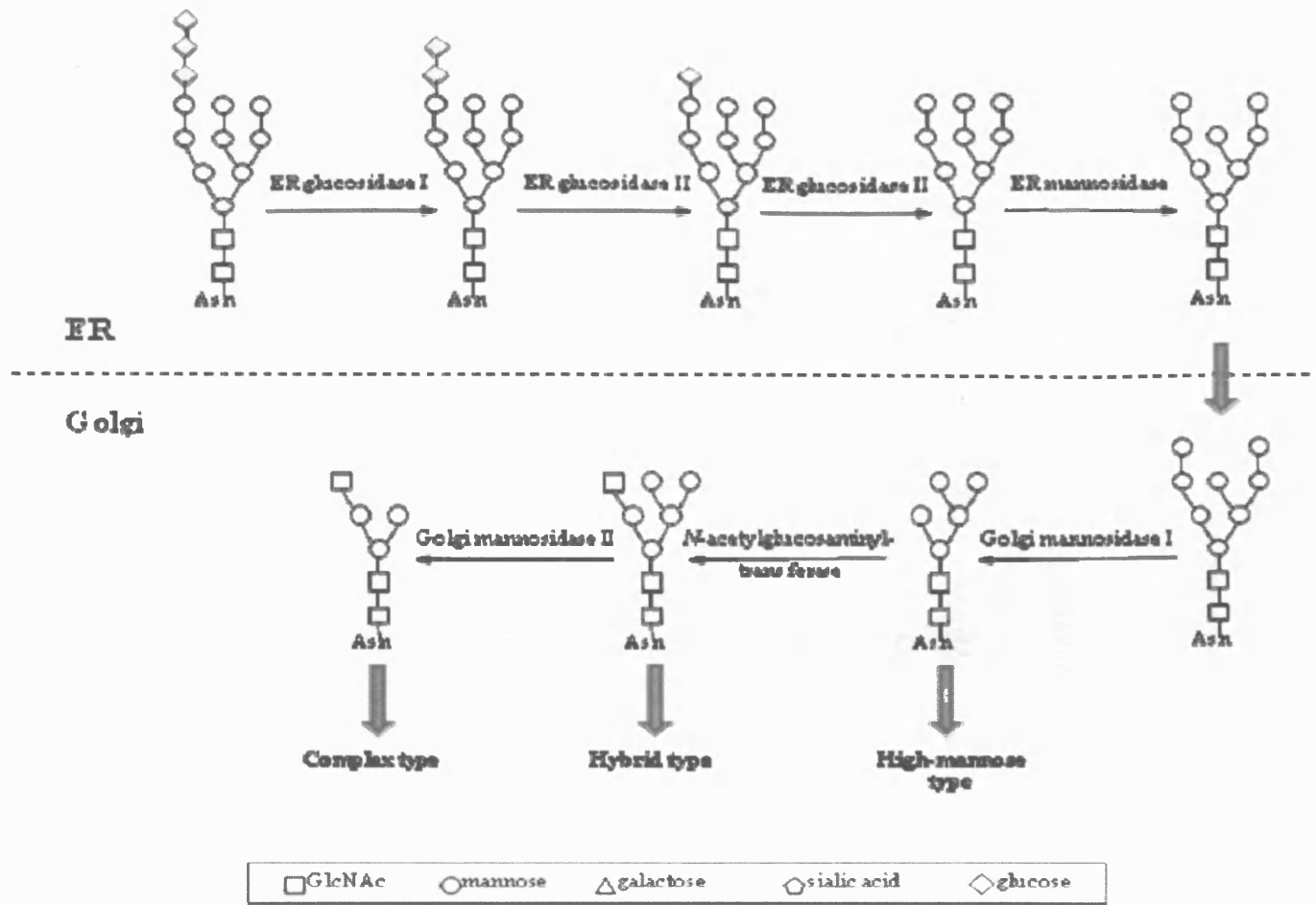


*Figure 1.9 Schematic of N-linked glycosylation*  
 (Legend on following page)

**Figure 1.9** continued. The glycosylation sequence is commenced in the lumen of the ER (above the broken line). The initial GlcNAc2Man9Glc3-oligosaccharide is synthesised while linked to a dolichol lipid. The glycan is then transferred to an Asn residue on the nascent peptide chain, catalysed by oligosaccharyltransferase. The three glucose residues are then enzymatically cleaved off by ER glucosidase I and II and one mannose residue is removed by ER mannosidase leaving a GlcNAc2Man8-oligosaccharide that can be exported from the ER to the Golgi by vesicular transport. In the Golgi three further mannose residues are cleaved off by Golgi mannosidase I, resulting in the GlcNAc2Man5 structure that is the precursor for the high-mannose type glycans where further mannose residues can be added. The GlcNAc2Man5 structure also serves as a precursor for the other two types of N-linked glycosylation; N-acetylglucosaminyl transferase adds a GlcNAc residue to create the GlcNAc3Man5 structure that can then be further processed as hybrid type glycans. The GlcNAc3Man5 structure in turn serves as a precursor for the complex type glycans when Golgi mannosidase II removes two mannose residues resulting in the GlcNAc3Man3 structure that can be further processed to obtain the different complex glycan structures.

### 1.7.3 Glycosylation of IgG

It is now of general knowledge that IgG exhibits *N*-linked glycosylation at asparagine (Asn) 297 (Beck et al, 2005), situated in the C<sub>H</sub>2 domain. The glycan at this site is of the complex type (Figure 1.8) and can therefore contain GlcNAc, fucose, mannose, galactose and sialic acid. However, the heterogenic nature of glycosylation means that the glycans vary in composition from species to species (Raju et al, 2000; Saba et al, 2002), for example between human and mouse IgG (Hossler et al, 2006), and so cell line selection is therefore of importance when producing therapeutic antibodies. There is, however, a predominant structure found among all IgGs; core-fucosylated asialo biantennary chains with varying levels of galactosylation, with small amounts of monosialyl and afucosyl oligosaccharides present (Kunkel et al, 2000; Saba et al, 2002). Figure 1.10 shows a schematic explaining the nature of these glycan structures; they most often have a fucose attached to the core structure and can have none (G0), one (G1) or two (G2) galactose residues attached to the GlcNAc residues on the antennae, and to a lesser extent sialic acid attached to the galactose. The most commonly observed glycan structure in human IgG is FucGlcNAc<sub>2</sub>Man<sub>3</sub>GlcNAc<sub>2</sub> (G0F) (Krapp et al, 2003). The glycans in Figure 1.10 are the most commonly observed in IgG; however, other variants of these structures have also been reported. Bailey et al, 2005, observed glycans where only one of the antennae was extended, generating structures like the examples shown in Figure 1.11. This has not been widely reported and so the frequency of their occurrence is most likely an exception rather than a rule. Up until recently most studies of glycosylation structures have involved a deglycosylation step to release the glycans from the peptide backbone in order to analyse separately. Using these methods it has been possible to map which glycans are present, but each IgG molecule has two glycan chains attached, one on each heavy chain, so the possibility of one IgG molecule having two different glycans attached was not commonly discussed. With the advancement of more powerful analytical techniques, the intact IgG can now be studied and it has

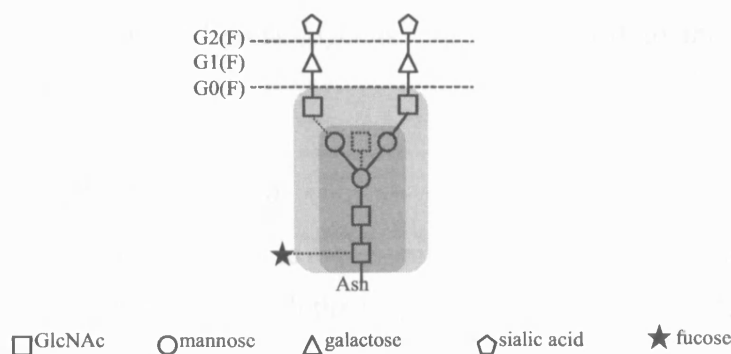


**Figure 1.10 Glycosylation of IgG**

The predominant glycosylation structure in IgG has a fucose residue attached to the first GlcNAc residue of the core structure common to all glycan types (dark grey-shaded area, with the exclusion of the bisecting mannose in dotted line) and is of a biantennary structure with one GlcNAc attached to each of the arms (light grey-shaded area) and with varying levels of galactosylation (G0, G1 and G2). There can also be small amounts of non-fucosylated glycans and glycans with sialic acid attached at the end of the arms. The bisecting GlcNAc (dotted line) occurs naturally in 5-10% of human IgG (Krapp et al, 2003), but is not commonly reported in studies.

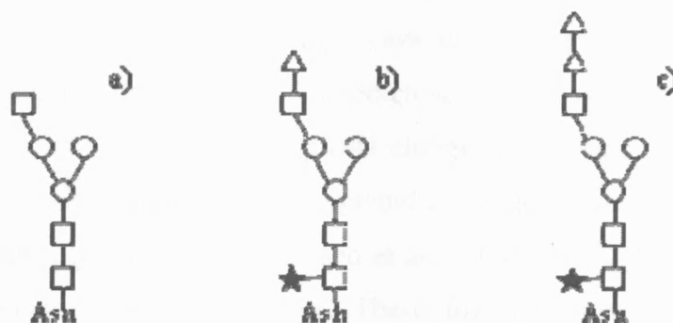


**Figure 1.11 Variations in glycosylation of IgG**

Bailey et al. (2005) reported some variations of the commonly observed IgG glycosylation from analysing IgG2 glycans. They observed a biantennary structure where only one of the antennae was extended as the examples in this figure; a) shows a G0 structure with one GlcNAc missing, b) shows a G1F structure with one GlcNAc missing and c) shows a G2F structure with a GlcNAc missing, with both galactose residues added on to the same arm.

become evident that two different glycans can be attached to the same IgG (Gadgil et al, 2006).

### 1.7.4 Effects of glycosylation

Glycosylation of IgG has proved to be essential for efficient activation of the response mechanisms associated with the Fc part (Lund et al, 1996; Mimura et al, 2000). It plays an important role in the recognition of the cellular receptors and complement. Studying the crystal structure of the IgGFc-Fc $\gamma$ RIII complex shows that the interaction site on the IgG is the hinge proximal region of the C<sub>H</sub>2 domain (Sondermann et al, 2001), indicating some importance of glycosylation. Interactions between amino acids of IgG (not Asn297) and sugar residues of its oligosaccharide chain and their influence on activity have also been investigated (Lund et al, 1996). Replacement of amino acid residues around Asn297 changed the interactions between the amino acid residues and the sugar molecules, which in turn changed the conformation of the hinge region. This resulted in decreased recognition of human chimeric IgG by guinea pig C, human C1q and human Fc $\gamma$ RI. Another study relates glycosylation to biological activity and also structural stability (Mimura et al, 2000). Here truncated glycoforms were examined and an increase in stability and activity was observed compared to the deglycosylated form. Stability studies were also carried out by Krapp et al. (2003). Truncated glycoforms of IgG-Fc showed conformational changes in the C<sub>H</sub>2 domain, which in turn affects the interaction with the cellular receptors. The effects of glycosylation on structure and stability have also been studied for other proteins. The thermostability of  $\beta$ -Lactoglobulin increased when the protein was modified through glycosylation (Broersen et al, 2004), although in this case the structural packing remained the same. These findings have led to ideas of improving protein function and stability through glycoengineering. One group managed to improve stability and *in vivo* activity of three different proteins (recombinant human erythropoietin, leptin and Mpl ligand) by introducing recognition sequences for glycosylation before expression (Elliott et al, 2003).

### 1.7.5 Factors affecting glycosylation

It has become obvious that glycosylation is a very important post-translational modification that confers important attributes to a glycoprotein and can affect efficacy and stability of the protein when used as a therapeutic. Glycosylation creates a heterogeneous product population, but how does the population change and what are the underlying factors? Already mentioned is that glycosylation is species-specific and so therefore will vary when using different cell lines. Several studies have also been carried out that show variations in glycosylation patterns with different culture methods and conditions; one group observed less sialylation and greater glycoform heterogeneity in human monoclonal IgM produced in mouse ascites compared to the IgM produced *in-vitro* in hollow-fibre perfusion or serum-free airlift cultures (Maiorella et al, 1993). Different levels of sialylation were also observed (Schweikart et al, 1999) when comparing the glycosylation patterns of murine monoclonal IgA produced in different cultivation systems (continuous stirred tank, fluidised bed and hollow fibre reactor). Again, Kunkel et al. (2000) noted variations in the relative amount of sialic acid residues when comparing a monoclonal IgG1 produced in two different bioreactors (LH Series 210 and New Brunswick Scientific CelliGen bioreactors). This group also found that different levels of dissolved oxygen (DO) concentrations affect the level of galactosylation with an increase in the relative amount of agalactosyl and a decrease in digalactosyl glycans at lower DO concentrations. One group observed higher levels of galactosylation in monoclonal IgG2 produced in static or spinner flasks compared to in ascites or a hollow-fibre system and that the influence of media content (protein free, low serum or high serum content) is more prominent in high cell-yield culture systems (Cabrera et al, 2005). The influence of media content was also studied (Serrato et al, 2007) when serum free and chemically defined media was observed to increase cell concentration and mAb titre but caused decreased sialylation and increased fucosylation as compared to a traditional serum-containing medium. They also observed lower levels of galactosylation with increased relative amounts of the G0 glycan in the IgG1 from serum free medium; however, this culture also displayed an increase in extracellular  $\beta$ -galactosidase activity, which could explain this observation. From the above-mentioned studies it becomes obvious that a greater understanding of

the effects of different factors during cell culture on glycosylation patterns is being obtained, but is a constantly ongoing process. What have not received a lot of attention up to date are the effects that further processing and purification could have on glycan structures.

### 1.7.6 Glycoengineering and current trends

One of the main problems associated with the use of murine Abs for therapeutic purposes is the fact that there are differences between for example mouse Abs and human Abs and the immunogenic responses these can cause. Although there are still some murine mAbs on the market, Zevalin being one of them, they are a minority. Today, the trend is to create mAbs by genetic engineering to create recombinant proteins (Dillon et al, 2004; Fotinopoulou et al, 2003; Wan et al, 2001). This ensures production of proteins that suit the purpose and more importantly, it ensures safety and efficiency of the immunisation, preventing an immune response upon injection of a foreign protein. In addition to the murine mAbs on the market, there are a few chimeric mAbs, i.e. with a murine variable region and a human constant region, for example Erbitux and Rituxan, and a couple of fully human mAbs, Humira (Abbott Laboratories, Abbott Park, IL) treating inflammatory diseases and Vectibix (Amgen Inc., Thousand Oaks, CA) for colorectal cancer. All other mAbs that are approved for therapeutic purposes are so called humanised, where murine hypervariable regions are introduced into human Abs, resulting in an almost entirely human Ab to keep the immunogenic response to a minimum.

Mammalian cells are currently the main means of producing therapeutic proteins and mAbs in particular. The main reason behind this is the glycosylation pattern produced by the cells that is most similar to human glycosylation, compared to bacteria, yeast or fungi. The mammalian cell system is the most appropriate one, but it is not perfect in this respect. One of the problems associated with therapeutic protein production using murine cell lines is the occurrence of the sialic acid N-glycolylneuraminic acid (Neu5Gc), which is absent in human Abs (Varki, 2001) and can therefore cause immunogenicity. The discrepancies in glycosylation patterns have led to *in vivo* engineering of the glycosylation

pathways and also N-glycan remodelling *in vitro*. One of the problems associated with mAbs is the high dosages required due to their relatively low activity *in vivo*. It has been shown that the ADCC activity can be increased through glycoengineering, especially non-fucosylated variants of IgG have shown improved efficiency. One group found that cytotoxicity was enhanced by the lack of core-fucosylation, with a 50-fold increase in binding to FcγRIIIA (Shields et al, 2002). Recently another group (Nechansky et al, 2007) found that a defucosylated IgG1 not only showed higher *in vitro* activity than the fucosylated native mAb, but also showed no inhibition from a high concentration of endogenous IgG in serum, which is normally the cause of the lower *in vivo* activity due to competition of binding to FcγRIII on the effector cells. It is not only the core-fucose that has an affect on ADCC. One group found that *in vitro* remodelled mAbs (Rituxan and Herceptin), with a high content of bisecting GlcNAc, showed a 10-fold increase in ADCC activity, while on the other hand CDC stayed essentially unaffected (Hodoniczky et al, 2005).

Glycoengineering is not only a useful tool for mAbs, it can also improve the efficiency of other therapeutic proteins. Elliott et al. (2003) recorded increased activity and half-life of glycoengineered recombinant human erythropoietin, which normally have three N-glycosylation sites, Mpl ligand, which normally only has O-linked glycosylation, and leptin, which is normally absent of any glycans.

The glycoengineering concept has also opened up new opportunities in cell line selection; monoclonal antibodies with human glycosylation structures, rather than their ordinary high-mannose type of N-glycosylation, have been successfully expressed in yeast strains, such as *Pichia Pastoris* (Li et al, 2006). This has been achieved by complex engineering of the glycosylation pathways, as reviewed by Hamilton and Gerngross, 2007 and opens up possibilities of using a high-yielding well-known expression system.

From the above mentioned findings and many others with them, it has become obvious that glycoengineering, either *in vivo* through cell engineering or *in vitro* by glycan remodelling, can be a powerful way of improving the efficiency of

mAbs. An increased in vivo activity can in turn decrease the dose required for treatment. It can also increase the half-life of the mAb so that the frequency of administration can be reduced. Glycoengineering has been the focus of many studies over the last few years and will most likely be a feature of future mAb production.

### **1.8 Protein analysis**

It is of vital importance that proteins to be used therapeutically maintain their biological structure in order to function properly. During production and processing the product will be exposed to unfavourable and sometimes harsh conditions that can alter the structure or lead to other unwanted product versions, such as aggregates. In order to achieve pure clinical products and to ensure consistency from batch to batch, careful monitoring is required. There is a vast array of analytical techniques available for protein analysis, with the possibility to obtain a range of information regarding concentration, structure, conformation and function. Not all of these techniques can be applied or are useful at any stage. Some techniques can only give one piece of information, for example the molecular weight, while others give more. Careful consideration has to be taken to map the pieces together, obtain all the necessary information at any given stage and not bypass any important aspects. Another way to vary the analysis is to use enzymatic digestion. This will cleave the protein into smaller fragments where for certain applications some can be discarded and others further analysed to collect more specific data. There are a few enzymes that are used in this area. First there are the two already mentioned regarding the IgG molecule (see section 1.6.3); papain, cleaving IgG into Fc and the two Fab fragments, and pepsin, cleaving into several parts of the Fc fragment and the F(ab')<sub>2</sub> fragment. Another enzyme that can be used is trypsin (Jung et al, 2005; Yang and Hancock, 2004). Trypsin cleaves proteins C-terminally of lysine and arginine with a relatively high specificity and results in a number of smaller peptides that can be analysed with better resolution. If the interest lies in glycosylation of the protein, release of the oligosaccharide chains can be carried out using *endo*- or *exoglycosidases* that cleave internal glycosidic bonds or cleave monosaccharides from the non-reducing end of the oligosaccharide respectively. The glycans can then be further

analysed using advanced techniques such as matrix-assisted laser desorption/ionisation mass spectrometry (MALDI-MS) (Colangelo and Orlando, 2001). Here follows an overview of some of the different techniques available and their possible uses in monitoring protein structure during processing. Not all of these techniques have been utilised in the research presented here, instead some of them have been selected to cover the areas of interest.

### **1.8.1 Electrophoresis**

Gel electrophoresis is a simple method for protein analysis and is the most widely used in research. Gels can be made up of agarose or polyacrylamide, depending on the application and they can be of constant or gradient concentration depending on resolution required. Other attributes to use in the gel is a pH gradient (as in isoelectric focusing) or addition of sodium dodecyl sulphate (as in SDS-PAGE). This provides a variation in the technique where proteins can be separated on a different basis, for example size (mass) or electric charge.

#### ***1.8.1.1 SDS-PAGE***

Sodium dodecyl sulphate-polyacrylamide gel electrophoresis (SDS-PAGE) is the most widely used technique for qualitative analysis of proteins. SDS is an anionic detergent that denatures proteins by binding to the backbone structure and conferring a negative charge on the protein relative to the length of the polypeptide. SDS is often combined with a reducing agent, for example  $\beta$ -mercaptoethanol or dithiothreitol) and then used for a polyacrylamide gel that will separate proteins according to size. This method can be used to determine the molecular weight of a protein or to investigate the purity of a sample. It is a basic, very simple technique, but is not very sensitive so different glycoforms would not be separated. However, it can be useful when looking at different proteins (Yang and Hancock, 2004) or when looking at aggregation or heavy and light chain complexes of incompletely assembled antibodies.

#### ***1.8.1.2 Isoelectric focusing***

Isoelectric focusing (IEF) is an electrophoresis technique that separates proteins according to their isoelectric points (pIs) and not their size as with SDS-PAGE.

The technique utilises a gel (usually polyacrylamide, but agarose can also be used) with a pH gradient. The gel contains carrier ampholytes that when an electric field is applied, arrange themselves according to pI from the anode to the cathode, creating a pH gradient. The protein sample is applied and migrates through the gel according to its charge until it reaches the pH that corresponds to its pI, where its net charge is zero. This results in proteins being separated on the basis of charge.

### **1.8.1.3 2D-gels**

Gels can also be used for two-dimensional analysis. The technique provides the possibility to analyse proteins and polypeptides in complex sample mixtures. This approach combines separation according to charge through IEF with separation on the basis of size by SDS-PAGE. First the sample mixture is loaded onto an IEF gel, which is run as normal. The first gel is then loaded onto the top surface of the second SDS gel. Here a gel with either a constant or a gradient polyacrylamide concentration can be used, depending on the desired resolution (Hanash, 1998). SDS-PAGE is carried out and the gel is then stained, usually by silver-staining, in order to reveal the separated proteins and to interpret the gel. 2D gels can be used for comparing proteins from cells, tissues or body fluids and provides the possibility of direct sequencing of glycan structures from the gels (Rudd and Dwek, 1997). This provides usefulness in the monitoring of glycosylation patterns during production and processing of therapeutic glycoproteins and could detect possible modifications.

### **1.8.2 ELISA**

Immunoaffinity measurements are another way to analyse proteins. These utilise the fact that for example antibodies have affinity for other proteins and bind to them accordingly. The affinities will be stronger or weaker depending on the structure of the protein and can therefore be used to detect modifications, or combined with for example a colourimetric detection method it can be used for concentration measurements. The enzyme-linked immunosorbent assay (ELISA) is a technique widely used in protein analysis. It can be used for all molecules to which an antibody can bind and provides a way of quantification as well as

detection. There are two basic types of ELISA; direct and indirect, with the latter being the most commonly used, providing high sensitivity and specificity. This method utilises two antibodies binding to different parts of the protein to be analysed. The primary antibody is first coated onto a solid phase and then the sample is applied and left for incubation. The excess is washed off and a secondary antibody is added. This antibody binds to a different part of the sample and is labelled with for example horseradish peroxidase. The excess secondary antibody is washed off and a substrate is added, the response usually being detected colourimetrically.

### **1.8.3 Chromatography**

#### ***1.8.3.1 Protein A/G affinity chromatography***

Protein A/G affinity chromatography is used for antibody purification (see section 1.2) but can also be used as an analytical method when measuring antibody concentration and is often the method of choice for monitoring product formation during cell culture. As mentioned, protein A/G affinity chromatography is highly specific and will therefore bind to and extract antibodies exclusively, eliminating any other proteins and will therefore give a very accurate measure of the antibody concentration through absorbance measurements at 280 nm. Due to the different binding characteristics of protein A and protein G (Aybay, 2003), protein A is normally used for intact antibodies while protein G is more suitable for antibody fragments such as Fab.

#### ***1.8.3.2 Lectin affinity chromatography***

Affinity chromatography of antibodies, or any glycoproteins for that matter, can also be carried out using lectins. Lectins are proteins that bind carbohydrates and therefore glycoproteins. They are widely found in nature and can be extracted for example from plants like *Trichosanthes dioica* (Sultan et al, 2004), or animals like the snail *Cepaea hortensis* (Gerlach et al, 2005). Different lectins have different saccharide specificities; the first mentioned being Gal/GalNAc specific while the latter is GalNAc/GlcNAc specific. Lectins can be used both as a purification/separation technique (Demelbauer et al, 2005; Yang and Hancock, 2004) and in analytical methods (Fotinopoulou et al, 2003; Jankovic and

Kosanovic, 2005b). One group used a multi-lectin column where lectins were bound to agarose that was then packed in a chromatography column to monitor changes in glycosylation patterns by use of displacers specific to the lectins in the column (Yang and Hancock, 2005). The isolated glycopeptides can be analysed further by LC-MS/MS in this case, or other advanced analytical techniques such as MALDI-TOF (Demelbauer et al, 2005) or the elution profiles can be used on their own (Jankovic and Kosanovic, 2005a). Lectins can also be used in other analytical techniques than chromatography, for example surface plasmon resonance (SPR) and ELISA (see section 1.8.2) and can be a useful tool in oligosaccharide profiling during production of monoclonal antibodies (Fotinopoulou et al, 2003).

### ***1.8.3.3 Size Exclusion Chromatography***

Size exclusion chromatography (SEC) is a technique that separates molecules on the basis of size. The technique utilises a semi-permeable polymeric gel, into which smaller molecules can enter, while larger ones can not and will therefore go straight through the column and elute first. SEC is widely used for protein purification but is also a valuable analytical technique. It can be used for identification and quantification of proteins, as well as for quality control. It is a useful tool for detecting product variants, such as aggregates.

### ***1.8.3.4 HPLC***

High-performance (or high-pressure) chromatography (HPLC) is widely used in biotechnology to separate protein mixtures. As the name indicates the technique utilises high pressures to achieve very high resolution that can separate for example peptides of similar size and charge. For the purpose of protein separation, HPLC is mainly used in reversed phase. A non-polar stationary phase is used together with a moderately polar aqueous mobile phase. The analytes will be retained in the column and then eluted by adding a less polar mobile phase, most often acetonitrile or methanol, according to the hydrophobicity of the analytes. Trifluoroacetic acid or formic acid can be added to the mobile phase to aid separation. HPLC can be used for purification purposes, but is mainly used as an

analytical technique, where it is sometimes coupled to mass spectrometry (see section 1.8.4.1), but can also be used as a stand-alone method.

### **1.8.4 Mass spectrometry**

Mass spectrometry (MS) is a high-throughput system that offers rapid protein and peptide analysis with extremely high sensitivity. During the last couple of decades the development of so called soft ionisation techniques, such as electrospray ionisation (ESI) and matrix-assisted laser desorption/ionisation (MALDI) has made MS a more and more popular technique. It shows great usefulness in the analysis of glycoproteins (Dell and Morris, 2001) and can analyse intact molecules or peptides. All MS techniques work on the same general basis; a detector measures the mass to charge ratio ( $m/z$ ) of an ionised sample. Mass is given in Daltons and the fundamental unit for charge (the charge of an electron) is used. The way ionisation is achieved is generally what differs in the different methods, as already mentioned.

#### **1.8.4.1 LC/ESI-MS**

In ESI-MS, the liquid sample is introduced into the ion source through a capillary to which voltages are applied, and also to a counterelectrode and the focusing optics, resulting in an aerosol. These highly charged microdroplets travel until they hit the drying gas where they transform into gaseous ions. These ions have a charge distribution that is proportional to the number of ionisable groups in the analyte. ESI-MS is a popular tool for analysis of glycoproteins. (It is extremely sensitive and can pick up structural changes such as deamidation Hagmann et al, 1998) when used with data from other analytical techniques (in this case IEF).

Samples can be injected directly into the mass spectrometer or, more commonly; it can be coupled with liquid chromatography (LC). LC-MS can for example be used for characterisation of intact recombinant antibodies and to study their heterogeneity (Dillon et al, 2004; Le and Bondarenko, 2005) and for qualitative characterisation of glycans (Saba et al, 2002). LC-MS can also be used for peptide mapping and has been of use for localisation of the glycosylation site (Hagmann et al. 1998) when comparing therapeutic proteins and their glycosylation patterns

(Ohta et al, 2002) and for characterisation and comparison of variants of recombinant proteins (Jung et al, 2005). LC-ESI-MS can also detect heterogeneity due to incomplete proteolysis or the modification of an amino acid (Stimson et al, 1999). RP-HPLC-ESI-MS was used by Wan et al. (2001) in the development of a method to investigate the heterogeneity in glycosylation of a recombinant antibody and the quantification of the different glycoforms. The HPLC was used to desalt and purify the samples and to separate heavy and light chain fragments. The sensitivity of the equipment also provides efficient analysis at low concentrations; only picomoles are required for good detection (Carr et al, 1993).

Mass spectrometry can also be utilised in tandem, i.e. MS/MS. The sample is analysed by MS, specific ions are then isolated and another round of MS is carried out. This technique provides a way of sequencing, confirming the primary structure that can be deduced from the first MS analysis (Demelbauer et al, 2005; Jung et al, 2005). LC-MS/MS can be used to specifically and selectively identify glycopeptides (Carr et al, 1993) and for structural analysis and assignment of isomers (Kawasaki et al, 2000).

#### ***1.8.4.2 MALDI-TOF***

The technique of laser desorption (LD) has been around for several decades, but it was only in the late eighties that development of MALDI took place (Karas et al, 1985). The basis of LD is that ions are produced by irradiating the sample with a high-intensity laser pulse. MALDI makes use of a matrix and is therefore applicable to proteins of a much higher molecular weight than LD. The matrix has to be volatile, e.g. 2,5-dihydroxybenzoic acid (Saba et al, 2002) or 2,4,6-trihydroxyacetophenon (Demelbauer et al, 2005) and is applied to the sample plate together with the sample and then dried. When the laser beam hits the solid sample preparation the matrix helps to excite the analyte molecules and then evaporates leaving the ionised molecule travelling to the detector in a time depending on its  $m/z$  ratio, hence the name MALDI-TOF (time-of-flight). This technique can be used to study glycosylation patterns in proteins and becomes very effective and specific when applied after release of glycans by glycosidases, as already mentioned (Colangelo and Orlando, 2001). MALDI is also suitable for semiquantification since the peak height or area is proportional to the amount of

carbohydrate in the sample (Saba et al, 2002). However, it is pointed out that if this technique is to be used for quantification, careful consideration has to be taken to the chemical properties of the analytes in the sample mixture, since oligosaccharides differing with certain monosaccharides in structure will have different ionisation efficiencies.

#### **1.8.4.3 SELDI-MS**

As mentioned, the use of MS has proved very successful for detailed analysis of biological compounds. However, when analysing samples from complex biologic materials, these often contain many different molecules and a high degree of salts, so there is a need for time-consuming and labour-intensive purification methods such as centrifugation, filtration or liquid chromatography due to the sensitivity of the MS equipment. Recent advances in surface-enhanced laser desorption/ionisation (SELDI) offers the possibility to bypass extensive sample preparation. As the name suggests, SELDI works on the same basic principles as MALDI; a laser beam provides the energy to ionise analytes from a solid sample on a sample plate. However, in SELDI, the surface plays an important role in the extraction of the analyte. For further details see review by Merchant and Weinberger, 2000. Commercially, SELDI is provided by Ciphergen's ProteinChip<sup>®</sup> Array System. The chips exhibit chromatographic capacity with binding on different basis: IMAC (immobilised metal affinity capture), ionic, reversed phase or hydrophobic or normal phase. A sample is applied to each one of the spots on the array and then washed with different buffers in order to facilitate the isolation of the analyte. This *in situ* technique provides the advantage of minimised sample loss when only small amounts are available. It also provides the possibility of working with relatively impure samples from various stages of the process of production and purification of therapeutic proteins.

#### **1.8.4.4 ESI-TOF**

Above are detailed some of the most commonly used mass spectrometry methods. These are by no means all of them and there are many variations on the basic techniques where different manufacturers combine different ionisation techniques

with different detectors. One example is electrospray ionisation coupled with a time-of-flight detector (ESI-TOF). This is the technique we used in the studies presented here, since it allows for analysis of the intact mAb. The principles of this technique are outlined in Figure 1.12.

## ***1.9 Aim***

The aim of the research carried out was to develop a combination of experimental techniques and protocols with the ultimate output of a tool-kit for in-process determination of structure and conformation of biopharmaceuticals such as mAbs.

## ***1.10 Objectives***

In order to reach the aim of the research a series of concerns around the production and purification of therapeutic proteins, such as mAbs, were raised that needed investigation:

- Would the method of harvesting impact the detailed structure of the mAb?
- Would there be any knock-on effects on the subsequent purification process due to intracellular material released due to shear?
- Are there other parameters during harvest that could impact the mAb structure, e.g. holding time and temperature?
- Is it possible to use at-line monitoring of mAb structure, providing results in hours instead of days?

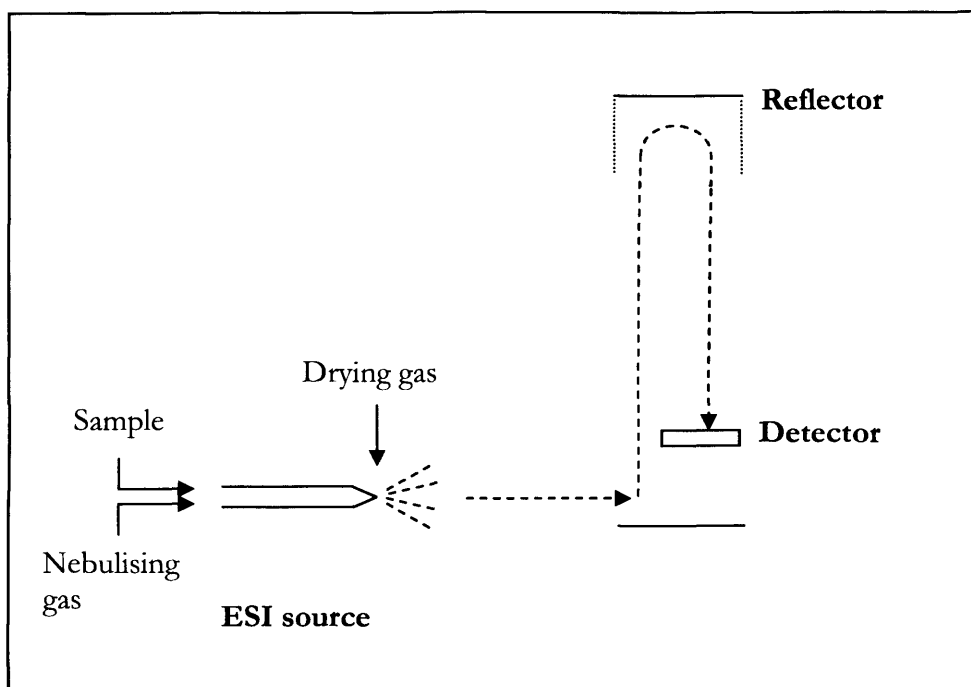


**Figure 1.12 Basic schematic of ESI-TOF**

The sample is introduced into a capillary that is situated inside the electrospray source. A high voltage is applied across the capillary resulting in the sample transforming into highly charged droplets that leave the capillary nozzle. Around the capillary is the nitrogen nebulising gas, which helps direct the emerging spray towards the analyser. At the end of the nozzle, the nitrogen drying gas is applied. This aids solvent evaporation of the droplets so that single ions evaporate from the droplets and can be introduced into the analyser that is kept under high vacuum. The vacuum is applied to avoid any interference of the flight path by air. The ions then travel through the flight tube and are sorted according to their mass-to-charge ratio. The heavier the ion, the longer it will take to reach the detector.

## 2 Materials and Methods

All reagents used were purchased from Sigma-Aldrich (Dorset, England) unless otherwise stated.

### 2.1 Cell culture

GS-CHO cells producing a chimeric IgG4 monoclonal antibody B72.3 were recultured in a fed-batch, 10L airlift vessel, working volume 8.5 L, at 37°C and pH 6.7-7.0. To monitor growth, cell count and viability were measured using a Vi-CELL™ (Beckman Coulter, Inc., Fullerton, CA, USA) while product formation was measured using protein A affinity chromatography. Three separate fermentations were carried out, providing samples for the different studies as indicated in results chapters.

### 2.2 Centrifugation for clarification

Samples were centrifuged (Eppendorf 5810R, Eppendorf, Cambridge, UK) at 200 x g for 20 min to separate cells from the product-containing supernatant. The supernatant was filtered through a 0.45 µm syringe filter (Low Protein Binding Durapore®, PVDF, Millipore, Co. Cork, Ireland) before storage at -20°C until further analysis. Cells were washed in PBS, centrifuged again at 200 x g for 10 min, liquid discarded and cells then stored at -80°C until further processing. Samples that were sheared (see section 2.3) before clarification were centrifuged at 3,200 x g for 40 min in order to achieve sufficient separation.

### 2.3 Shear

For the purpose of studying the effect of shear during the first clarification step after fermentation, a USD shear device was used (Levy et al, 1999). The device consists of a stainless steel chamber 12 mm high with a diameter of 50 mm and inside it a 1mm thick rotating disc of diameter 40 mm. The sample volume used was 20 mL and the standard conditions of shearing at 15,000 rpm for 30 s were used except where stated otherwise. When studying the effect of different shearing conditions the following four sets of conditions were used; control with no shear, 15,000 rpm for 30 s, 15,000 rpm for 90 s, and 20,000 rpm for 30 s. The

tip speed can be related to the maximum energy dissipation rate experienced, with 15,000 rpm corresponding to a maximum energy dissipation rate in the region of  $10^6 \text{ W kg}^{-1}$  and 20,000 rpm corresponds to  $10^7 \text{ W kg}^{-1}$ . Various maximum energy dissipation rates and their corresponding large-scale centrifuge are listed in Table 2.1, where it can be seen that the former of the two shear rates chosen corresponds to the shear experienced in a large-scale multichamber-bowl centrifuge under non-flooded conditions. The faster tip speed was chosen to investigate the impact of even higher energy dissipation rates to examine the effects of more extreme shear on the protein structure and conformation. In order to study the effect of shear on both the broth and the pure antibody in solution, some samples were sheared before centrifugation and some after as will be explained further at a later stage.

## ***2.4 Holding***

When studying the effects of holding time and conditions in between stages, samples of broth were held in 50 mL centrifuge tubes at two different temperatures;  $+4^\circ\text{C}$  and  $+37^\circ\text{C}$ . Samples were then removed at certain times; 0, 2 h, 4 h and 24 h, clarified as above (see section 2.2) and then purified using protein A affinity chromatography or sheared as described previously (see section 2.3) and then clarified and purified.

## ***2.5 Disruption of cells for purification of intracellular material***

Cells were resuspended in PBS pH 7.4 after thawing. They were disrupted using a Lab 40 high-pressure homogeniser (Gaulin Micron Lab40, APV Gaulin, Lubeck, Germany) for complete release and then centrifuged (GS-6R centrifuge, Beckman Coulter) at  $6,400 \times g$  for 45 min. The debris was discarded and the mAb containing supernatant was filtered ( $0.45\mu\text{m}$  Durapore, Millipore) and then purified using protein A chromatography.

## ***2.6 Protein A affinity chromatography for purification***

Both intra- and extracellular material was purified using protein A affinity chromatography. A 1 mL HiTrap rProteinA Fast Flow column (GE Healthcare UK Ltd, Buckinghamshire, England) was used together with an ÄKTA™explorer system and UNICORN™ software (both GE Healthcare). A sample (10 mL of

<b>Maximum energy dissipation rate (W kg<sup>-1</sup>)</b>	<b>Large-scale equivalent</b>
2 x 10 <sup>5</sup>	Disc stack centrifuge operated at 15-80 L/hr and at 165 rps
6 x 10 <sup>5</sup>	Multichamber-bowl centrifuge under flooded conditions, operated at 22 L/hr and at 167 rps
12 x 10 <sup>5</sup>	Multichamber-bowl centrifuge under non-flooded conditions, operated at 22 L/hr and at 167 rps
14 x 10 <sup>5</sup>	CARR Powerfuge™ operated at 20 L.hr and at 255 rps

**Table 2.1 Maximum energy dissipation rates of large-scale centrifuges**

*The above table shows the maximum energy dissipation rate experienced in various large-scale centrifuges (Boychyn et al, 2004). The values described in the right hand column represent the flow rates and the bowl rotational speeds of the centrifuges.*

supernatant or 20 mL of clarified homogenised cells) was loaded onto the column using 10 mM PBS, pH 7.4, at a flow rate of 1 mL/min. Non-binding material was washed off using five column volumes of loading buffer and gradient elution then carried out with 10 mM sodium citrate, pH 3, from 0 to 100 % over 15 min. The eluted material was collected and immediately neutralised by the addition of 1M Tris, pH 9 and protein concentration measured by absorbance at 280 nm (Genesys 10vis, Thermo Scientific, Waltham, MA, USA). Samples were then diluted with 0.1 M sodium acetate, pH 6.4, to a concentration of ~1 mg/mL.

## ***2.7 Sample modification***

### **2.7.1 Deglycosylation**

For deglycosylation of the mAb, a denaturation step was first carried out by addition of 0.2% SDS in 100 mM mercaptoethanol to the protein solution (1 mg/ml), which was then heated to 100°C for 10 min. After the denaturation step 4 units of PNGase F in 5mM potassium phosphate, pH 7.5, was added to the protein solution and kept at 37°C overnight.

## ***2.8 Antibody profiling by gel electrophoresis***

### **2.8.1 Lab-on-a-chip**

Samples were analysed using an Agilent 2100 bioanalyzer (Agilent Technologies, Santa Clara, CA, USA), protein 200 assay, non-reducing conditions, following manufacturer's recommendations. The bioanalyzer is a lab-on-a-chip technology separating proteins on the basis of molecular weight.

## ***2.9 Mass spectrometry***

For detailed analysis of the molecular structure of the mAb, as well as the overall composition of the product stream, HPLC coupled to electrospray-time-of-flight mass spectrometry (ESI-TOF) was used.

### 2.9.1 LC/MSD-TOF

For analysis of intact mAbs, LC/MSD-TOF (Agilent Technologies) was used. A Poroshell 300-SB C18 reverse phase column (75 mm x 1 mm i.d., 5  $\mu$ m pore size, Agilent Technologies) was injected for online desalting with 2  $\mu$ L sample at 1  $\mu$ g/ $\mu$ L, heated to 70°C and the product eluted using a gradient starting at 5 % (v/v) acetonitrile in 5 % (v/v) formic acid in water rising to 95 % over 10 min with a flow rate of 200  $\mu$ L/min. Proteins eluting from the column were ionised by an electrospray source, and the ions were analysed using a time-of-flight mass spectrometer. For the samples from the first fermentation, the drying gas temperature was set to 300°C at 8L/min. The protocol was reviewed and further optimised for the samples from the second and third fermentation in order to minimise noise levels and to allow for a deeper analysis. Therefore the gas temperature was increased to 350°C at 11 L/min. Agilent BioConfirm Software (Version A.02.00) was used for deconvolution of spectra. The deconvolution was carried out using the following parameters; step mass 1 Da, signal-to-noise threshold 5, isotope width 30 Da, and average mass 50 % of the peak.

## 3 Structural analysis of IgG

### 3.1 *Basic structure and sequence*

The subject of this research was a monoclonal immunoglobulin G4 (IgG4). The IgG molecule is built up of two heavy and two light chains linked together by disulphide bonds. This structure forms the basis of the molecular weight, which depends on the amino acid composition. The amino acid sequence is translated from the mRNA that has in turn been transcribed from the DNA nucleotide sequences of the heavy and light chains (Figure 3.1 and Figure 3.2 respectively). The sequence is made up of the nucleotides adenosine (A), cytosine (C), guanine (G) and thymine (T) (uracil (U) in the case of RNA). Three nucleotides together form a codon, which is transcribed and translated into an amino acid.

Figure 3.3 and Figure 3.4 show the translated amino acid sequence for the heavy and light chain respectively. The signal sequence has been cleaved off and the stop codon is no longer included so that the first and last amino acids of the heavy chain are glutamine and lysine respectively and of the light chain are aspartic acid and cysteine.

### 3.2 *Modifications*

After the protein backbone of IgG has been formed, post-translational modifications take place, the main one being glycosylation (see section 1.7). IgG has one site of *N*-linked glycosylation at asparagine 297 on each of the heavy chains. The glycosylation is of the complex type and can therefore contain all or some of the following monosaccharides; *N*-acetylglucosamine, mannose, glucose, galactose, fucose and sialic acid (*N*-acetylneuraminic acid). The structure is most commonly of a core-fucosylated biantennary structure as can be seen in Figure 3.5. Each finished glycan structure is built up of several monosaccharides; each of which contributes different masses (Table 3.1) to the basic molecular weight of the IgG creating a heterogeneous population.

```

ATGGAATGGA GCTGGGTCTT TCTCTTCTTC CTGTCAGTAA CTACAGGTGT
CCACTCCCAG GTTCAGCTGC AGCAGTCTGA CGCTGAGTTG GTGAAACCTG
GGGCTTCAGT GAAGATATCC TGCAAGGCTT CTGGCTACAC CTTCACTGAC
CATGCTATTC ACTGGGCGAA GCAGAAGCCT GAACAGGGCC TGGAATGGAT
TGGATATATT TCTCCCGGAA ATGATGATAT TAAGTACAAT GAGAAGTTC A
AGGGCAAGGC CACACTGACT GCAGACAAAT CCTCCAGCAC TGCCTACATG
CAGCTCAACA GCCTGACATC TGAGGATTCT GCAGTGTATT TCTGTAAAAG
ATCGTACTAC GGCCACTGGG GCCAAGGCAC CACTCTCACA GTCTCCTCAG
CCTCCACCAA GGGCCCATCC GTCTTCCCCC TGGCGCCCTG CTCCAGGAGC
ACCTCCGAGA GCACAGCCGC CCTGGGCTGC CTGGTCAAGG ACTACTTCCC
CGAACC GGTTGTCGT GGAACCTCAGG CGCCCTGACC AGCGGCGTGC
ACACCTTCCC GGCTGTCCTA CAGTCTCAG GACTCTACTC CCTCAGCAGC
GTGGTGACCG TGCCCTCCAG CAGCTTGGGC ACGAAGACCT ACACCTGCAA
CGTAGATCAC AAGCCCAGCA ACACCAAGGT GGACAAGAGA GTTGAGTCCA
AATATGGTCC CCCATGCCCA TCATGCCCAG CACCTGAGTT CCTGGGGGGA
CCATCAGTCT TCCTGTTCCC CCAAAAACCC AAGGACACTC TCATGATCTC
CCGACCCCT GAGGTCACGT GCGTGGTGGT GGACGTGAGC CAGGAAGACC
CCGAGGTCCA GTTCAACTGG TACGTGGATG GCGTGGAGGT GCATAATGCC
AAGACAAAGC CGCGGGAGGA GCAGTTCAAC AGCACGTACC GTGTGGTCAG
CGTCCTCACC GTCCTGCACC AGGACTGGCT GAACGGCAAG GAGTACAAGT
GCAAGGTCTC CAACAAAGGC CTCCCCTCCT CCATCGAGAA AACCATCTCC
AAAGCCAAAG GGCAGCCCCG AGAGCCACAG GTGTACACCC TGCCCCCATC
CCAGGAGGAG ATGACCAAGA ACCAGGTCAG CCTGACCTGC CTGGTCAAAG
GCTTCTACCC CAGCGACATC GCCGTGGAGT GGGAGAGCAA TGGGCAGCCG
GAGAACAAC TACAAGACCAC GCCTCCCCTG CTGGACTCCG ACGGCTCCTT
CTTCCCTTAC AGCAGGCTAA CCGTGGACAA GAGCAGGTGG CAGGAGGGGA
ATGTCTTCTC ATGCTCCGTG ATGCATGAGG CTCTGCACAA CCACTACACA
CAGAAGAGCC TCTCCCTGTC TCTGGGTAAA TGA

```

**Figure 3.1 Nucleotide sequence of the cB72.3 heavy chain**

*A; adenosine, C; cytosine, G; guanine, T; thymine. The sequence begins with the start codon ATG, which is part of the 57 nucleotide long signal sequence. This is the highlighted region, which is later cleaved off so that the first amino acid is glutamine (Q) from the CAG codon and the last amino acid is lysine (K) from the AAA codon, followed by the end codon TGA.*

```

ATGAGTGTGC CCACTCAGGT CCTGGGGTTG CTGCTGCTGT GGCTTACAGA
TGCCAGATGT GACATCCAGA TGACTCAGTC TCCAGCCTCC CTATCTGTAT
CTGTGGGAGA AACTGTCACC ATCACATGTC GAGCAAGTGA GAATATTTAC
AGTAATTTAG CATGGTATCA ACAGAAACAG GGAAAATCTC CTCAGCTCCT
GGTCTATGCT GCAACAAACT TAGCAGATGG TGTGCCATCA AGGTTTCAAGT
GCAGTGGATC GGGCACACAG TATTCCCTCA AGATCAACAG CCTGCAGTCT
GAAGATTTTG GGAGTTATTA CTGCCAACAT TTTTGGGGTA CTCCGTACAC
GTTCCGGAGGG GGGACCAGGC TGGAAATAAA ACGTACGGTG GCTGCACCAT
CTGTCTTCAT CTTCCCAGCA TCTGATGAGC AGTTGAAATC TGGAAGTACC
TCTGTTGTGT GCCTGCTGAA TAACTTCTAT CCCAGAGAGG CCAAAGTACA
GTGGAAGGTG GATAACGCC TCCAATCGGG TAACTCCCAG GAGAGTGTC
CAGAGCAGGA CAGCAAGGAC AGCACCTACA GCCTCAGCAG CACCCTGACG
CTGAGCAAAG CAGACTACGA GAAACACAAA GTCTACGCCT GCGAAGTCAC
CCATCAGGGC CTGAGCTCGC CCGTCACAAA GAGCTTCAAC AGGGGAGAGT
GTTAG

```

**Figure 3.2 Nucleotide sequence of the cB72.3 light chain**

The sequence begins with the start codon ATG, as for the heavy chain, but the highlighted signal sequence is in this case 60 nucleotides long so that the first amino acid is aspartic acid (D) from the codon GAC and the last amino acid is cystein (C) from the codon TGT, followed by the stop codon TAG.

```

QVQLQQSDAE LVKPGASVKI SCKASGYTFT DHAIHWAKQK PEQGLEWIGY
ISPGNDDIKY NEKFKGKATL TADKSSSTAY MQLNSLTSED SAVYFCKRSY
YGHWGQGTTL TVSSASTKGP SVFPLAPCSR STSESTAALG CLVKDYFPEP
VTVSWNSGAL TSGVHTFPAV LQSSGLYSLS SVVTVPSSSL GTKTYTCNVD
HKPSNTKVDK RVESKYGPPC PSCPAPPEFLG GPSVFLFPPK PKDTLMISRT
PEVTCVVVDV SQEDPEVQFN WYVDGVEVHN AKTKPREEQF NSTYRVVSVL
TVLHQDWLNG KEYKCKVSNK GLPSSIEKTI SKAKQPREP QVYTLPPSQE
EMTKNQVSLT CLVKGFPYPSD IAVEWESNGQ PENNYKTPPP VLDSGDSFFL
YSRLTVDKSR WQEGNVFSCS VMHEALHNHY TQKLSLSLGLG K

```

**Figure 3.3 Amino acid sequence of the heavy chain**

The codons have now been transcribed and translated, from the nucleotide sequence in Figure 3.1, to the amino acid sequence above. The signal sequence has been cleaved off so that what can be seen here is the actual heavy chain that is used for assembly of the IgG; however it is still subject to further modifications (see section 3.2).

```

DIQMTQSPAS LSVSVGETVT ITCRASENIY SNLAWYQQKQ GKSPQLLVYA
ATNLADGVPS RFGSGSGTQ YSLKINSLQS EDFGSYQCQH FWGTPYTFGG
GTRLEIKRTV AAPSVFIFPP SDEQLKSGTA SVVCLLNNFY PREAKVQWKV
DNALQSGNSQ ESVTEQDSKD STYLSLSTLT LSKADYEKHK VYACEVTHQG
LSSPVTKSFN RGEK

```

**Figure 3.4 Amino acid sequence of the light chain.**

The codons have here been transcribed and translated, from the nucleotide sequence in Figure 3.2, to the amino acid sequence and the signal sequence has been cleaved off.

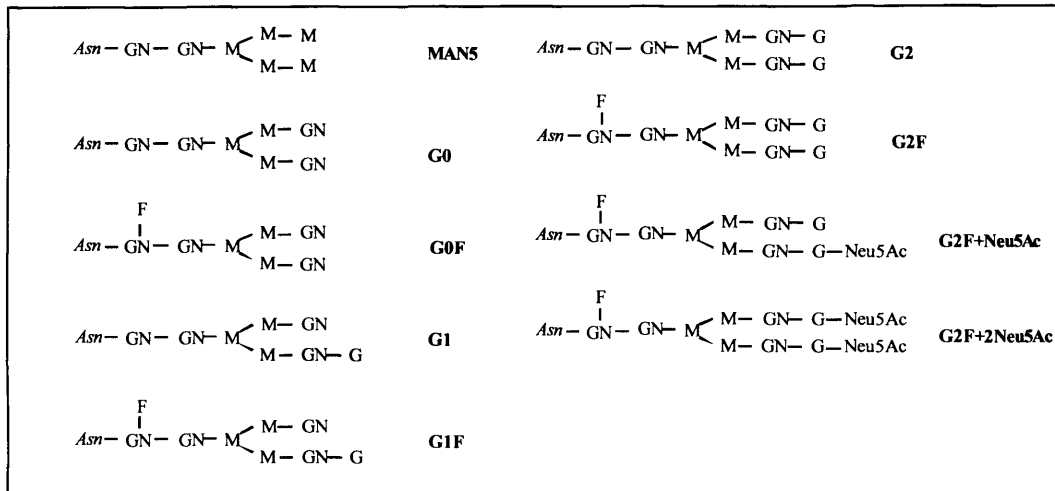


**Figure 3.5 Glycosylation structures in IgG**

Asn; asparagine 297, GN; N-acetylglucosamine, F; fucose, M; mannose, G; galactose. Glycosylation in IgG is of the complex type with variable glycan structures. Most common is the core-fucosylated biantennary structure, as can be seen here, built up of two N-acetylglucosamine residues attached to asn297, followed by three mannose residues as the general core structure. Fucose may be attached to the first N-acetylglucosamine. Attached to the mannose are two more GN residues followed by none, one or two galactose. Sialylation at the galactose residues can also occur, but to a lesser extent. Problems with detection and quantification of sialylated versions occur since loss of sialic acid residues can occur.

Glycan	MW (Da)
Fucose (F)	146
Galactose (G)	162
Mannose (M)	162
N-Acetylglucosamine (GN)	203
Sialic acid (Neu5Ac)	291

**Table 3.1 Average masses of the glycan building blocks**

Galactose and mannose are both hexoses, while fucose is a hexose deoxy sugar (a hydroxyl group has been replaced with a hydrogen) and therefore of a lower molecular weight. N-acetylglucosamine is an eight carbon derivative of glucose while sialic acid is a derivative of the nine carbon monosaccharide neuraminic acid.

In addition to glycosylation, IgG is prone to other modifications. One example is the proteolytic degradation of the C-terminal lysine residues (see section 1.6.5). Each heavy chain of the IgG has a lysine residue at its C-terminal that can be cleaved off, so that theoretically it is possible to end up with a population of mAbs with none, one or two C-terminal lysine residues, resulting in a shift in the molecular weight of -128 Da per clipped lysine.

Another common modification of IgG is the cyclization of *N*-terminal glutamine to pyroglutamic acid (see section 1.6.5). Each heavy chain has a glutamine (Q) residue at its *N*-terminal, which can be converted into pyroglutamic acid (pE) with the loss of an amino group, causing the mass shift of -34 Da (-17 Da per glutamic acid). This causes further heterogeneity in the mAb population where again none, one or two modifications can take place.

These are some of the main modifications that can be detected when analysing intact mAbs on LC/MSD-TOF. Taking them all into consideration, it is obvious a large amount of different combinations can occur with a wide range of different masses, which are summarised in Table 3.2. What is not known is if all of these different structures can be present at the same time, or if some of them are more favoured than others. From experience, it seems that some structures are more common than other, especially when it comes to glycosylation profiles of mAbs (Rehder et al, 2006) where three or four main glycan structures are present rather than a more widely heterogeneous population.

	Ab	MAN5	G0	G0F	G1	G1F	G2	G2F	G2F+sial	G2F+2sial
<b>2K, Q</b>	143867	146301	146465	146757	146789	147081	147113	147405	147987	148569
<b>2K, pE</b>	143833	146267	146431	146723	146755	147047	147079	147371	147953	148535
<b>1K, Q</b>	143739	146173	146337	146629	146661	146953	146985	147277	147859	148441
<b>1K, pE</b>	143705	146139	146303	146595	146627	146919	146951	147243	147825	148407
<b>0K, Q</b>	143611	146045	146209	146501	146533	146825	146857	147149	147731	148313
<b>0K, pE</b>	143577	146011	146175	146467	146499	146791	146823	147115	147697	148279

**Table 3.2 Calculation of theoretical masses of the IgG used in the study**

The masses listed in the table result from heterogeneity in the glycosylation pattern together with a few other commonly occurring modifications. The first column indicates what modifications the mAb has been subject to. The native mAb has a lysine residue (K) at the C-terminal of each heavy chain, but these are prone to being cleaved off resulting in mAbs with two, one or no terminal lysines (2K, 1K or 0K) on the heavy chains, corresponding to a mass shift of -128 Da per lysine residue (see Figure 1.6). The other modification refers to the cyclization of the N-terminal glutamine (Q) to pyroglutamic acid (pE) which corresponds to a mass shift of -34 Da (see Figure 1.7), accounting for even more variants as shown. The top row shows the nature of the glycan structure (see Figure 3.5); for sake of demonstration the table shows the masses of the mAb with the two glycan structures being the same on both heavy chain, so the top row should read (G0F)<sub>2</sub> etc. From this point forward, the structures of the mAbs will be referred to in coherence with the headings of this table, e.g. (G0)<sub>2</sub>-0K-Q, (G1F)<sub>2</sub>-1K-pE. When the glycan structures on the heavy chains of the same mAb are different, e.g. one is G0F and the other is G1F, the structure will be referred to as G0F/G1F-0K-pE etc.

### ***3.3 HL complexes***

The IgG molecule is built up by two heavy and two light chains linked together by disulphide bonds. The heavy and light chains are synthesized separately and then assembled into the covalently linked IgG tetramer structure  $H_2L_2$  of a mass of approximately 146,000 Da. The IgG subclasses differ in their structure of the hinge region, which has an effect on their ability to create these disulphide bonds between the two heavy chains. The structure at the hinge region of the IgG4 subclass causes a non-covalently linked  $H_2L_2$  tetramer to be co-secreted with the covalently linked tetramer (see section 1.6.4). The tetramers lacking the disulphide bonds between the heavy chains can disassociate into HL dimers, resulting in complexes at half the mass of the intact mAb, i.e. approximately 73,000 Da.

The mAb used in this research is an IgG4, serving as a model antibody, and will therefore be subject to the presence of HL dimers as will become evident when looking at the results.

### ***3.4 Analysis of mass spectra***

Mass spectrometric analysis of intact mAbs creates complex data that needs to be processed and interpreted. This was carried out with the help of Agilent's BioConfirm software (version A.02.00). The data can be viewed in different forms. Firstly a total ion chromatogram (TIC) is produced (Figure 3.6) from the online desalting where the mAb is captured by the chromatography column through hydrophobic interactions and then released to be introduced into the ionisation source. This records all the ions present in one signal and is therefore not very informative, but can be a useful tool to confirm that the run is working properly.

Secondly a mass spectrum is created for the compound (Figure 3.7). This is a plot of intensity against the mass-to-charge ratio ( $m/z$ ) where all the ions are recorded. Deconvolution is then carried out with the help of the software in order to create a

plot of intensity against molecular weight (Daltons). The initial spectrum contains a distribution of multiply charged ions. The deconvolution algorithm uses the data to calculate the charge states of the ions and the molecular weight of the analyte. The plot of the deconvoluted spectrum can be viewed as a whole profile (Figure 3.8) where all species in the sample can be seen. However, to get more detailed information regarding the molecular weight the plot can be zoomed in to focus on one area in particular, for example the intact mAb (Figure 3.9). This provides the molecular weights of all the different variants in this group showing the heterogeneity of the sample, especially regarding the various glycoforms.

Once the mass spectrum has been created showing the molecular weights of the variants, the data needs to be interpreted. As can be seen from Figure 3.9 the data is rather complex, although some main trends can be observed. The peaks represent different glycoforms, but also different modifications such as C-terminal lysine cleavage and N-terminal glutamine cyclization. The different peaks need to be matched up with the mass variations displayed in Table 3.2. To illustrate the evaluation process when assigning the peaks in the spectra to different structures, the spectrum in Figure 3.9 has been used as an example and the peaks have been numbered as can be seen in Figure 3.10, for easier referral.

A first attempt to assign structures to the different peaks was made by looking at the masses of the peaks and then simply trying to find masses in Table 3.2 that matched up to the measured ones, as detailed in Table 3.3. This way of interpretation leaves a few peaks unidentified as well as several peaks with a large mass error. The data from this type of mass spectrometry on such a large molecule is not exact, but more likely to have an error of up to about  $\pm 5$  Da (from experience in these studies), which has to be kept in mind when interpreting the results. The peaks that are possible to assign also appear to be a bit random, with a mixture of the number of C-terminal lysine and N-terminal glutamine residues. It seems this assignation method falters in several ways. Instead the mass spectrum was viewed as a whole and patterns became obvious. The main peaks are all approximately 162 Da apart, which corresponds to the mass of a galactose or a mannose. Looking closer at the other peaks, they are all showing patterns with set distances from the main peaks and this was used as a basis for the spectral

interpretation. Figure 3.11, Figure 3.12, Figure 3.13 and Figure 3.14 show the thought process where one set of peaks has been identified in each one of the figures for clarity. First the main peaks were identified in Figure 3.11, where the peaks correspond to the same basic mAb structure with both C-terminal lysine residues cleaved off (0K) and both N-terminal glutamine residues converted to pyroglutamic acid (pE). The peaks are approximately 162 Da apart, corresponding to a galactose residue, resulting in the different glycan structures as detailed in Table 3.4, with the exception of peak number one, which is 147 Da smaller than the following peak, corresponding to the absence of the core-associated fucose. The mass difference of 162 Da also corresponds to the mass of a mannose; however the mass patterns do not fit with a high-mannose structure and is therefore ruled out. The second set of peaks, identified in Figure 3.12, also differ by 162 Da, corresponding to the different glycan structures listed in Table 3.5. The peaks in this set also form a pattern with the main peaks in Figure 3.11; each one with a mass of +34 Da compared to the associated peak. This corresponds to the difference between two pyroglutamic acid residues and two glutamine residues, which indicates that the basic mAb structure of the second set of peaks has both C-terminal lysine residues cleaved off (0K) but the N-terminal glutamine residues (Q) have not been converted. The third set of peaks, identified in Figure 3.13, again differ by 162 Da, corresponding to the glycan structures described in Table 3.6. The peaks again form a pattern with the main peaks in Figure 3.11, but in this case they are shifted by +128 Da. This corresponds to the mass of a lysine residue, meaning the basic mAb structure of the third set of peaks have both N-terminal glutamine residues converted (pE), as with the first set, but still have one of the two C-terminal lysine residues intact (1K). The fourth and last set of peaks, identified in Figure 3.14, are also 162 Da apart, corresponding to the glycan structures in Table 3.7. The peaks in this set are shifted from the main peaks by +256 Da. This corresponds to the mass of two lysine residues, so the basic mAb structure in this case is determined to have the N-terminal glutamine residues converted (pE), but still have both C-terminal lysines intact (2K).

The one peak that has not been identified here using this method is peak number two. It could be expected that this peak would be linked to peak number one in the same way as the third set of peaks were associated with the other main peaks, i.e.

with a mass difference of +128 Da. However this is not the case, the difference is +94 Da, and by the assignment method used here the identity of this peak still remains unclear. Going back to the glycan structures observed by Bailey et al. (2005; see Figure 1.11), this could give an explanation to the mass of this peak, with a few different possible combinations, however this would open up countless possible structures and since these structures have not been commonly observed, the peak assignment method from Figure 3.11-3.14 has been adhered to. This means there are several possible explanations to the appearance of peak number two, but with the method used here it was left unidentified. This has not been a major concern in the work presented here, since the spectra have mainly been compared in order to spot possible differences and trends. In addition, the peaks of most importance are the main peaks identified in Figure 3.11, since they are the most prominent and therefore the main contributors to the efficacy of the mAb.

The ESI-TOF analysis has proved to be a very useful tool in the analysis of intact mAb. Despite the size of the protein the instrument can detect the masses of the sample with great accuracy. Looking at the discrepancies in the sample spectrum in Figure 3.10 the average error, when comparing the measured mass with the theoretical mass, is less than 30 ppm.

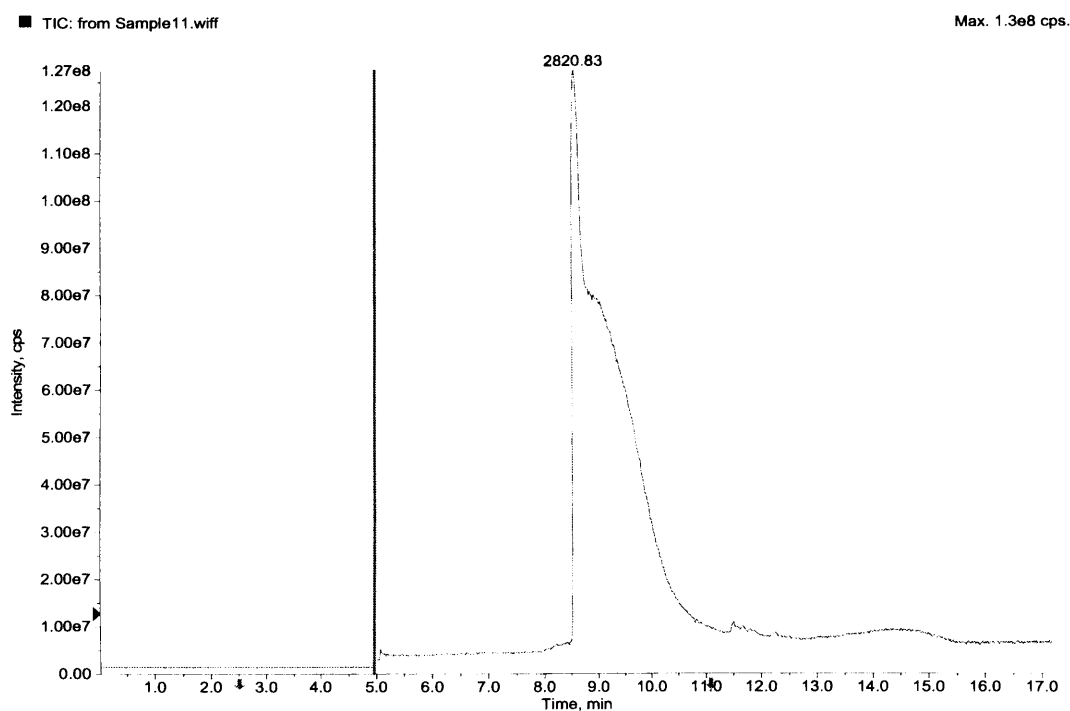


**Figure 3.6 Sample total ion chromatogram of an intact mAb**

*The TIC records all ions present in the sample in one combined signal. It measures the signal intensity over time and corresponds to the liquid chromatogram with a slight shift in time since it will be slightly delayed in comparison. The data is not selective and does not give any detailed information other than confirming the presence of an analyte in the sample.*

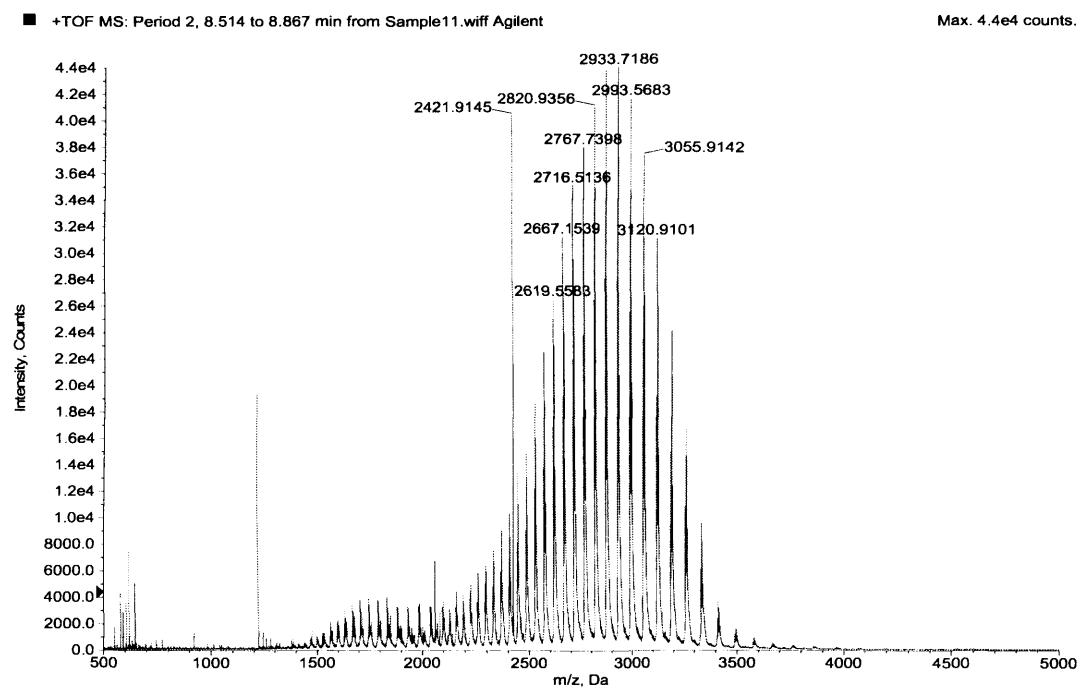


**Figure 3.7** Mass spectrum; sample raw data before deconvolution

The distribution of multiply charged ions is plotted as intensity against mass-to-charge ratio. The ions that can be seen at 1222 and 2422 Da are from the calibration solution used to achieve accurate mass. From the charge envelope the deconvolution algorithm calculates the charge states of the ions and from this determines the molecular weight of the compound.

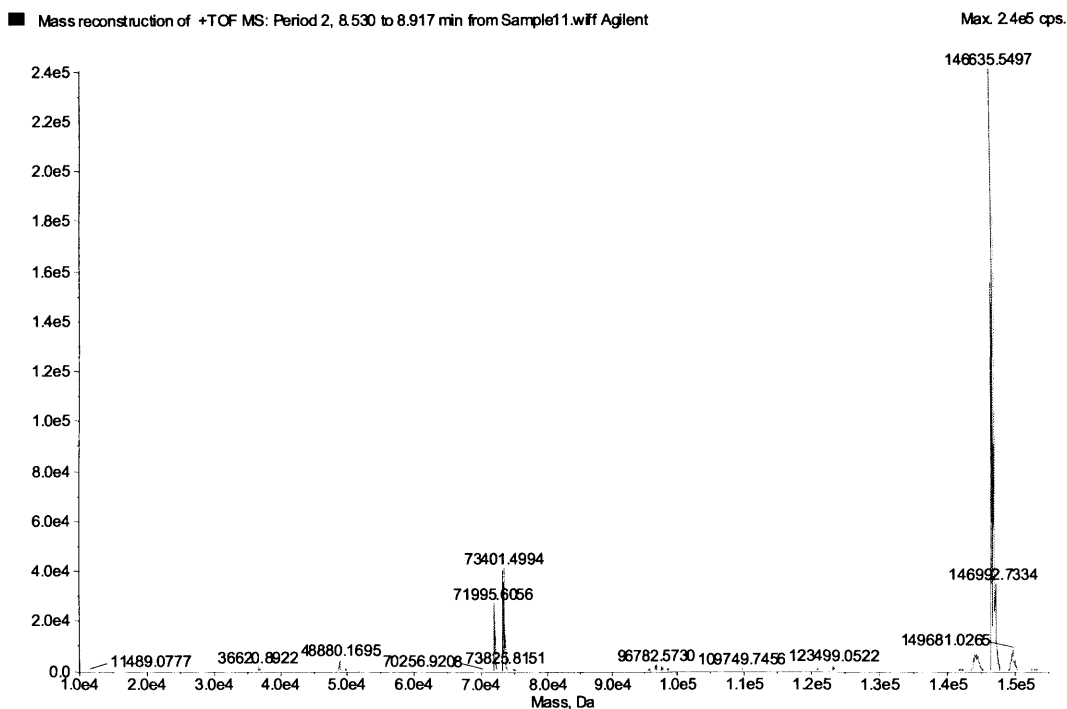


**Figure 3.8 Deconvoluted mass spectrum of the whole mass range**

After deconvolution the spectrum is plotted as intensity against mass in Da. Here it can be seen that there are two main groups of compounds in the sample – one around 73,402 Da and one around 146636 Da. The latter one represents the intact mAb while the first one corresponds to half mAbs, i.e. one light and one heavy chain. The peak at mass 71,995 Da is non-glycosylated half-antibodies. Some minor peaks can also be seen; one at around 48,900 Da, representing the heavy chain on its own and also one at around 98,000 Da, which is a complex of two heavy chains.

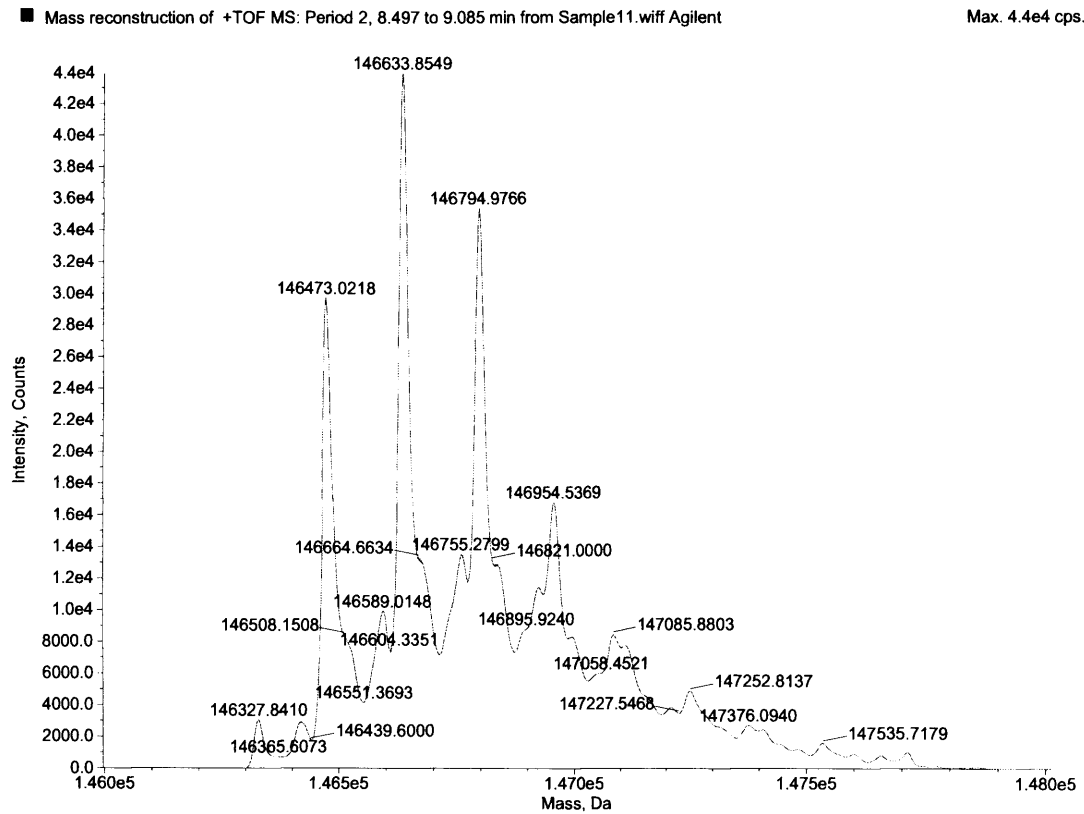


**Figure 3.9 Deconvoluted mass spectrum of the intact mAb.**

*This represents the group at 146,636 Da from Figure 3.8. The deconvolution was this time focused on the area around 146,636 Da to create more detailed data. The plot still shows intensity against mass in Dalton. Here the heterogeneity of the sample can be seen with variants of the intact mAb shown. The different modifications and glycoforms show up as different peaks in the spectrum.*

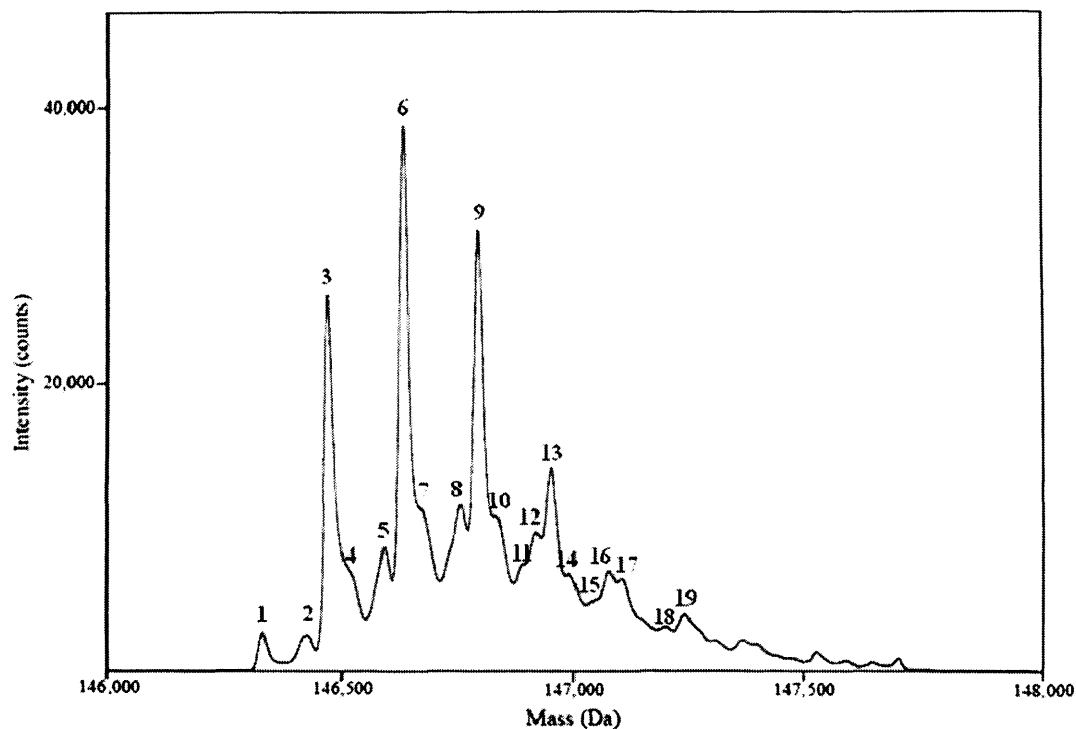


**Figure 3.10** Mass spectrum with assigned peaks

Each peak detected by the MS software has been numbered and listed in Table 3.3 together with the interpretations of their structure. The peaks towards the upper end of the spectrum have been ignored on the basis of being too small and indistinct.

Peak no.	Measured mass (Da)	Possible structures (discrepancy in Da in brackets)
1	146326	G0-1K-Q (+11)
2	146420	G0-2K-pE (+11)
3	146473	G0-2K-Q (-8) or G0F-0K-pE (-6)
4	146505	As above + O <sub>2</sub> (±0) or G0F-0K-Q (-4) or G1-0K-pE (-6)
5	146592	G0F-1K-pE (+3)
6	146634	G0F-1K-Q (-5) or G1-1K-pE (-7)
7	146674	As above + O <sub>2</sub> (-8) or + 2xH <sub>2</sub> O (-4) or + 2xNa (+6)
8	146755	G0F-2K-Q (+2) or G1-2K-pE (±0)
9	146795	G1-2K-Q (-6) or G1F-0K-pE (-4)
10	146828	As above + O <sub>2</sub> (-1) or + 2xH <sub>2</sub> O (+3) or G1F-0K-Q (+3) or G2-0K-pE (-5)
11	146890	?
12	146921	G1F-1K-pE (-2)
13	146955	G1F-1K-Q (-2) or G2-1K-pE (-4)
14	146992	As above + O <sub>2</sub> (-5) or 2xH <sub>2</sub> O (-1) or G2-1K-Q (-7)
15	147046	G1F-2K-pE (+1)
16	147085	G1F-2K-Q (-4) or G2-2K-pE (-6)
17	147114	G2-2K-Q (-1) or G2F-0K-pE (+1)
18	147211	?
19	147250	G2F-1K-pE (-7)

**Table 3.3 Interpretation of the mass spectrum in Figure 3.10**

The peaks detected by the software are listed in the table above detailing their assigned peak number, their masses in Dalton and the possible theoretical structures at or near the measured masses. For explanations of the structures listed see section 3.2. All but two peaks could be correlated to at least one mAb structure. The unidentified peaks (11 and 18) are barely visible and may not be of great importance, but could indicate that there are other modifications present that have not been possible to determine in this study. Most peaks in the table above have more than one possible structure correlated to its mass. It is of course

*possible that multiple structures make up one peak, but in this case it becomes a matter of judgement of what is most likely, drawing from earlier experience in the field. First of all, for this particular mAb, the N-terminal glutamine residue will have been converted to a pyroglutamic acid, so that the structures including the Q residues can be scrapped, cutting the possibilities essentially by half. This leaves peaks 2, 3, 5, 6, 8, 9, 12, 13, 15, 16, 17 and 19 with only one possible structure assigned. The first is now without assignation. The second peak has one possible structure, but the calculated mass of this structure is 11 Da bigger than the measured value, causing doubt as to whether this is actually the correct structure. Peak number four still has two possibilities. Judging the spectrum, it looks more likely to be an adduct being so closely linked to the previous peak. Peak seven is an adduct of the previous peak, but from the spectrum it is not possible to determine what kind of adduct. Peak ten has two possible structures, but again it looks more likely to be an adduct. Peak fourteen is an adduct, but could be either oxygen or water.*

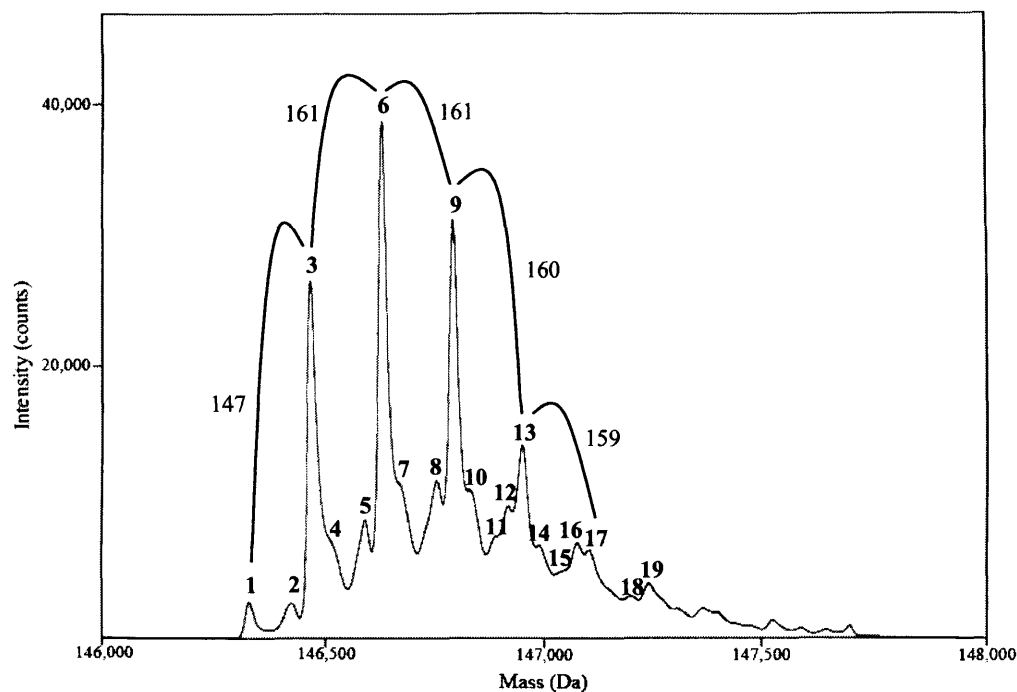


**Figure 3.11 Interpretation of mass spectra, main peaks**

The most prominent peaks were used as the basis when determining the structures behind the masses of the spectral peaks. A distinct pattern can be seen between peak 3, 6, 9, 13 and 17; they are all around 162 Da (159 Da to 161 Da) apart, with a maximum error of -3 Da. A mass of 162 Da corresponds to a hexose. Looking firstly at peak number three, it has a measured mass of 146,473 Da. From Table 3.2, this is close to the theoretical mass of either  $(G0)_2-2K-Q$  (146,465 Da) or  $(G0F)_2-0K-pE$  (146,467 Da). Since it is more common that the glutamine is converted to pyroglutamic acid than not and the likelihood of having 2 intact lysines is small, this peak is determined to be  $(G0F)_2-0K-pE$ . The 162 Da addition to this structure corresponds to one galactose, resulting in the structure  $G0F/G1F-0K-pE$ . The structure with a second addition of 162 Da then represents  $(G1F)_2-0K-pE$  or  $G0F/G2F-0K-pE$ , the third  $G1F/G2F-0K-pE$  and the fourth  $(G2F)_2-0K-pE$ , as detailed in Table 3.4. Peak number one is included in the pattern, but with a mass 147 Da lower than that of peak number three. This instead corresponds to the absence of the core-associated fucose (146 Da) and represents the structure  $G0/G0F-0K-pE$ . All mAbs behind the peaks mentioned above include the same modifications; they have both C-terminal lysine residues cleaved off (0K) and both N-terminal glutamine residues converted to pyroglutamic acid (pE).

Peak no.	Measured mass (Da)	Glycan	Theoretical mass (Da)
1	146,326	G0/G0F	146,321
3	146,473	(G0F) <sub>2</sub>	146,467
6	146,634	G0F/G1F	146,629
9	146,795	(G1F) <sub>2</sub> or G0F/G2F	146,791
13	146,955	G1F/G2F	146,953
17	147,114	(G2F) <sub>2</sub>	147,115

**Table 3.4 Peak assignment from Figure 3.11**

The table lists the first set of peaks with their measured mass in Dalton. All peaks in this set have the same modifications; they have both C-terminal lysine residues cleaved off (OK) and both N-terminal glutamine residues converted to pyroglutamic acid (pE). Their respective glycan structures are listed in the table as well as their theoretical calculated masses in Dalton. With these peak assignments the measured masses are correct with errors from -1 Da to +6 Da.

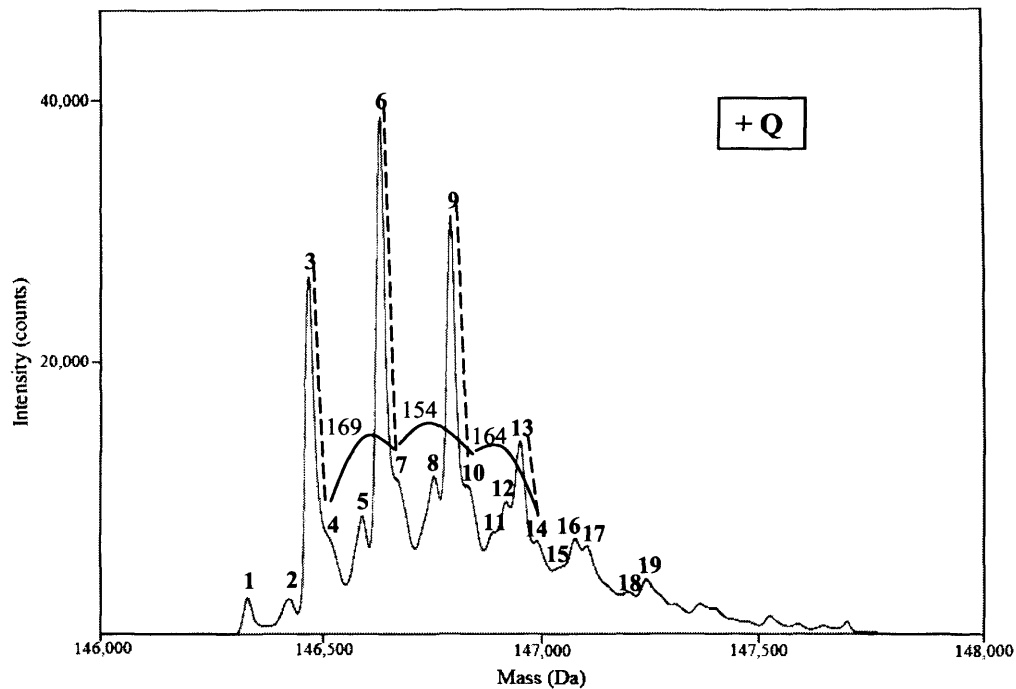


**Figure 3.12 Interpretation of mass spectra, glutamine not converted**

A second set of peaks can be detected that are also around 162 Da (154 Da to 169 Da) apart. The reason for the greater variability in masses is that these peaks (4, 7, 10 and 14) are closely associated with the main peaks and are therefore not as prominent. They differ from the main peaks they are associated with by +36 Da  $\pm$  4 Da, the connection indicated by dotted lines. The mass difference corresponds to the difference between two pyroglutamic acid residues and two glutamine residues (+34 Da). The basic structure of the mAb behind this set of peaks can therefore be determined to have the two C-terminal lysine residues cleaved off as before (0K), but do not have the N-terminal glutamine converted (Q). The glycan structures corresponding to the peaks are (G0F)<sub>2</sub> (peak number 4), G0F/G1F (7), (G1F)<sub>2</sub> or G0F/G2F (10) and G1F/G2F (14), as detailed in Table 3.5.

Peak no.	Measured mass (Da)	Glycan	Theoretical mass (Da)
4	146,505	(G0F) <sub>2</sub>	146,501
7	146,674	G0F/G1F	146,663
10	146,828	(G1F) <sub>2</sub> or G0F/G2F	146,825
14	146,992	G1F/G2F	146,987

**Table 3.5 Peak assignment from Figure 3.12**

*The table lists the second set of peaks with their measured mass in Dalton. All peaks in this set have the same modifications; they have both C-terminal lysine residues cleaved off (OK) but differ from the peaks in the first set (Figure 3.11 and Table 3.4) by having the N-terminal glutamine residues intact (Q). Their respective glycan structures are listed in the table as well as their theoretical calculated masses in Dalton. With these peak assignments the measured masses are correct with errors from +4 Da to +9 Da. The greater discrepancies in this set compared to the first is due to the small mass difference (+34 Da) between these peaks and the main peaks and the inability of the software to correctly make a distinction of this much smaller peak from the main peak it is associated with.*

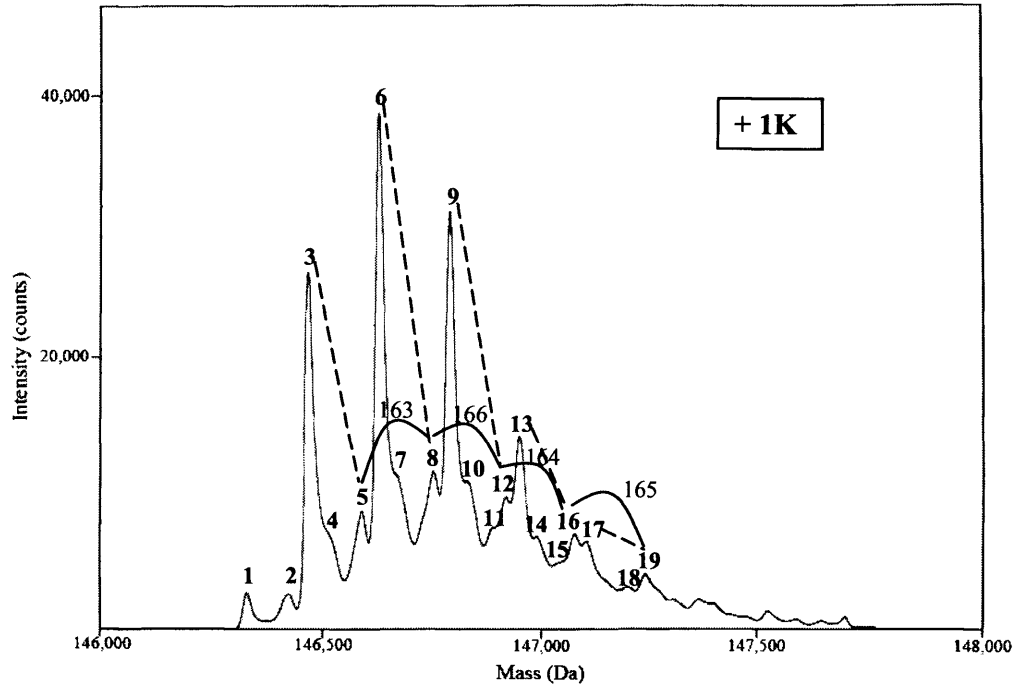


**Figure 3.13 Interpretation of mass spectra, one intact lysine**

A third set of peaks can be detected that are again around 162 Da (163 Da to 166 Da) apart. They differ from the main peaks they are associated with by  $+127.5 \text{ Da} \pm 8.5 \text{ Da}$ , the connection indicated by dotted lines. This mass difference corresponds to the mass of one lysine residue, indicating that the basic structure of the mAb behind this set of peaks have the N-terminal glutamine converted (pE) as in the first set of peaks but only have one of the two C-terminal lysine residues cleaved off (1K). The glycan structures corresponding to the peaks are (G0F)<sub>2</sub> (peak number 5), G0F/G1F (8), (G1F)<sub>2</sub> or G0F/G2F (12), G1F/G2F (16) and (G2F)<sub>2</sub> (19), as detailed in Table 3.6.

Peak no.	Measured mass (Da)	Glycan	Theoretical mass (Da)
5	146,592	(G0F) <sub>2</sub>	146,595
8	146,755	G0F/G1F	146,757
12	146,921	(G1F) <sub>2</sub> or G0F/G2F	146,919
16	147,085	G1F/G2F	147,081
19	147,250	(G2F) <sub>2</sub>	147,243

**Table 3.6 Peak assignment from Figure 3.13**

The table lists the third set of peaks with their measured mass in Dalton. All peaks in this set have the same modifications; they have both N-terminal glutamine residues converted (pE) but differ from the peaks in the first set (Figure 3.11 and Table 3.4) by having one of the C-terminal lysine residues intact (1K). Their respective glycan structures are listed in the table as well as their theoretical calculated masses in Dalton. With these peak assignments the measured masses are correct with errors from -3 Da to +7 Da.

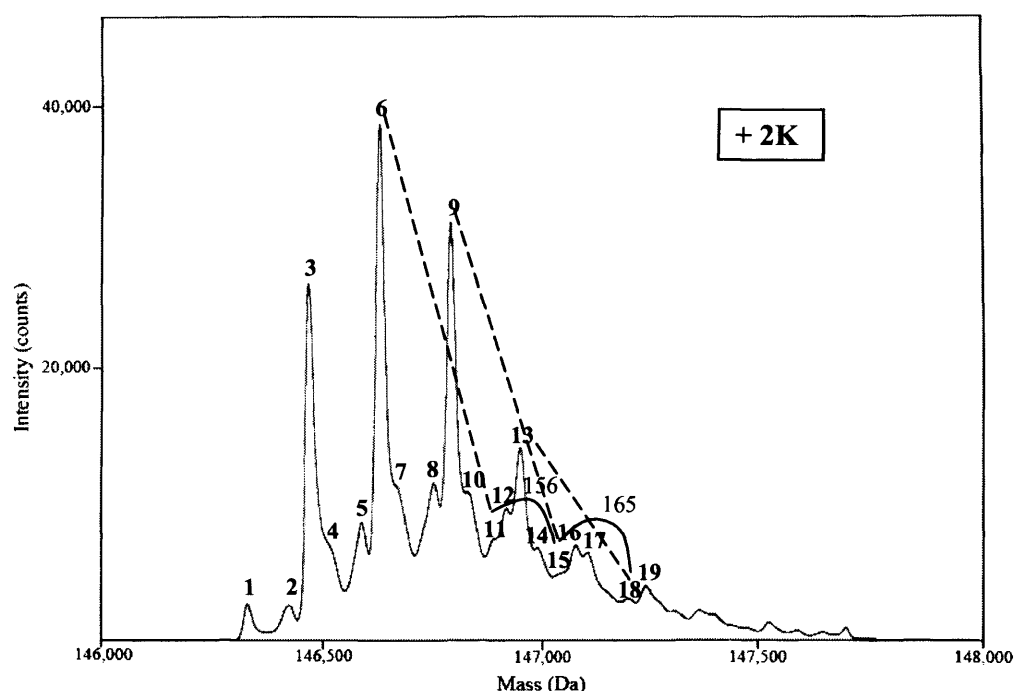


**Figure 3.14 Interpretation of mass spectra, two intact lysines**

A fourth set of peaks can be detected that are again around 162 Da (156 Da and 165 Da) apart. They differ from the main peaks they are associated with by  $+253.5 \text{ Da} \pm 2.5 \text{ Da}$ , the connection indicated by dotted lines. This mass difference corresponds to the mass of two lysine residues, indicating that the basic structure of the mAb behind this set of peaks have the N-terminal glutamine converted (pE) as in the first set of peaks but have both C-terminal lysine residues intact (2K). The glycan structures corresponding to the peaks are G0F/G1F (peak number 11), (G1F)<sub>2</sub> or G0F/G2F (15) and G1F/G2F (18), as detailed in Table 3.7. This set of peaks could possibly have the addition of a peak directly to the left of peak number eight, since that is a wider peak that could hide the integration of a smaller peak that the software finds difficult distinguishing from the other one.

Peak no.	Measured mass (Da)	Glycan	Theoretical mass (Da)
11	146,890	G0F/G1F	146,885
15	147,046	(G1F) <sub>2</sub> or G0F/G2F	147,047
18	147,211	G1F/G2F	147,209

**Table 3.7 Peak assignment from Figure 3.14**

The table lists the fourth set of peaks with their measured mass in Dalton. All peaks in this set have the same modifications; they have both N-terminal glutamine residues converted (pE) but differ from the peaks in the first set (Figure 3.11 and Table 3.4) by having both C-terminal lysine residues intact (2K). Their respective glycan structures are listed in the table as well as their theoretical calculated masses in Dalton. With these peak assignments the measured masses are correct with errors from -1 Da to +5 Da.

## 4 Effect of harvest time on the molecular structure and conformation of a mAb

This study examines the effect of time of harvest on the molecular structure of the recombinant IgG B72.3. The glycosylation status of whole recombinant IgG at different stages of fermentation was compared. Two separate fermentations were compared where the same cell line, media and culture conditions were used (for details see section 2.1).

### 4.1 Growth profiles

Figure 4.1 shows the growth profile of the first fermentation that was investigated. Samples were taken on day 6, 7, 11, 14 and 17 to obtain coverage throughout the different stages of fermentation. Figure 4.2 shows the logarithmic growth curve providing an overview of the growth phase of the cells during the fermentation. Table 4.1 details the conditions for each sampling point, which will be of importance when interpreting the data. Figure 4.1 and Table 4.1 show that between day 11 and day 14 the fermentation is starting to reach higher mAb titres, but at the same time cell viability is also significantly starting to suffer. There is an obvious decrease in cell viability between day 14 and day 17 when harvest was carried out. It is important to note here that most mammalian cell cultures of this kind are normally harvested on day 14 or 15. The reason for keeping the fermentation going to day 17 was to look at how the mAb concentration and overall performance of the culture change over the last couple of days. From this data it can be seen that there is no significant increase in product titres from day 14 to day 17, while there are significant decreases in cell viability, explaining the industry choice of harvesting after 15 days.

In order to confirm the findings from fermentation 1, a second fermentation was carried out. This time the culture was only kept until day 15, rather than day 17, when harvest was carried out, which is more representative of commercial standards for this application. The second fermentation showed a slightly slower start, both in terms of growth and product formation, especially the latter, as can be seen in Figure 4.3. However, after the first two days the growth and product

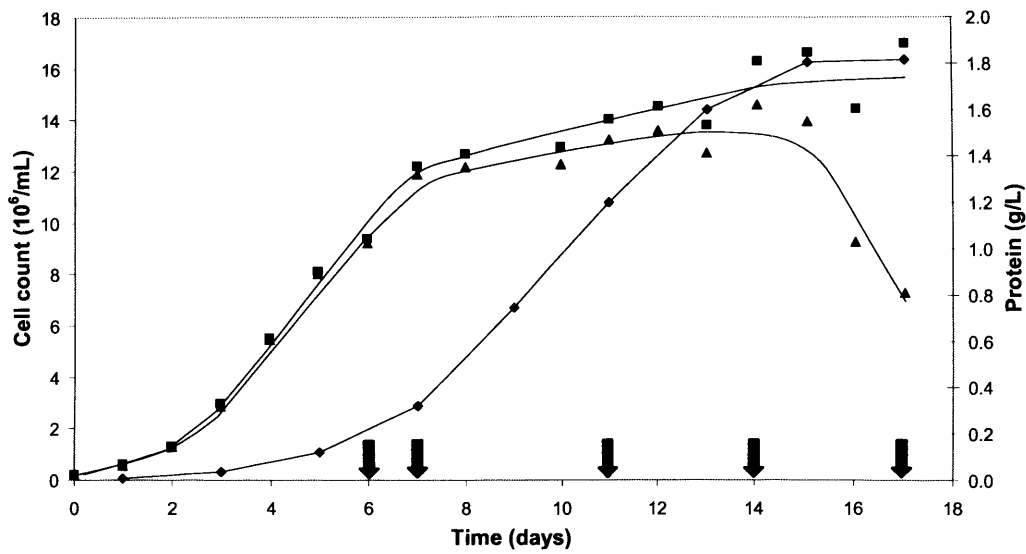


**Figure 4.1 Growth profile of cell culture, 1<sup>st</sup> fermentation**

Symbols represent total number of cells (■); number of viable cells (▲); mAb formation (◆). Points are single measured values and lines were drawn as best fit by eye. A 10 L fermenter was used with a working volume of 8.5 L, fed batch (see section 2.1). The arrows indicate time points when samples were taken (days 6, 7, 11, 14 and 17).

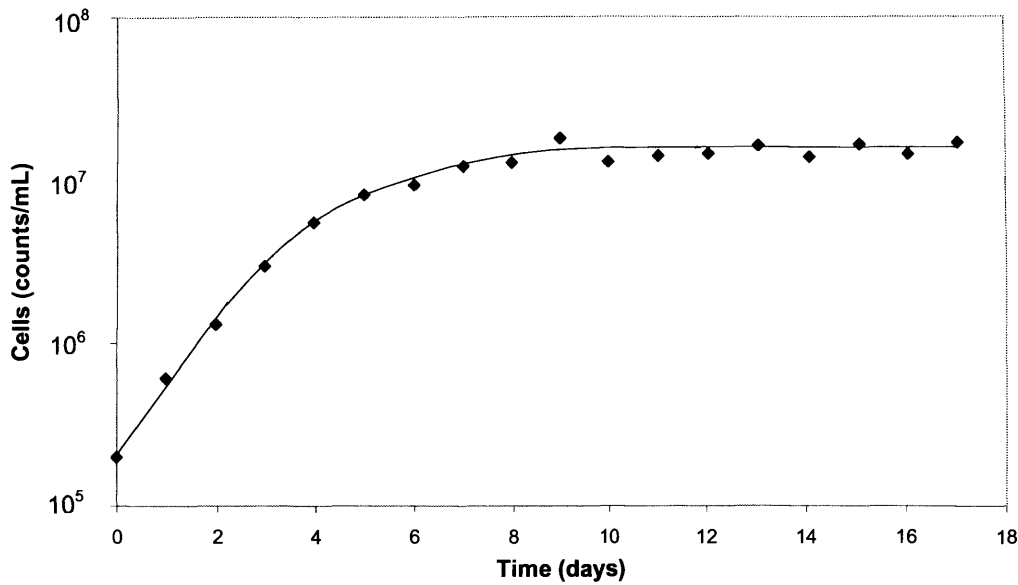


**Figure 4.2 Logarithmic growth curve, 1<sup>st</sup> fermentation**

*Lag phase was absent in this fermentation and instead exponential phase was experienced immediately for the first four days after which the cells entered stationary phase, which then lasted for the remainder of the fermentation.*

Sample	Growth phase	Antibody titre (g/L)	% cell viability
Day 6	Early stationary	0.2	98
Day 7	Early stationary	0.3	97
Day 11	Late stationary	1.2	94
Day 14	Death phase	1.7	90
Day 17	Death phase	1.8	43

**Table 4.1 Growth characteristics, 1<sup>st</sup> fermentation**

*Six samples were taken and analysed at different stages of the fermentation; during early stationary (day 6 and 7), late stationary (day 11 and 14) and finally at time of harvest (day 17). Cell viability was high and stayed steady over the first two samples, starting to decrease around day 11 and from day 14 the cells started to die rapidly with significant cell death at time of harvest and last sampling point.*

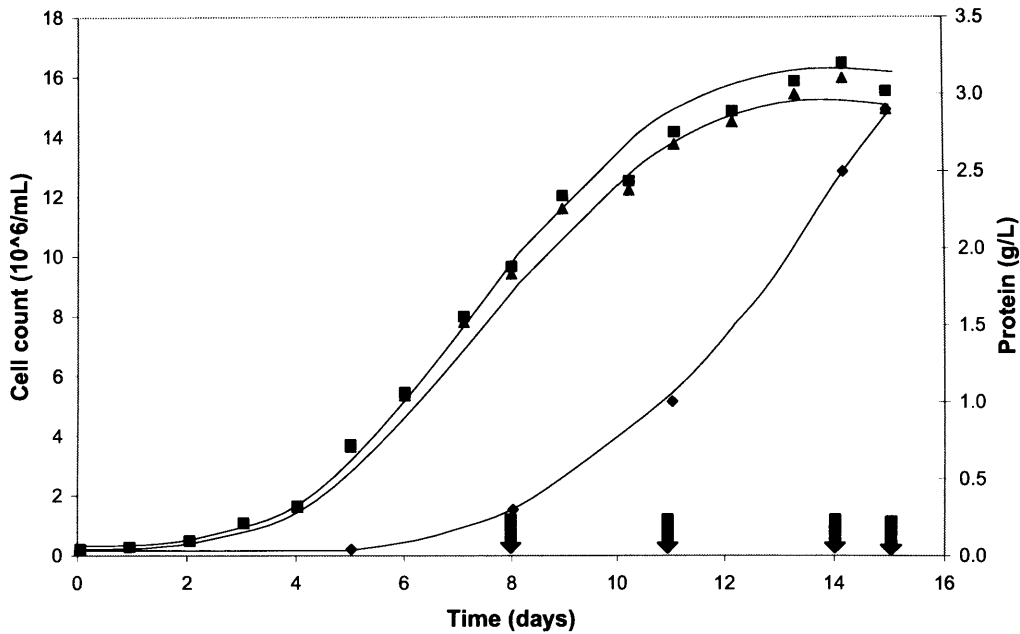


**Figure 4.3** Growth profile of cell culture, 2<sup>nd</sup> fermentation

Symbols represent total number of cells (■); number of viable cells (▲) and mAb formation (◆). Points are single measured values and lines were drawn as best fit by eye. A 10 L fermenter was used with a working volume of 8.5 L, fed batch (see section 2.1). The arrows indicate time points when samples were taken (day 8, 11, 14 and 15).

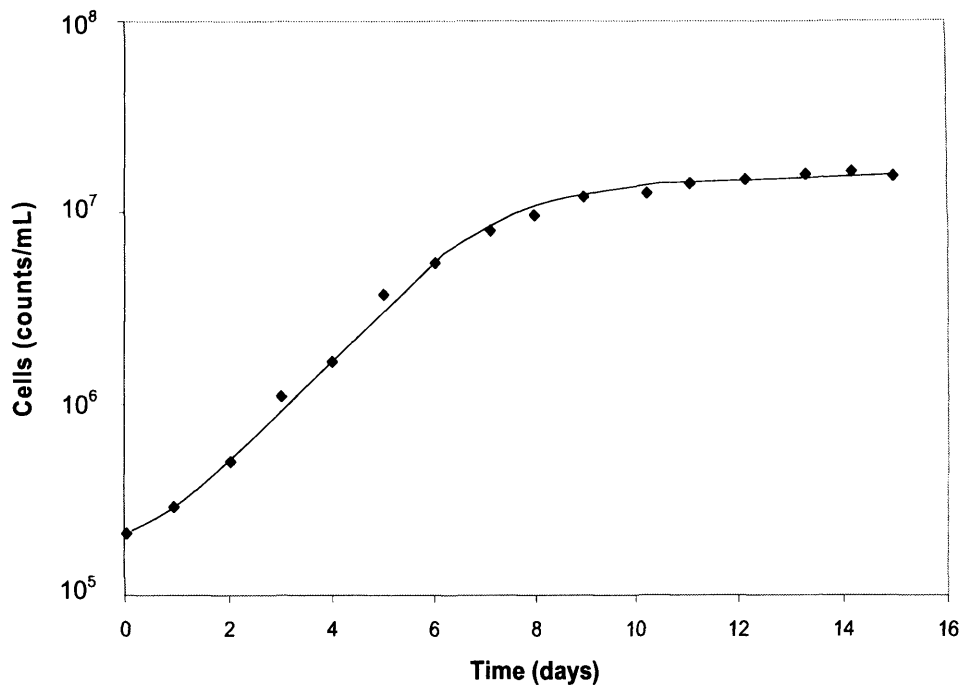


**Figure 4.4** Logarithmic growth curve, 2<sup>nd</sup> fermentation

Lag phase was experienced for the first day or two before the cells went into exponential phase from day 2 to 7. From day 10 stationary phase was experienced for the remainder of the fermentation.

Sample	Growth phase	Antibody titre (g/L)	% cell viability
Day 8	Early stationary	0.3	97
Day 11	Stationary	1.0	97
Day 14	Late stationary	2.5	97
Day 15	Late stationary	2.9	96

**Table 4.2** Growth characteristics, 2<sup>nd</sup> fermentation

Four samples were taken and analysed at different stages of the fermentation; during early stationary (day 8), mid stationary (day 11), late stationary (day 14) and finally at time of harvest (day 15). Cell viability was high and stayed level over the main part of the culture with only small losses in viability towards time of harvest.

formation rate was very similar to that of the first fermentation. From the log growth curve in Figure 4.4 it becomes obvious that this second fermentation had a slight lag phase before exponential phase was reached by day two. A consequence of this is that the viability stays high for the duration of the fermentation until time of harvest. Samples were taken during different growth phases on days 8, 11, 14 and 17, with conditions for each sampling point with regard to growth phase and cell viability detailed in Table 4.2.

## 4.2 *Glycosylation profiles*

The samples taken were purified (see sections 2.2 and 2.6), analysed by LC/MSD-TOF (for conditions see section 2.9.1) and deconvoluted. The mass spectra were then normalised so that the areas of all spectra were identical, in order to compare the relative amounts of each peak (Figure 4.5). Due to the noise levels from the solvents the spectra are rather complex and the smaller peaks have at this point not been investigated closer; instead the focus has been on trends among the main peaks. The peaks were assigned as detailed in section 3.4. The identified peaks all have the same modifications to the basic mAb structure; both C-terminal lysine residues have been cleaved off and the N-terminal glutamine residues have been converted to pyroglutamic acid (see section 1.6.5). One mAb can have either two of the same glycans attached to each heavy chain, or two different ones. As can be seen from the spectra, the glycans vary from G0 to G2F (for structures see section 3.2, Figure 3.3) and the overall trend is that the level of galactosylation decreases over time of culture. On day six, the most abundant glycoform is (G1F)<sub>2</sub>, however this shifts with time; on day seven the most abundant glycoform is 162 Da smaller, representing the G0F/G1F glycoform. Towards the later stages of culture it has shifted even further by another 162 Da and the most abundant glycoform is (G0F)<sub>2</sub> on days 11, 14 and 17. The whole spectrum shifts towards the left, clearly showing that the glycans are becoming less complex over time of fermentation.

The data from the first fermentation gives clear information related to the major peaks. In order to better interpret the smaller peaks, the protocol was redesigned for the second fermentation (for conditions see section 2.9.1). The drying gas temperature was increased to provide a clearer spectrum with less noise as can be

seen in Figure 4.6. Looking at the main peaks, the trends agree well with the observations from the first fermentation; the level of galactosylation decreases with time of culture. There is a shift in the main glycoform from G0F/G1F on day 8 towards (G0F)<sub>2</sub>, with an obvious decrease in the (G1F)<sub>2</sub> glycoform at the same time as the (G0F)<sub>2</sub> variant is increasing. The lower noise levels in these spectra also allow a more detailed analysis, taking all peaks into consideration and not only the most intense ones. In these spectra, not only the different glycoforms can be detected, but also other modifications to the basic mAb structure (see section 1.6.5). Small, incompletely resolved peaks are evident at a mass of +34 Da from each main peak. This corresponds to the difference in mass between pyroglutamic acid and glutamine, indicating that the mAbs behind these second peaks have not had the N-terminal glutamines converted. The spectra also show resolved peaks corresponding to mAbs with the same glycoforms as the main peaks, but with different amounts of intact C-terminal lysines; peaks at +128 Da with one intact lysine as well as peaks at +256 Da, with both lysines intact.

### 4.3 Glycoform production

In order to understand better the reasons behind the changes in glycoform production, the total product formed in picograms per cell per day (PCD) was calculated and plotted in Figure 4.7. During the first stages of culture while the cells are in exponential phase, the product formation per viable cell remains approximately constant rather than increasing, which could be due to the cells focusing on growth rather than mAb formation. During the later stages of the exponential phase, the mAb production per viable cell increases rapidly and stays steady during early stationary phase, which is when the cell specific activity is at its highest. During this stage, the cells are no longer focusing on growth, but are still in a good state and this is where most of the product is being formed. The mAb production per viable cell then decreases until time of harvest when it almost reaches zero. This could be due to the state of the viable cells during this stage and the counting method used (the Vi-Cell is based on the trypan blue method). Even if the cells are still counted as viable, they will not be in a favourable state and will have decreased functionality. Apoptotic cells will have shut down certain protein production mechanism for example.

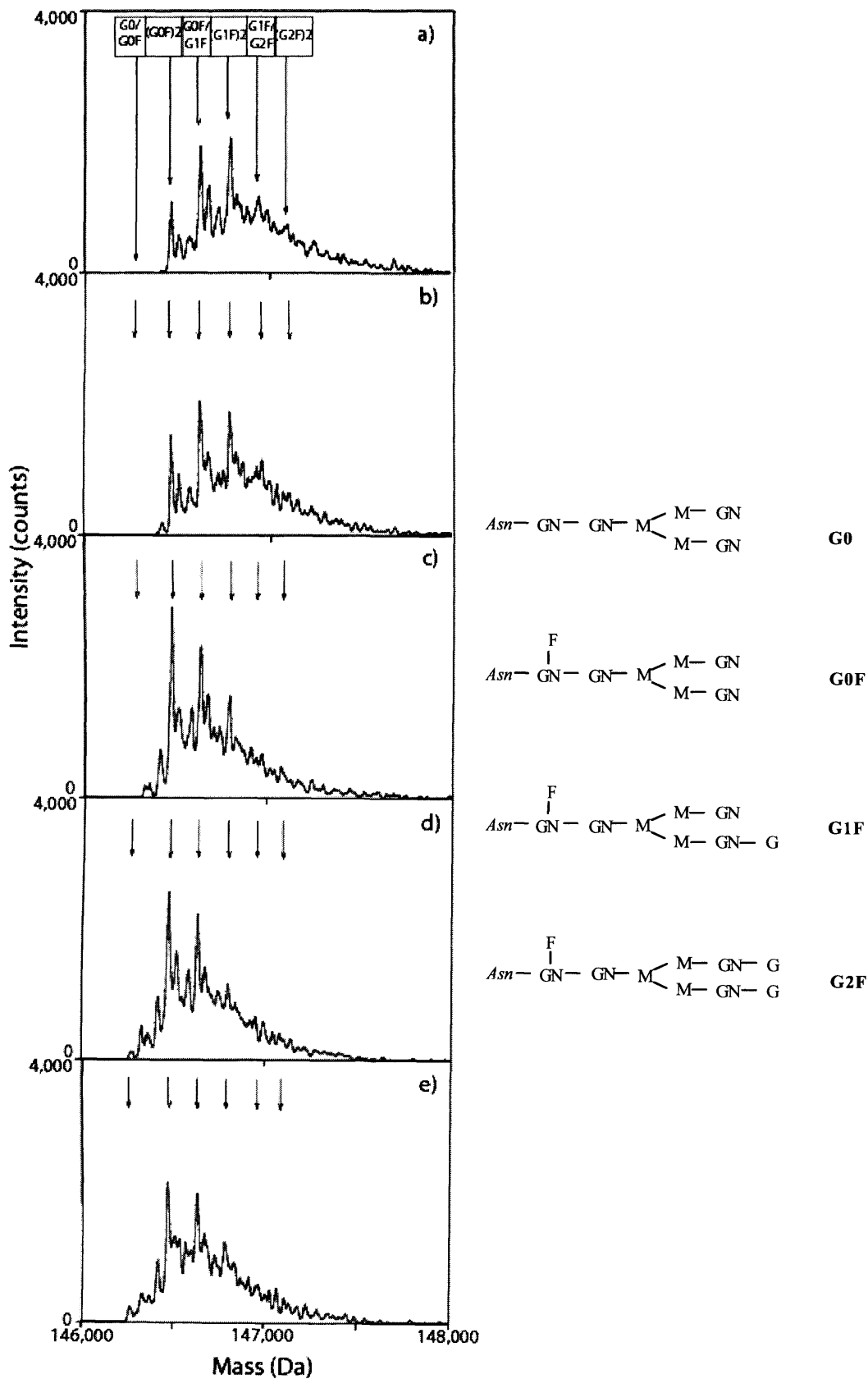


**Figure 4.5** Effect of harvest time on the glycosylation pattern of an IgG, 1<sup>st</sup> fermentation.

Legend on following page.

*Figure 4.5 continued. The figure shows the mass spectra from day 6 (a), 7 (b), 11 (c), 14 (d) and 17 (e) of culture. LC/MSD-TOF was used to analyse the intact antibody, resulting in the above spectra. Looking at the most prominent peaks, these create a pattern, separated by approximately 162 Da, corresponding to the mass of a galactose, with the exception of the first and second main peaks that instead are separated by 146 Da; the mass of a fucose. The figure indicates the basic glycoforms G0, G0F, G1F and G2F (see Figure 3.5) and how they are represented in pairs on the intact mAb (one on each of the two heavy chains). The mAbs are also prone to other modifications, such as C-terminal lysine cleavage and cyclization of the N-terminal glutamine residue (see section 1.6.5). All of the main peaks have the same modifications in this respect; both lysines have been cleaved off (OK) and the glutamine has been converted to pyroglutamic acid (pE) (for more details see Table 3.2). The other peaks that can be seen in the spectra are variations of these modifications, causing the heterogeneity in the mAb population. There is also a certain level of noise from the solvents involved in the analysis, which is the reason the smaller peaks have not been given more attention. The most prominent peaks are obviously the main contributors to the mAb population, so these have been analysed in more detail. Looking at the two extremes as shown in a) the profile from day six and e) the profile from day seventeen, a shift in masses can be seen over the course of culture. In a) the lowest masses start at 146,400 Da, while in e) the whole mass spectrum has shifted towards the left with masses starting at 146,200 Da. The main peak has shifted by 324 (2x162) Da from 146,795 Da on day 6, corresponding to the G1F glycan attached to both heavy chains, to 146,471 Da on days 11, 14 and 17, corresponding to the G0F glycan attached to both heavy chains. The shift in the spectra indicates that the sugars are becoming less complex towards the end of fermentation.*

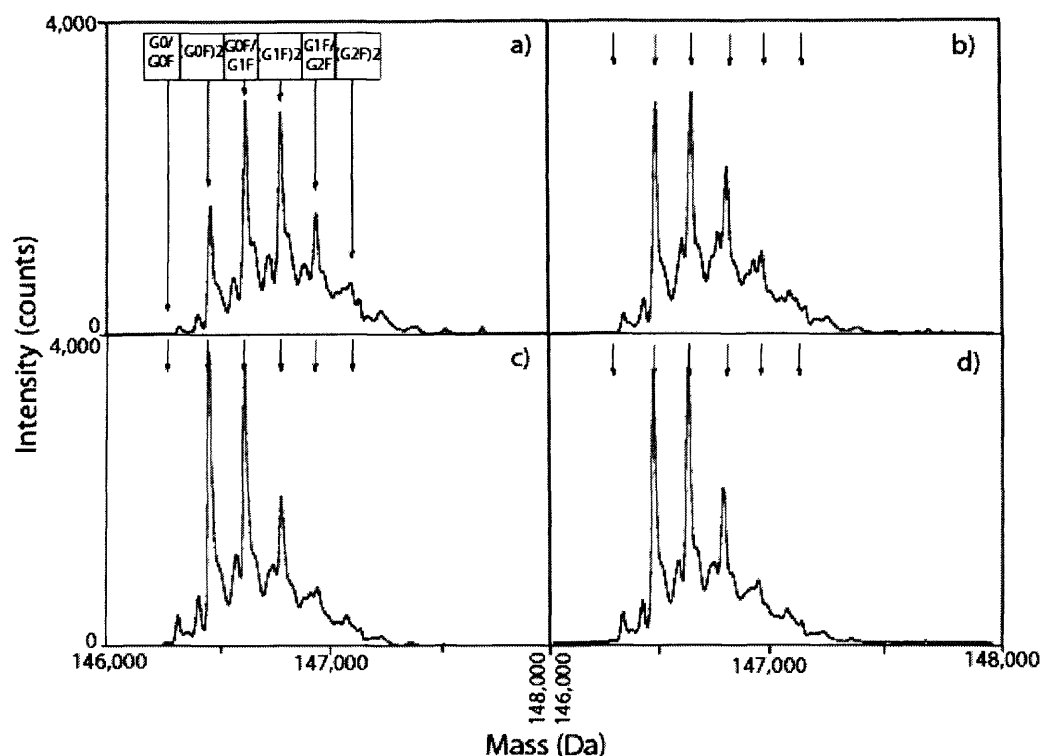


**Figure 4.6 Effect of harvest time on the glycosylation pattern of an IgG, 2<sup>nd</sup> fermentation**

The figure shows the mass spectra from day 8 (a), 11 (b), 14 (c) and 15 (d) of culture. As in Figure 4.5, the basic glycoforms are indicated; G0, G0F, G1F and G2F and how they are represented in pairs on the intact mAb and again all of the main peaks have the same modifications to the basic structure; both lysines have been cleaved off (OK) and the glutamine has been converted to pyroglutamic acid (pE). The observations made for the first fermentation are well supported by this second fermentation. There is an increase in the lower masses over time of culture at the same time as there is a decrease in the higher masses. The main glycans shift with time from G0F/G1F on day 8 towards (G0F)<sub>2</sub>, the level of galactosylation decreasing with time. The lower noise levels in these optimised spectra also make it possible to start looking closer at the less intense peaks. All of the main peaks have a “heel” on them, indicating there is a second peak there that has not been completely resolved due to the similarity in mass of the two peaks. This second peak has a mass of +34 Da compared to the main peak it is connected to. This corresponds to the difference in mass between pyroglutamic acid and glutamine, indicating that these second peaks have the same glycans attached as the main peaks, but the N-terminal glutamines have not been converted. There is also another peak at +128 Da from each main peak. This

---

*corresponds to a mAb carrying the same glycans but still has one C-terminal lysine intact. If looking closely, an additional peak can be detected, at +256 Da from each main peak, which in turn corresponds to the same mAb structure but with both C-terminal lysines intact. For a more detailed explanation of interpretations see section 3.4.*

The total amount of mAb produced per cell per day was then used to investigate the production rate of the different glycoforms. The areas of the peaks in the spectra from Figure 4.5 were measured and the amount of each glycoform produced per viable cell per day was calculated and plotted in Figure 4.8. With the exception of the G0/G0F glycoform, all lines seem to follow the development of the total product formed, just with different magnitudes, which is the trend that might have been expected. The increase in G0/G0F formation is concurrent with a decrease in cell viability and could be related to increased stress levels.

As for the first fermentation, the total product formed per viable cell per day was calculated and plotted in Figure 4.9. The trend of this curve is very similar to what was observed for the first fermentation, only with a slightly later response due to the lag phase experienced at the beginning of the culture. Again the production rate is staying rather level for the early stages, during exponential growth phase to then increase sharply towards the end of the growth phase and reaching the highest values during early stationary phase when a large amount of the product is being formed. In contrast to the first fermentation, total product formed per viable cell per day in this second fermentation does not reach zero towards time of harvest. This can be explained by the lag phase experienced as well as the earlier harvest time.

The amount of each glycoform produced per viable cell per day was then calculated using the areas of the peaks of the spectra in Figure 4.6 and plotted in Figure 4.10. As for the first fermentation, the (G0F)<sub>2</sub> and the G0F/G1F glycoforms seem to follow the development of total mAb formed per viable cell per day. In contrast to before, the G0/G0F glycoform now also follows the trend of the total product formed and can therefore be grouped together with the two first mentioned. The formation of (G1F)<sub>2</sub>, G1F/G2F and (G2F)<sub>2</sub> in this case seems to increase with time for reasons not fully understood. A possible explanation is that due to the lag phase and delay in product formation the production rates for these glycoforms have not yet dropped off, but if harvest had been carried out a few days later the decrease would have been visible.

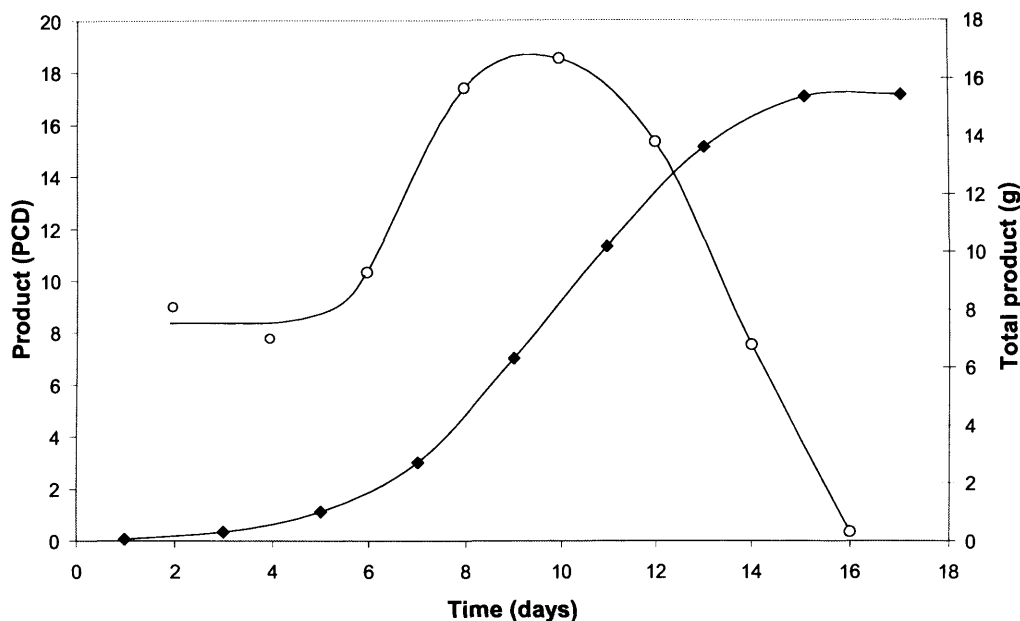


**Figure 4.7 Product formation, 1<sup>st</sup> fermentation**

Shown here is the product formation over time of culture (◆) (in grams) and product formation (○) in picograms per viable cell per day (PCD). The total amount of mAb produced per cell per day was calculated as an average between two measured points and plotted with the axis on the left. Up until day six the product formation per viable cell is staying fairly steady rather than increase. After day six, as the culture is reaching the later stages of the exponential phase, the mAb production per viable cell increases sharply until day nine when the cells reach stationary phase. It then decreases rapidly until time of harvest when product per viable cell per day almost reaches zero.

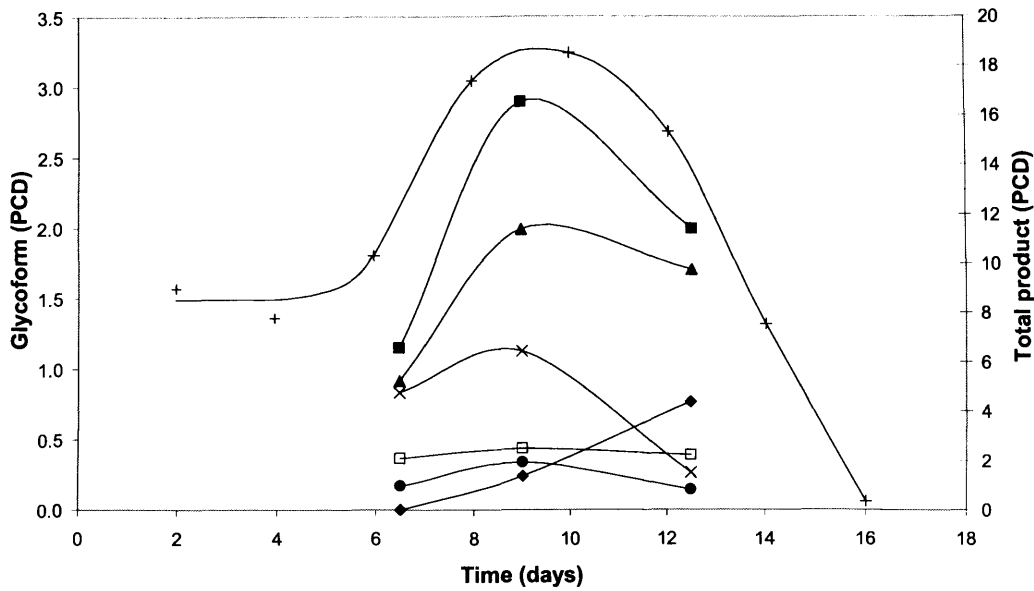


**Figure 4.8** Formation of different glycoforms per viable cell per day, 1<sup>st</sup> fermentation

The total amount of mAb produced per cell per day was plotted with the axis on the right. To generate the lines representing the amount of each glycoform formed per viable cell per day the areas of the peaks of the mass spectra from Figure 4.5 were calculated, and the relative amounts of the glycans representing the main peaks were calculated. This value was then multiplied with the total amount of mAb produced per cell per day. The symbols represent the following: (+) Total product, (◆) G0/G0F, (■) (G0F)<sub>2</sub>, (▲) G0F/G1F, (x) (G1F)<sub>2</sub>, (□) G1F/G2F, (●) (G2F)<sub>2</sub>. Looking at the trends of the lines, G0/G0F (◆) is the only glycoform that increases with time. The (G0F)<sub>2</sub> (■), G0F/G1F (▲) and (G1F)<sub>2</sub> (x) glycoforms more or less follow the development of the total product being formed, which is the trend that might have been expected. The last and most complex glycoforms, G1F/G2F (□) and (G2F)<sub>2</sub> (●), seem to stay almost constant at a first glance. However, when expanding the axis for these two lines they both follow the trend of the total product formed and the other glycoforms, except G0/G0F, only with smaller variations.

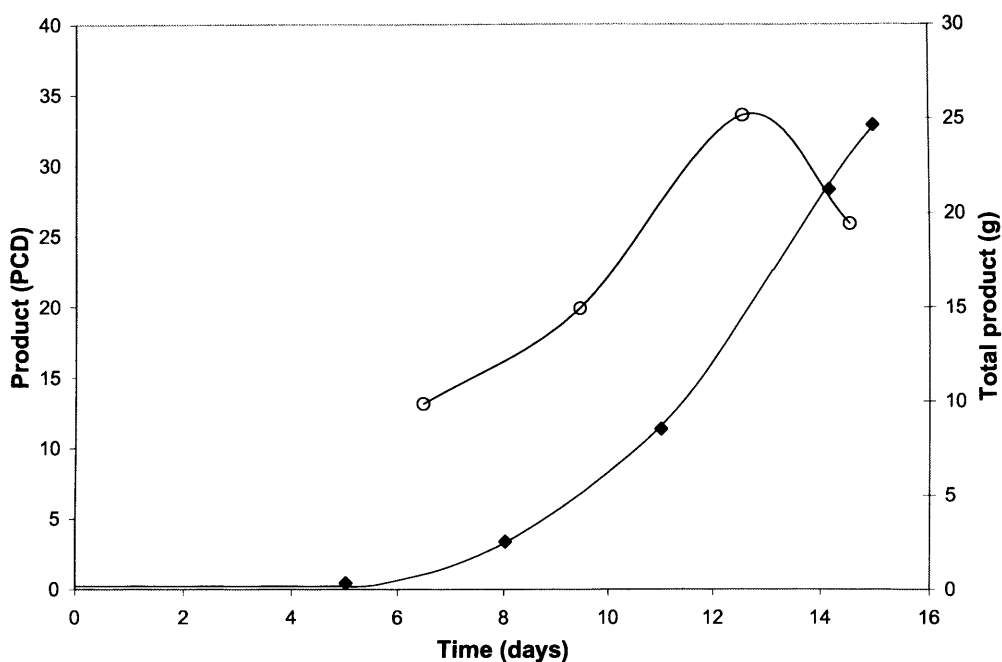


**Figure 4.9 Product formation, 2<sup>nd</sup> fermentation**

Shown here is the product formation over time of culture (◆) (in grams) and product formation in picograms per viable cell per day (○). Product formation per viable cell per day increases for the duration of the exponential growth phase and during early stationary phase, up until day 12. From this point onwards, the viable cells produce decreasing amounts of product per day, while the cells are in stationary phase.

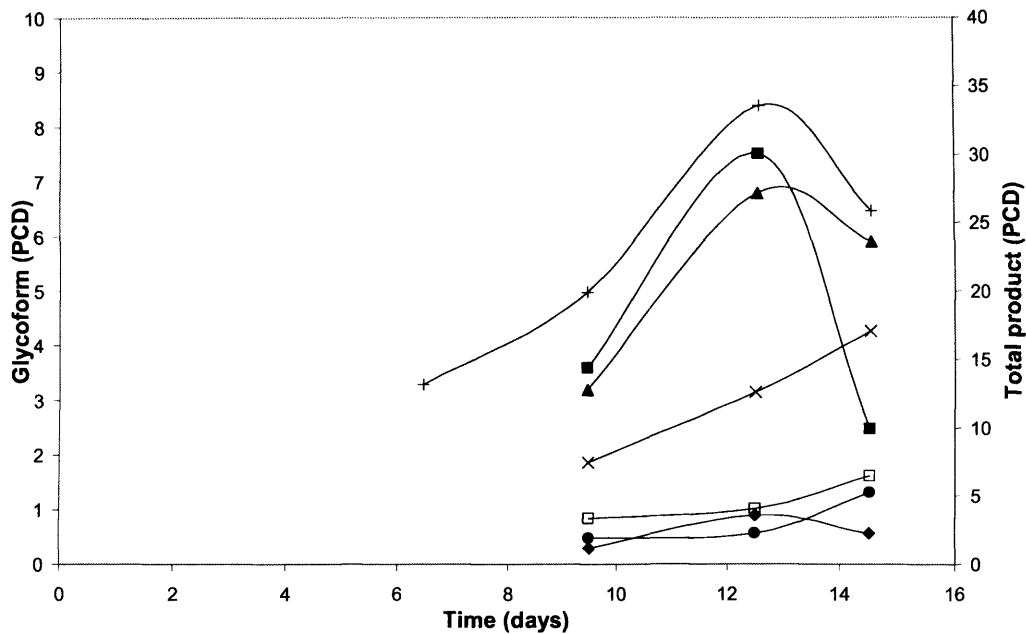


**Figure 4.10** Formation of different glycoforms per viable cell per day, 2<sup>nd</sup> fermentation

The lines representing the amount of glycan formed per viable cell per day were generated as detailed in the legend for Figure 4.8 but using the mass spectra in Figure 4.6 rather than Figure 4.5. The symbols represent the following: (+) Total product, (◆) G0/G0F, (■) (G0F)<sub>2</sub>, (▲) G0F/G1F, (x) (G1F)<sub>2</sub>, (□) G1F/G2F, (●) (G2F)<sub>2</sub>. The trends of the lines can divide the glycoforms into two groups. In this case, the G0/G0F (◆) glycoform, upon expansion of the axis, follows the trend of the total product formed per viable cell per day and can therefore be grouped together with (G0F)<sub>2</sub> (■) and G0F/G1F (▲). The formation of (G1F)<sub>2</sub> (x) per viable cell in this case seems to increase with time as do G1F/G2F (□) and (G2F)<sub>2</sub> (●).

#### 4.4 *Half antibodies*

So far, the focus has been on the molecular structure of the intact mAb and its glycosylation pattern. If instead looking at the overall composition of the product, the intact mAb is not the only evident structure that has been purified by protein A chromatography, as detailed in Figure 4.11. This shows everything that was detected in a wider mass range; from 10,000 Da up to 155,000 Da. The noise levels in these spectra make the data rather messy and difficult to interpret, however, it still becomes obvious that in addition to the intact mAb at approximately 147,000 Da, there is another structure present, giving rise to peaks at 73,000 Da, approximately half the mass of the intact mAb. This structure is the HL dimer, or so called half-antibody (see section 1.6.4) that is the result of the non-covalently bound  $H_2L_2$  tetramer, which in this case has fallen apart into two HL dimers. Looking more closely at these structures it becomes clear that the tetramers that are non-covalently bound have the same glycosylation pattern as the covalently bound tetramers, with the main glycoform shifting from G1F on days six and seven, to G0F on days 11, 14 and 17. This justifies only taking the intact mAb into account when doing the glycan analysis detailed above.

Figure 4.12 shows the mass spectra of the samples from the second fermentation with the wider mass range from 10,000 Da to 155,000 Da, where the intact mAb as well as the non-glycosylated and glycosylated half-antibody is visible. Due to the lower noise levels in these spectra it becomes possible to do a more detailed interpretation of the data. By visual inspection it looks like the proportion of half-antibodies is decreasing over time of culture; the non-glycosylated half-Abs seem to only slightly decrease, while the glycosylated dimers seem to decrease more notably. As for the first fermentation, the mass of the glycosylated half-Ab shifts from having the G1F glycoform on day 8 towards having the G0F glycoform on days 11, 14 and 15, supporting the observations from Figure 4.6.

Due to the different ionisation potentials of the HL dimer and the  $H_2L_2$  tetramer the amounts are not quantifiable, but the general trend can be studied by looking at the relative amounts; the peak of highest intensity was set to 1 and the ratios of the intensities of the other peaks to the highest were calculated as detailed in

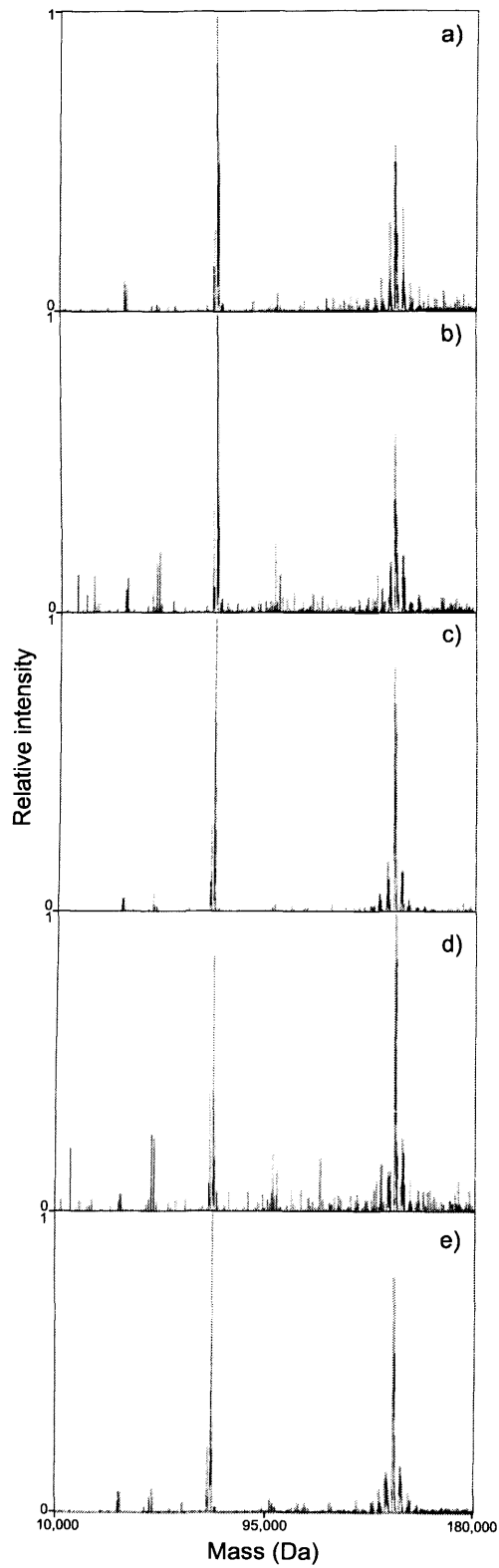


**Figure 4.11** Effect of harvest time on the overall mAb composition, 1<sup>st</sup> fermentation.

Legend on following page.

*Figure 4.11 continued. The traces correspond to the samples in Figure 4.5, but here the whole mass range is shown as an overview; from 10,000 Da to 180,000 Da. The spectra contain a lot of noise due to solvents, so no detailed information can be obtained from this figure. However, it still becomes obvious that there are two main peak clusters; one with masses around 73,000 Da and one with masses around 146,000 Da. The higher mass peak cluster, at 146,000 Da, corresponds to the intact antibody, while the lower mass peak cluster corresponds to a “half-antibody” made up of one heavy and one light chain (see section 1.6.4). Looking closer, there are two distinct peaks here; the one of the lower mass, less than 72,000 Da, corresponds to a non-glycosylated HL dimer, while the one with a slightly higher mass, over 73,000 Da, corresponds to a glycosylated HL dimer. The mass of the latter peak shifts from 73,396/7 Da in a) and b) (day 6 and 7) to 73,234/7 in c), d) and e) (day 11, 14 and 17). The mass during day 6 and 7 corresponds to a HL dimer with the C-terminal lysine on the heavy chain cleaved off and the N-terminal glutamine on the heavy chain converted to pyroglutamic acid, plus the G1F glycan attached at Asn297. On day 11, the mass of the peak shifts to correspond to a HL dimer with the same basic structure, but instead of the G1F glycan, it has the G0F glycan attached. This data correlates nicely with the findings from figure 4.3; the complexity of the glycans decreases over time of culture and also shows that the glycosylation patterns are the same for the non-covalently bound H<sub>2</sub>L<sub>2</sub> tetramers, that here have dissociated into dimers, as for the covalently bound tetramer.*

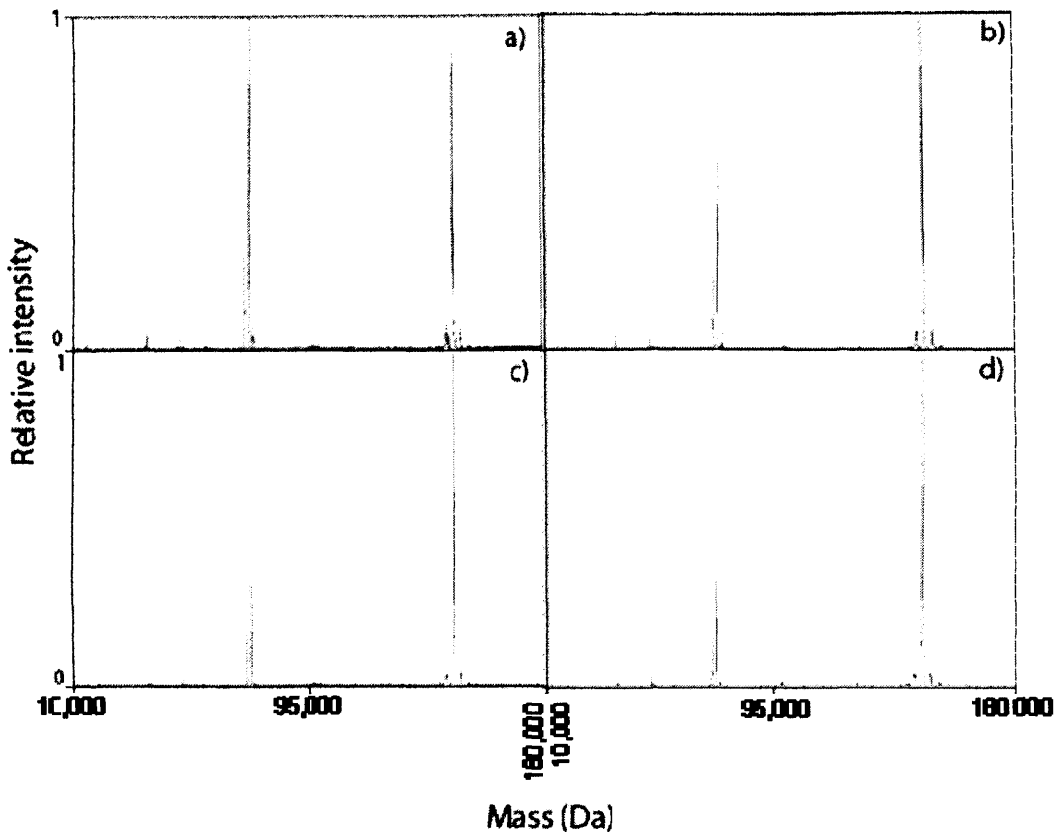


**Figure 4.12** Effect of harvest time on the overall mAb composition, 2<sup>nd</sup> fermentation

The traces correspond to the samples in Figure 4.6, but here the whole mass range is shown as an overview; from 10,000 Da to 180,000 Da. The peak of highest intensity was set to 1 and from this the relative amount of each structure could be determined. Three main distinct peaks can be seen that are actually clusters of peaks when looking more closely, corresponding to the different modifications and glycosylation patterns present. There is one group just under 72,000 Da, which corresponds to non-glycosylated HL dimers, i.e. “half-Abs” (see section 1.6.4). The second one is the glycosylated form of the HL dimer, with masses on 73,000 Da. The third peak is the intact Ab, with the main peak at 146,636 Da, corresponding to the basic antibody structure with both C-terminal lysines cleaved off (0K), the N-terminal glutamines converted to pyroglutamic acid (pE) and with the G0F/G1F glycoform. From determination by eye, it seems the proportion of HL dimers is decreasing over time of culture, from day 8 to day 15. The non-glycosylated half-Abs seem to only slightly decrease, while the glycosylated half-mAbs seem to decrease more notably. The mass of the latter shifts from 73,396 Da on day 8 towards 73,234 Da on days 11, 14 and 15. A mass

of 73,396 Da corresponds to the HL dimer with both lysines cleaved off (OK), the glutamine converted to pyroglutamic acid (pE) and with the G1F glycoform attached to the heavy chain, while a mass of 73,234 Da corresponds to the same basic mAb structure, but with the G0F glycoform attached. These findings correlate nicely with the observations from Figure 4.6; the level of galactosylation decreases with time of culture. From this it can also be concluded that the non-covalently bound H<sub>2</sub>L<sub>2</sub> tetramers carry the same glycoforms as the covalently bound tetramers.

Day	Half-mAb (non-glyc)	Half-mAb	Intact mAb
8	0.28	: 1	: 0.9
11	0.22	: 0.57	: 1
14	0.16	: 0.31	: 1
15	0.17	: 0.32	: 1

**Table 4.3 Effect of harvest time on the proportion of HL dimers, 2<sup>nd</sup> fermentation**

From Figure 4.12 the relative amounts of non-glycosylated half-mAb, glycosylated half-mAb and intact mAb were measured and the ratios of the three were calculated as can be seen in the table above. The first figure represents the non-glycosylated HL dimers, the second represents the glycosylated HL dimers and the last is the intact mAb. These calculations confirm the initial observations from Figure 4.12; the relative amounts of both non-glycosylated and glycosylated half-Abs decrease with time, by 40% and 70% respectively.

Table 4.3. The calculated values support the observations made by eye from Figure 4.12; the proportion of half-Abs decreases with time, the non-glycosylated dimer by 40% and the glycosylated dimer by 70%.

#### ***4.5 Lysine and glycoform levels***

The lower noise levels of the mass spectra in the second fermentation allow for a comparison of lysine levels on the mAb in samples from different times in culture, represented by a histogram in Figure 4.13. This shows that the predominant structure has both lysine residues cleaved off (0K) at a level of 60-67% of the mAb population while structures with one or two intact lysines make up 20-25% and 12-16% respectively. This was also confirmed by analysis of a deglycosylated mAb (Figure 4.14), which shows one main peak representing the intact mAb with both N-terminal glutamine residues converted to pyroglutamic acid and both lysines cleaved off. It also shows a second peak where the mAb still has one intact lysine, representing approximately 17% of the population and a third peak where both lysines are still intact, representing approximately 5%. Since the lysine levels stay more or less constant over the time course of culture, regardless of glycan structure, it was thought justified the decision to concentrate on the main peaks (both lysine residues cleaved) for the glycan analysis. A more detailed analysis of the amounts of the different glycoforms was also carried out. The relative amount of each glycoforms was calculated from the spectra in Figure 4.6, taking into account all lysine variants (0K, 1K and 2K) and then plotted as a histogram in Figure 4.15. This gives an overview of how the proportions of the glycoforms change over time of culture and aids in showing how the glycoforms with a lower degree of galactosylation, G0/G0F and (G0F)<sub>2</sub>, increases in proportion over time, while the more complex glycans, (G1F)<sub>2</sub>, G1F/G2F and (G2F)<sub>2</sub> decreases. This agrees nicely with the initial observations made by visual inspection of Figure 4.6.

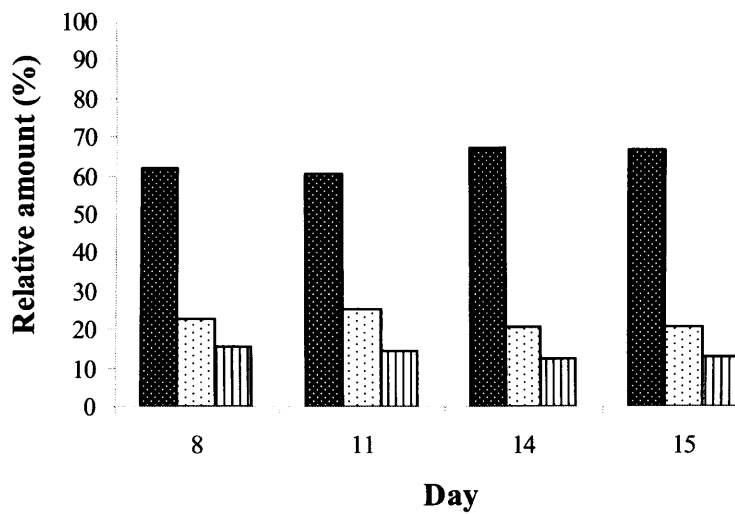


**Figure 4.13 Lysine levels over time, 2<sup>nd</sup> fermentation**

The relative intensities of the peaks representing different numbers of lysines were compared. All mAb versions (i.e. different glycan forms) of 0K (■), 1K (▨) and 2K (▩) were added together and the relative amount was calculated for each of them and plotted as a histogram, above. The predominant structure (60-67%) has had both lysine residues cleaved off, 0K, with structures of one and two intact lysines representing 20-25% and 12-16% respectively. The above representation shows that the lysine levels stay fairly constant over time of culture, possibly with a slight increase in the 0K variant towards the end of fermentation.

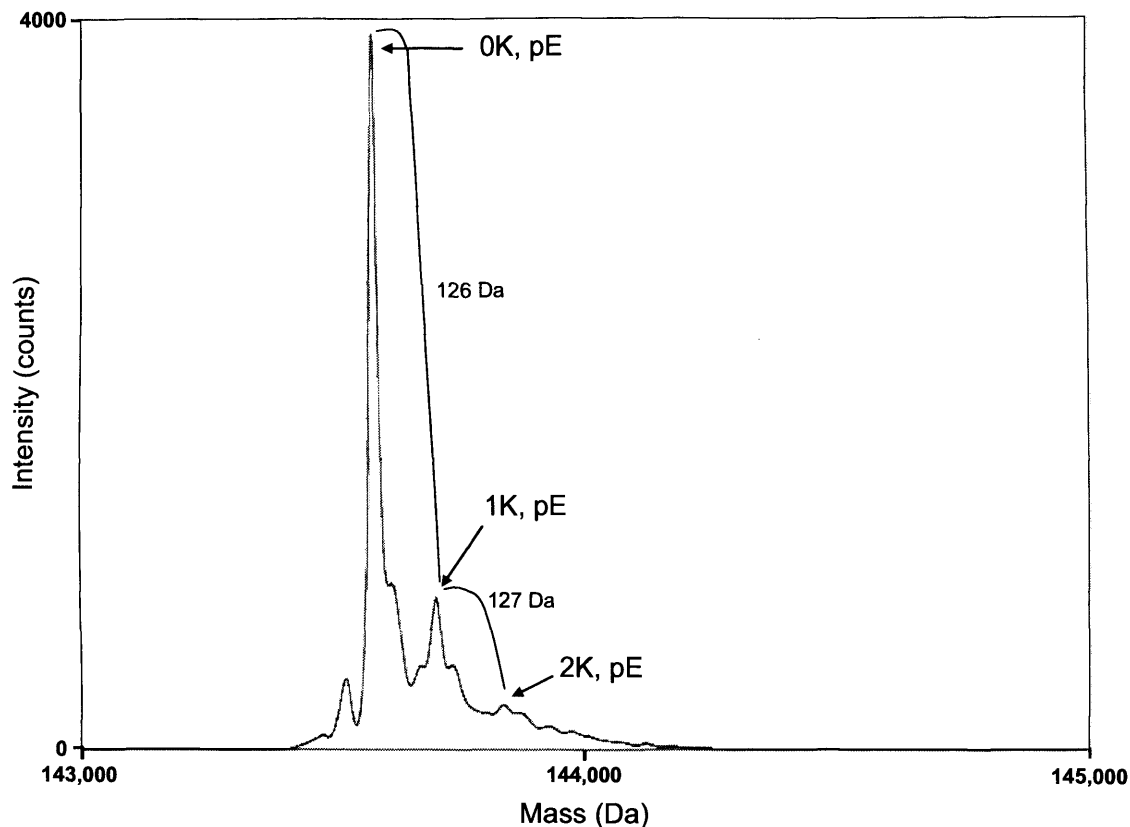


**Figure 4.14 Deglycosylated mAb**

Deglycosylation of the mAb was carried out (for conditions see section 2.7.1) and the mAb was then analysed again using LC/MSD-TOF resulting in the spectrum above. The main peak at 143,583 Da represents the intact deglycosylated mAb with both lysines cleaved off and both glutamine residues converted to pyroglutamic acid (theoretical mass 143,577 Da). The second prominent peak has a mass increase of 126 Da as compared to the main peak, representing the intact deglycosylated mAb with one lysine intact (theoretical mass 143,705 Da). A third peak is also visible at +253 Da compared to the main peak, representing the intact deglycosylated mAb with both lysines still intact (theoretical mass 143,833 Da).

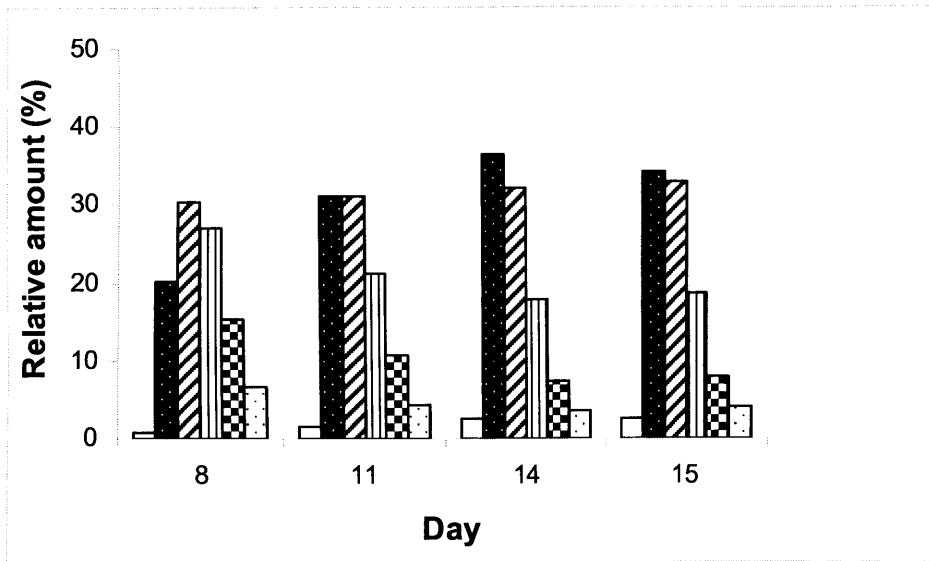


**Figure 4.15 Glycoform levels over time, 2<sup>nd</sup> fermentation**

From Figure 4.6 the area of each peak was measured and the relative amounts of the glycoforms were calculated, taking into account all lysine variants (0K, 1K and 2K). The resulting histogram gives an overview of how the proportions of the glycoforms change over time of culture. The bars represent the following glycoforms; (□) G0/G0F, (■) (G0F)<sub>2</sub>, (▨) G0F/G1F, (▩) (G1F)<sub>2</sub>, (▣) G1F/G2F, (▤) (G2F)<sub>2</sub>. The figure shows clearly how the glycoforms with a lower degree of galactosylation, G0/G0F and (G0F)<sub>2</sub>, increases in proportion over time, while the more complex glycans, (G1F)<sub>2</sub>, G1F/G2F and (G2F)<sub>2</sub> decreases over time. The G0F/G1F mAb contains one glycoform with lower levels of galactosylation and one with higher and shows a nice correspondence by staying at a constant proportion over time.

## 4.6 Discussion

The two separate fermentations were carried out using the same cell line, media and culture conditions. If the slight lag phase that was experienced during the second culture is disregarded, the two fermentations were very similar with respect to cell growth and they should therefore give good indications to the reproducibility of the results on mAb structure and conformation as well as any variations between batches. The combined results help us gain a better understanding of the events determining structure.

The first fermentation was kept until day 17 in order to look at how the mAb concentration and overall performance of the culture change over the last couple of days. From this data it can be seen that there is no significant increase in product titres from day 14 to 17, while there is a very marked decrease in cell viability during the same period. With dying cells there is an increase in cell lysis, which would then lead to the release of intracellular material. This could in turn make subsequent purification steps harder, making it important to reach a balance between mAb production and cell death. The rapid decrease in viability and the relatively small increase in product titres over these last two to three days of culture explain the reasons behind the industry standard to harvest on day 15.

The main focus of this study was to look at the integrity of the molecular structure of the mAb over time of culture. It is of common knowledge that the C-terminal lysine residues of mAb produced by mammalian cell culture are prone to cleavage. MAb populations with almost complete absence of C-terminal lysines have previously been reported (Beck et al, 2005; Harris et al, 1990). In contrast, here it was shown that approximately two thirds of the final product have had both lysines removed, 20-25% have one lysine and 12-16% still have both lysines intact, similar to observations made by Santora et al. (1999). We have shown that the lysine levels of the mAb population stay relatively constant over time of culture, possibly with a slight decrease in intact lysine residues. This is however not of great importance with respect to the efficacy of the mAb, since the presence

of a C-terminal lysine residue does not impact the activity. However it could be of concern for validation purposes.

What is of greater importance is the glycosylation pattern due to its relationship to crucial attributes, such as stability (Broersen et al, 2004; Krapp et al, 2003; Mimura et al, 2000) and activity (Lund et al, 1996). The peak distribution of the mass spectra shows that two different glycans can be attached to the heavy chains of a mAb H<sub>2</sub>L<sub>2</sub> tetramer, which has been reported previously (Gadgil et al, 2006). From the mass spectra of both fermentations it becomes evident that the glycosylation pattern of the mAb is changing over time of culture. The main glycoform shifts from (G1F)<sub>2</sub>, when the cells are in late exponential/early stationary phase, to (G0F)<sub>2</sub>, towards the end of culture, i.e. a decrease in the level of galactosylation is experienced. The G0F glycan is the most abundant at time of harvest, which is in accordance with previous findings (Krapp et al, 2003). The explanation for the observations of decreased levels of galactosylation over time can be one or more of several: the antibodies could be modified while in the broth by for example proteolytic degradation; glycosylation could be compromised due to production of high antibody titres, i.e. the cells are stressed and therefore failing to attach additional galactose residues; the cells could be starting to lyse. The two last mentioned explanations would both lead to the release of incompletely processed material, such as glycoforms with lower levels of galactosylation. It is at this point difficult to determine which one or what combination of the factors are the underlying reason for the observations made, but subsequent experiments (discussed in chapter 6) have been designed to rule out some hypotheses.

Glycosylation is affected by various changes in the operating environment; previous studies have reported changes in glycosylation patterns with different culture methods (Cabrera et al, 2005; Kunkel et al, 2000; Maiorella et al, 1993; Schweikart et al, 1999), culture conditions (Kunkel et al, 2000; Maiorella et al, 1993) and media composition (Cabrera et al, 2005; Serrato et al, 2007) to mention a few. There have been some previous studies monitoring glycosylation over the time-course of culture, to which similarities can be drawn from the results presented here. One was carried out by Goldman et al, 1998, who studied the glycosylation site-occupancy of interferon-gamma (IFN- $\gamma$ ), which has three glycosylation sites, produced by NS0 cells. They did not observe any major

variations in site-occupancy during perfusion culture, but noticed a slight decrease towards the later stages of stirred-tank culture. They also recorded changes in levels of sialylation over time; an increase in sialylation during the first 200 h of perfusion culture and then more constant levels, while sialylation during stirred-tank culture was fairly constant and then started to decrease after 200 h of culture. They reported that for both culture methods, maximal sialylation was associated with periods of rapid cell growth. Similarly, this is true for the highest levels of galactosylation recorded here as well, where decreased galactosylation was observed from early stationary phase and onwards. Goldman et al. (1998) suggest some similar explanations to those reported here when trying to explain the observed decreases; the action of extracellular sialidases released from lysed cells or compromised cellular sialylation (in our case galactosylation). They also suggest it could be due to the build-up of toxic metabolites, such as ammonia, which could possibly change the pH inside the cell to a sub-optimal one for sialyltransferase activity. Another report looking at glycosylation over time of culture was carried out by Robinson et al, 1994. This group characterised an IgG1 produced through a prolonged fed-batch culture of NS0 cells over 22 days. Glycosylation of proteins produced by NS0 cells differ to that of those produced by CHO cells, but the main overall finding of an increase in truncated glycoforms is along the lines of our observations of an increase in glycoforms with lesser complexity later in culture. Robinson et al. (1994) also noted an increase in the amount of high-mannose oligosaccharides, which was not observed in our study. They ruled out glucose starvation and ammonia inhibition as possible reasons behind the behaviour and concluded that mAb production by non-viable cells and the release of incompletely processed mAb by lysed cells were negligible. Overall, the findings of this group support our hypothesis that the cells produce mAb with less complex glycans towards the later stages of culture, perhaps due to the high rates of product formation. No matter what the reasons behind the change in the glycosylation profile are, it is important to draw attention to the fact that they do take place. As mentioned, glycosylation is a post-translational modification of importance to for example stability and activity and therefore the efficacy when used as a pharmaceutical. Changes in the glycosylation profile have to be taken into careful consideration when designing the production process. It should be an important factor, along with cell growth and viability and mAb titres,

in the decision making process as to when to harvest. The level of heterogeneity that is acceptable has to be agreed and the reproducibility is crucial for validation purposes. This study has not taken into consideration which is the most efficacious glycoform, but this has to be determined for each individual case and cause. The way forward then has to be discussed; is it feasible to harvest at the point when the desired glycoform is in abundance? It seems that glycoengineering would be a beneficial option, both in order to achieve highest possible efficacy of the product, but also to achieve batch-to-batch consistency and minimise any heterogeneity present.

The other aspect of the mAb structure that was closer looked at in this study is the overall composition of the H<sub>2</sub>L<sub>2</sub> tetramer. From the spectra, it is obvious that a proportion of the mAb is present as HL dimers rather than tetramers, which is a trait of the IgG4 subclass and due to non-covalent bonds (Angal et al, 1993; Bloom et al, 1997; Deng et al, 2004; King et al, 1992; Zhang and Czupryn, 2002). The measurements are not quantifiable but give a good indication as to what is happening; the proportion of HL dimers is decreasing over time of culture. The reason for the decrease is not clear, but the important aspect from a process economics point of view is their existence. The HL dimers are not fully functional products and due to their different conformation they would be separated and removed during the last polishing steps in the purification process, for example by size exclusion or ion exchange chromatography. This means parts of the produced mAbs will be, despite being functional in theory, removed and discarded, resulting in a loss in yield. The sizes of these losses are not known and are outside the scope of this study; it is difficult to make an estimation due to the non-quantifiable detection methods, as well as possibly sub-optimal purification and storage procedures, compared to industrial processes. However, they could be substantial. One way of overcoming these problems is to use a different subclass than IgG4, or use genetic engineering to change the hinge region to that of for example IgG1 or IgG2 (Angal et al, 1993; Bloom et al, 1997). However, if the IgG4 subclass is preferred, extensive research has to be carried out in order to minimize any losses due to these HL dimers. Attempts have been made to reduce their existence by for example media additions, such as copper sulphate, which creates an oxidative environment, facilitating the formation of disulphide bonds

(Chaderjian et al, 2005) or by preventative screening for the most promising clone during cell line development (Deng et al, 2004).

The presence of the half-mAbs also brings further questions, such as; what physical conditions affect the proportion of dissociated tetramers? Are there more non-covalently bound mAbs in the final product? And if there are, will they stay bound or will they dissociate upon processing, formulation and storage? Some of these queries have been dealt with in the following studies in order to get a better understanding of the effect of processing on the conformation of the H<sub>2</sub>L<sub>2</sub> tetramer structure, as well as the glycosylation profile.

## **5 Effect of harvest on the molecular structure and overall conformation of a mAb**

### ***5.1 Effect of shear on the glycosylation profile of a mAb***

This study examines the effect of means of cell removal after cultivation on the molecular structure of recombinant IgG. Ultra scale-down tools were applied to allow better prediction of the effects of early stage cell recovery by centrifugation on the structural authenticity of the protein. A shear-device mimicking the conditions at the inlet of a large-scale disc stack centrifuge was used to compare samples processed with or without shear.

#### **5.1.1 Sampling overview**

A 10 L fed-batch airlift fermenter was used (fermentation 1 from Chapter 4, for conditions see section 2.1) and samples were taken on three separate days for comparison (days 7, 14 and 17). Figure 5.1 shows the overview of the sampling protocol, for shearing and centrifugation conditions see sections 2.3 and 2.2 respectively. Sample a) was not sheared and used as control, sample b) was sheared after centrifugation to study the effect of shear on the mAb itself, while sample c) was sheared prior to centrifugation in order to mimic the large scale process and study the effect of shear on the whole cell broth. Sample c) should also confirm whether the decreased complexity of the glycoforms observed in chapter 4 is due to the release of incompletely processed mAbs from lysed cells. All samples were purified using protein A chromatography (see section 2.6) and the intact mAb analyzed using the Agilent Bioanalyzer (see section 2.8.1) and time-of-flight mass spectrometry (see section 2.9.1).

#### **5.1.2 Structural analysis**

The Agilent Bioanalyzer was used to confirm the purity of the samples as well as investigate the effect of shear on the overall conformation of the mAb. Figure 5.2 shows the electrophoresis data of the samples from days 7, 14 and 17. Proteins are present as intact mAbs at approximately 160 kDa and half-mAbs at 80 kDa, with no other contaminating proteins visible. Densitometric analysis of the gel reveals

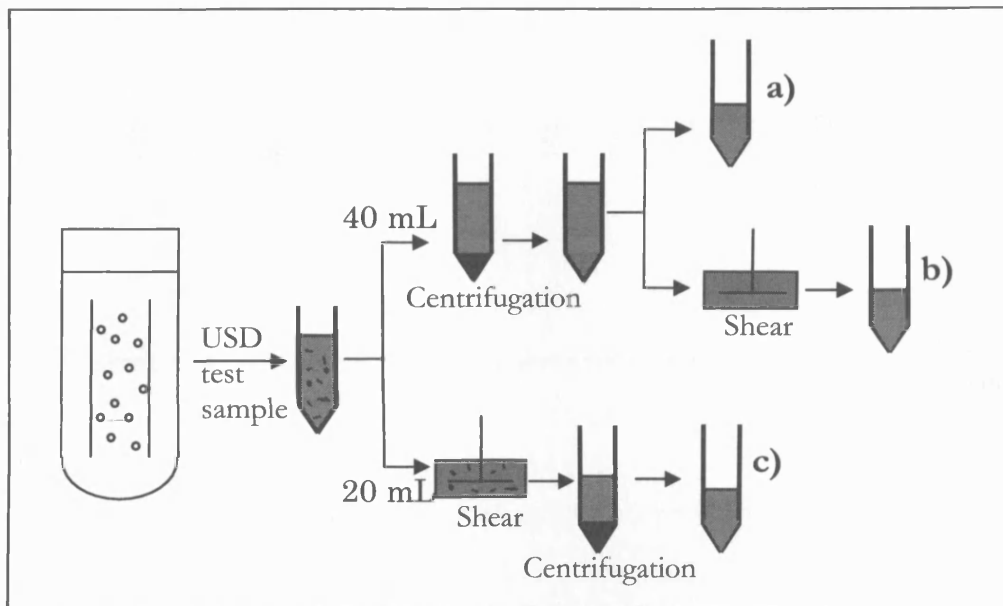


**Figure 5.1 Sampling overview**

Each day of sampling, 60 mL broth was removed from the fermenter. 40 mL was centrifuged as described previously (see section 2.2), the cells were discarded while the supernatant was split in two. The first part (a) was not treated with any shear, but only purified using protein A affinity chromatography (see section 2.6) and used as standard in the comparison. The second part (b) was sheared using standard conditions (see section 2.3) after removal of cells but prior to protein A purification, to study the effect of shear directly on the mAb. The remaining 20 mL (c) were sheared using standard conditions before centrifugation and purification so that the effect of shear on the whole cell broth could be examined. The following denotations will be used; a) standard, b) sheared supernatant, c) sheared broth.

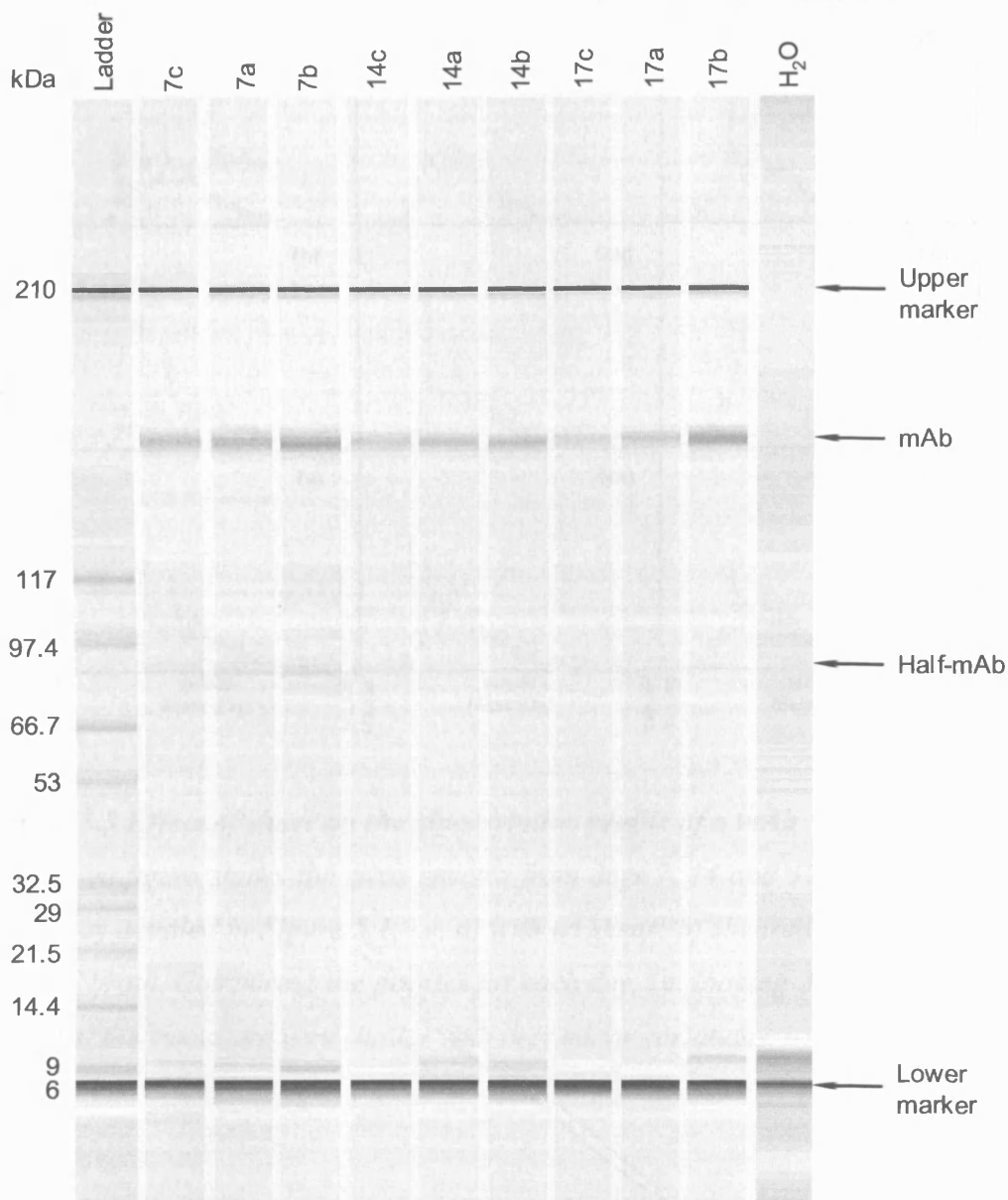


**Figure 5.2** Effect of shear on mAb conformation

Bioanalyzer protein 200 assay after protein A chromatography. The samples are from days 7, 14 and 17, with the annotations from Figure 5.1: a) no shear; b) sheared clarified mAb; c) sheared cell broth. The intact mAb can be seen with an approximate mass of 160 kDa and a small proportion of half-mAbs can also be seen at approximately 80 kDa. No other contaminating proteins are present. Water was used as control.

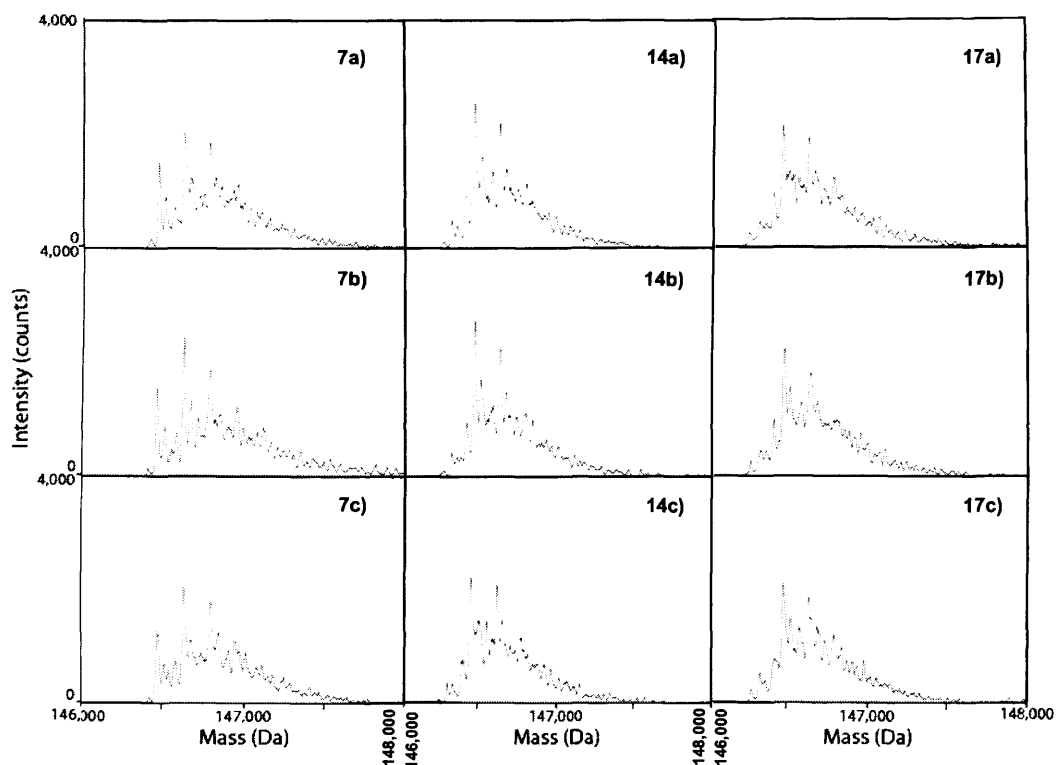


**Figure 5.3** Effect of shear on the glycosylation profile of a mAb

The above figure shows the mass spectra from days 7, 14 and 17. Samples were treated as detailed in Figure 5.1, i.e. a) with no shear; b) sheared supernatant; c) sheared broth. Comparing the profiles for each day, i.e. looking down each of the columns, the traces are very similar with only minor variations.

there are no significant differences between samples treated with no shear, sheared clarified mAb or sheared cell broth, with regards to product composition and proportion of half-mAbs. There is one exception to this; the sheared clarified supernatant from day 7 shows half the proportion of HL dimers as compared to the non-sheared and the sheared cell broth. The reason behind this is unclear, but could just be due to a misrepresentative sample, since no trends are visible among the other samples. The analysis shows a decrease in the proportion of half-mAbs with time of culture, from ~40% on day 7 to ~9% on day 17, supporting the results from section 4.4. The traces from the mass spectrometry analysis can be seen in Figure 5.3. For each of the days, the glycosylation profiles are very similar; no clear differences seem to have been caused by shear, either on the antibody itself (b) or the overall profile when intracellular material was released into the product stream (c). The minor differences that can be seen are most likely due to the deconvolution process. The results presented here indicate that shear during the first clarification step does not have an impact on the glycosylation pattern of mAbs, however, in order to confirm these findings, further experiments were designed and carried out as detailed in section 5.2.

## ***5.2 Effect of shear rate and time***

From the previous investigation of the effect of shear on the glycosylation profile of the mAb (section 5.1) it looked as if shear during the first clarification step does not have an impact. In order to confirm this, a further shear study was carried out on a third fermentation. Here the rate and time of shearing was taken into consideration, since these would vary with the flow rate of a continuous large scale centrifuge and with the model used. Two different shear rates were used in addition to a control sample treated with no shear. Two different shear times were also used in addition to the control sample.

### **5.2.1 Sampling overview**

Figure 5.4 shows the overview of the sampling protocol. In order to study the effect of both shear rate and time, two sets of samples were compared: a, b and d

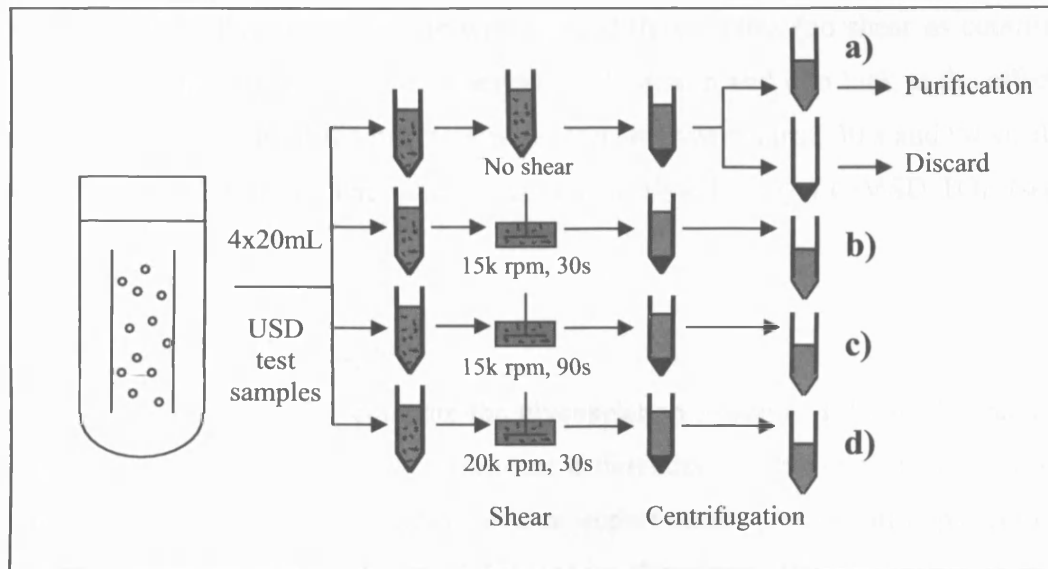


**Figure 5.4 Sampling overview of shear investigation**

A sample of 100 mL was taken on day 13 of culture and split into four. Each 20 mL sample was purified the same way but with different shearing conditions. The first sample (a) was not sheared and used as control in the comparison. The remaining samples were sheared as follows; b) 15,000 rpm for 30 s, c) 15,000 rpm for 90 s and d) 20,000 rpm for 30 s. All samples were centrifuged (see section 2.2), the cell pellet discarded and the product-containing supernatant purified by protein A chromatography (see section 2.6).

to look at the effect of shear rate with three different rates (no shear as control, 15,000 rpm and 20,000 rpm), all sheared for 30 s; a, b and c to look at the effect of shearing time with three different times (no shear as control, 30 s and 90 s), all sheared at 15,000 rpm. The intact mAb was analysed using LC/MSD-TOF (see section 2.9.1).

### 5.2.2 Structural analysis

The spectra in Figure 5.5 compare the glycosylation patterns of the mAbs treated with different shear rates. No significant differences can be seen in the traces, suggesting that shear rate does not have an impact on the glycosylation pattern of the mAb. The spectra in Figure 5.6 compare the glycosylation patterns of the mAbs exposed to shear for different lengths of time. Again no significant differences can be seen in the traces suggesting that the time the mAb is exposed to shear does not affect the glycosylation pattern either.

The spectra in Figure 5.7 look at the overall composition of the product stream with respect to half-mAbs and intact mAbs, after treatment with different shear rates. By visual inspection the proportion of HL dimers seem to increase upon treatment with shear, i.e. when comparing a) (treated without shear as a control) with b) and c) (sheared for 30 s at 15,000 rpm and 20,000 rpm respectively). However, when comparing the two different shear rates, i.e. 15,000 rpm and 20,000 rpm in b and c respectively, there seems to be no difference in the half-mAb proportion. This indicates that shear increases the proportion of dimers, but only to a certain extent; there seems to be an upper limit in how much the dimers can increase. In Table 5.1 the relative amounts of HL dimers and intact mAbs were calculated and the ratios were compared between the samples treated with different shear rates. The calculated ratios confirm the initial observations from Figure 5.7; there is an increase in half-mAb by approximately 9% upon shearing, but no increase from shearing at a higher rate. If then looking at the effect of shearing time on the overall conformation (Figure 5.8), similar results are observed. There is an increase in the proportion of half-mAbs upon shearing, i.e. comparing a) (no shear) with b) and c) (sheared at 15,000 rpm for 30 s and 90 s respectively), but no apparent increase when shearing for a longer time

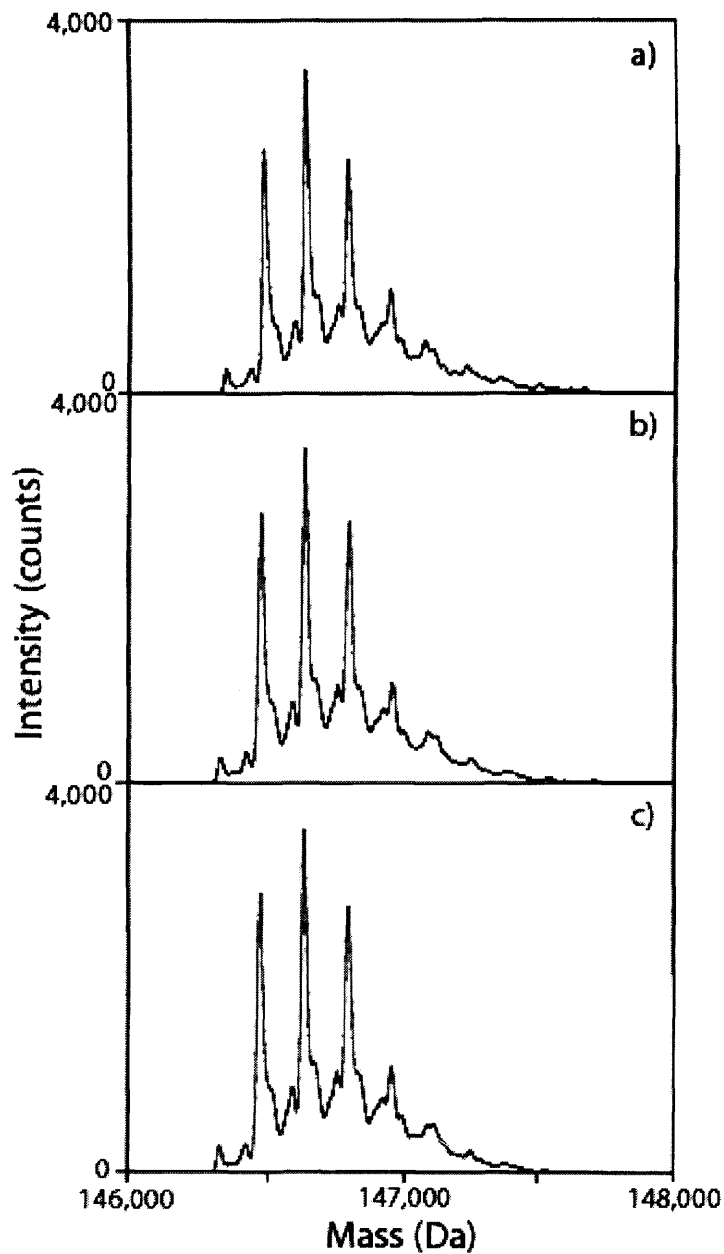


**Figure 5.5** Effect of shear rate on the glycosylation profile of a mAb

The above figure shows the mass spectra of the samples treated as detailed in Figure 5.4, i.e. a) with no shear; b) sheared at 15,000 rpm; d) sheared at 20,000 rpm. No significant differences can be seen for the different shear rates.

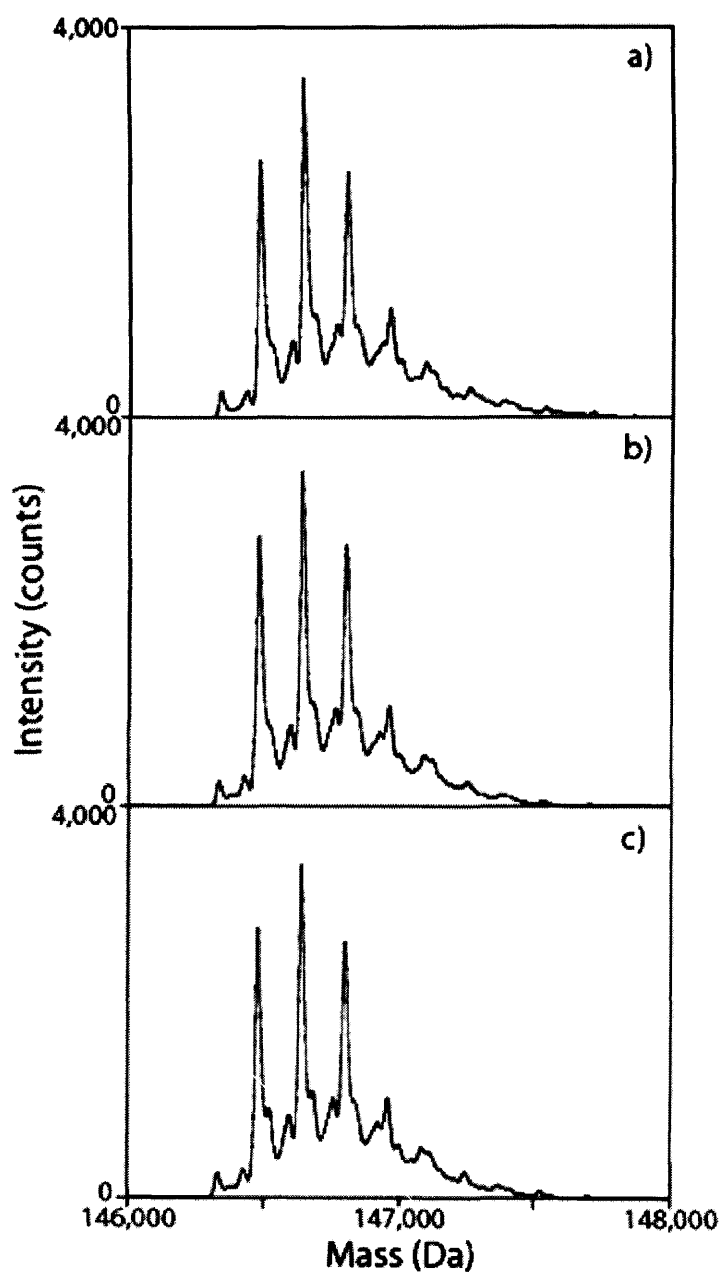


**Figure 5.6** Effect of shearing time on the glycosylation profile of a mAb

The above figure shows the mass spectra of the samples treated as detailed in Figure 5.4, i.e. a) with no shear; b) sheared for 30 s; c) sheared for 90 s. No significant differences can be seen for the different shearing times.

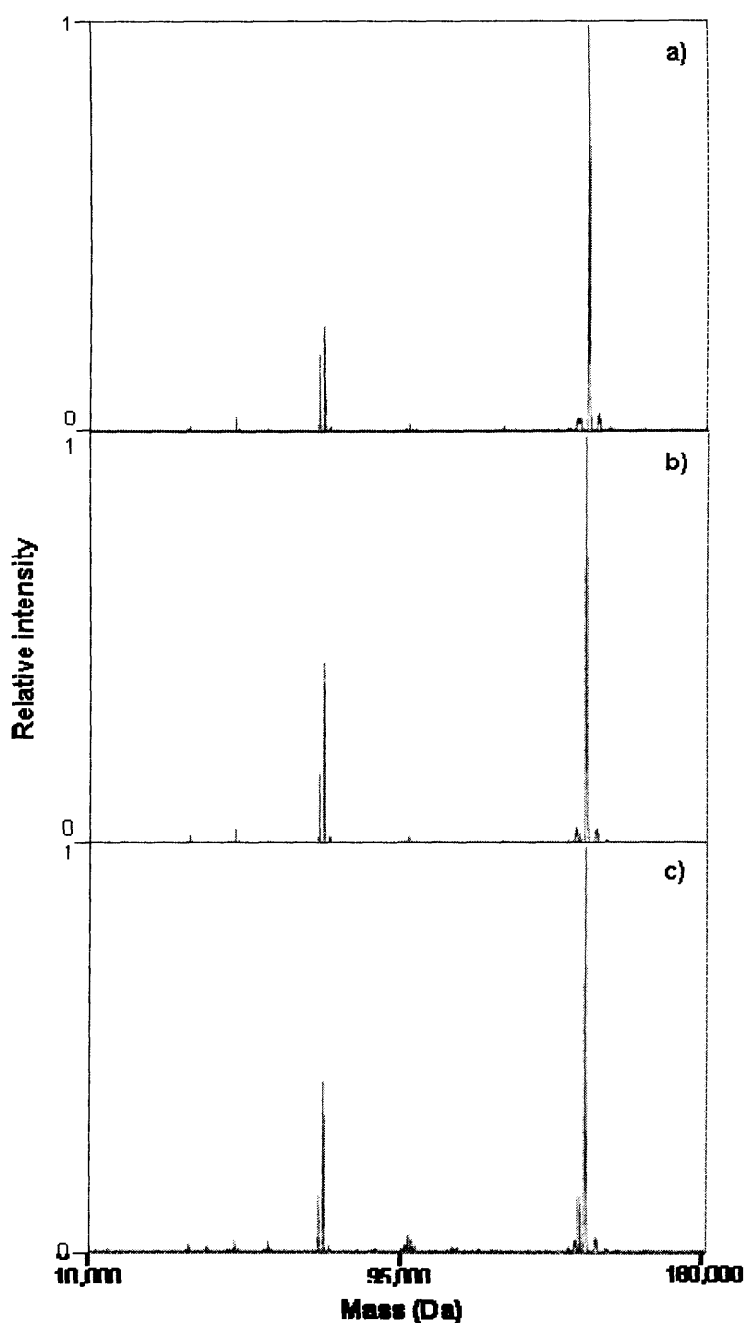


**Figure 5.7** *Effect of shear rate on the conformation of a mAb*

The above figure corresponds to the spectra with the same denotation in Figure 5.5, with a) being treated with no shear as control, b) sheared at 15,000 rpm and c) sheared at 20,000 rpm. There are three main peaks visible: non-glycosylated half-mAb; glycosylated half-mAb and intact mAb. By looking at the intensity of the half-mAb peak, as compared to the intact mAb, b) and c) seem to be of similar proportions, while a) has a slightly lower proportion of half-mAb.

Sample	Half-mAb (non-glyc)	Half-mAb	Intact mAb
0 rpm 0 s	0.19	: 0.26	: 1
15k rpm 30 s	0.17	: 0.44	: 1
20k rpm 30 s	0.14	: 0.42	: 1

**Table 5.1 Proportion of HL dimers after shearing at different rates**

From Figure 5.7 the relative amounts of non-glycosylated half-mAbs, glycosylated half-mAbs and intact mAbs were measured and the ratios of the three were calculated as can be seen in the table above. The first figure represents the non-glycosylated HL dimers, the second represents the glycosylated HL dimers and the third is the intact mAb, i.e.  $H_2L_2$  tetramers. The spectral data is not quantifiable but any changes in proportions give an indication to differences between the samples. The data here supports the initial observations observed by eye in Figure 5.7; there is an increase in the proportion of glycosylated half-mAb upon shearing (comparing a with b and c), but there seems to be no increase when shearing at a higher rate (comparing b and c).

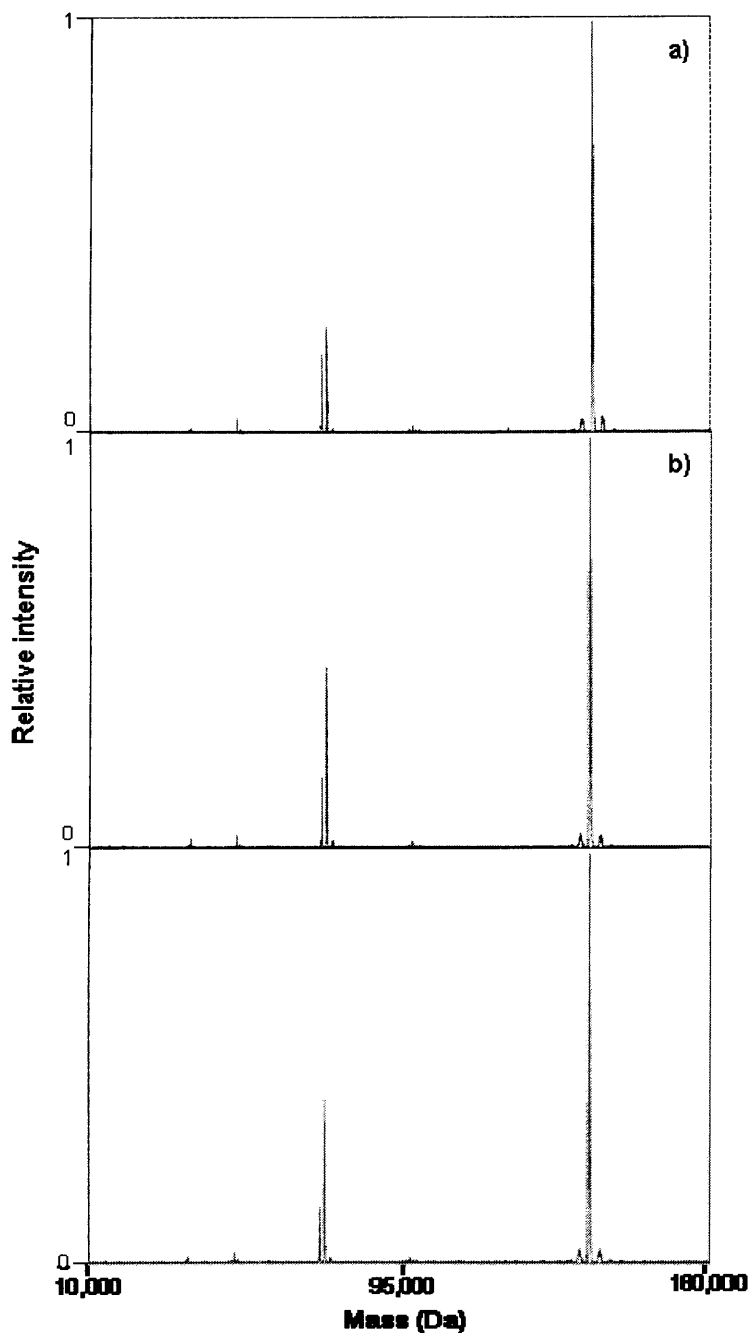


**Figure 5.8** *Effect of shearing time on the conformation of a mAb*

The above figure corresponds to the spectra with the same denotation in Figure 5.6, with a) being treated with no shear as control, b) sheared for 30 s and c) sheared for 90 s. There are three main peaks visible: non-glycosylated half-mAb; glycosylated half-mAb and intact mAb. By looking at the intensity of the half-mAb peak, as compared to the intact mAb, b) and c) seem to be of similar proportions, while a) has a slightly lower proportion of half-mAb.

Sample	Half-mAb (non-glyc)	Half-mAb	Intact mAb
0 rpm 0 s	0.19	: 0.26	: 1
15k rpm 30 s	0.17	: 0.44	: 1
15k rpm 90 s	0.14	: 0.40	: 1

**Table 5.2 Proportion of HL dimers after shearing for different times**

From Figure 5.8 the relative amounts of non-glycosylated half-mAbs, glycosylated half-mAbs and intact mAbs were measured and the ratios of the three were calculated as can be seen in the table above. The first figure represents the non-glycosylated HL dimers, the second represents the glycosylated HL dimers and the third is the intact mAb, i.e.  $H_2L_2$  tetramers. The data here supports the initial observations observed by eye in Figure 5.8; there is an increase in the proportion of glycosylated half-mAb upon shearing (comparing a with b and c), but there seems to be no increase when shearing for a longer time (comparing b with c).

(comparing b and c). Table 5.2 confirms these observations and shows that there is an increase in half-mAb by approximately 8% upon shearing, but no increase when shearing for a longer time.

### ***5.3 Comparison of intra- and extracellular mAb***

In order to get a better understanding of the impact the release of intracellular material could have on the overall composition of the mAb, an investigation comparing the intra- and the extracellular mAb was carried out. The experiments detailed below were designed to determine any effects the release of intracellular material, due to cell lysis, could have on the overall composition of the product stream.

#### **5.3.1 Sampling overview**

Samples were taken on days 9 and 13 from the third GS-CHO fermentation as detailed in Figure 5.9. The sample was centrifuged to separate the cells from the product-containing supernatant. The cells were resuspended and homogenised to release any intracellular material, while the supernatant was immediately purified. Both samples were purified using protein A chromatography.

#### **5.3.2 Structural analysis**

After purification the intact mAb was analysed using time-of-flight mass spectrometry as before. The deconvoluted spectra from the analysis can be seen in Figure 5.10, showing the overall composition of the product. The extracellular material (9a and 13a) contains mainly HL dimers and intact mAbs. The proportion of HL dimers decreases from day 9 to day 13 in accordance with the findings from section 4.4. The intracellular material on the other hand (9b and 13b), contains barely any intact mAb, suggesting the mAbs are secreted immediately after assembly. The intracellular material is instead made up of single heavy chains, HL dimers and heavy chain dimers (HH). The proportion of each complex was calculated and listed in Table 5.3. This shows that the intracellular material from day 9 and day 13 are similar in composition, with the exception that the material from day 13 contains a larger proportion of non-glycosylated HL dimers and a smaller proportion of glycosylated single heavy chains.

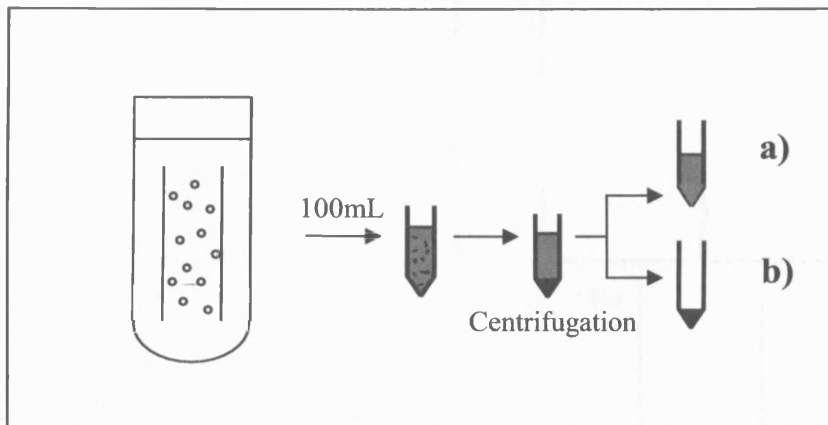


**Figure 5.9 Sampling overview**

A sample of 100 mL was taken on days 9 and 13 of a 10 L fed-batch fermentation (see section 2.1). The sample was spun down using a bench-top centrifuge (for conditions see section 2.2) in order to separate the cells from the liquid broth. The mAbs were then purified from the supernatant (a) using protein A chromatography (for conditions see section 2.6). The cells (b) were resuspended and homogenised (see section 2.5) to release any intracellular material. The cell debris was then removed by centrifugation and the mAbs in the supernatant were purified by protein A. The mAbs were then purified using protein A chromatography as before.

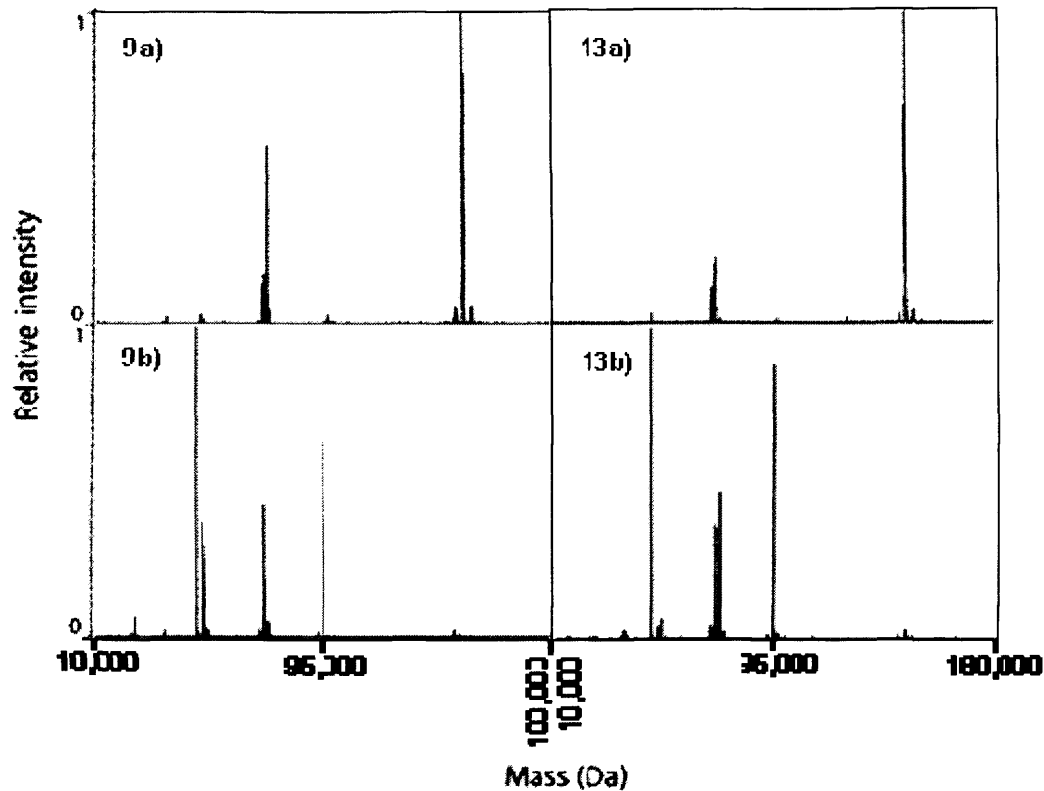


**Figure 5.10 Comparison of intra- and extracellular mAb**

The figure above shows the spectra from days 9 and 13 where the samples were treated as detailed in Figure 5.9, with a) representing the extracellular product composition and b) the intracellular mAb composition. There are four main peaks visible in the spectra: a single heavy chain with a mass of approximately 48 kDa; HL dimers at 73 kDa; complexes of two heavy chains at ~96 kDa; intact mAb at 146 kDa. The extracellular material only shows the presence of HL dimers and intact mAb, while the intracellular material show barely any intact mAb, some HL dimers, but also a large proportion of single heavy chains as well as complexes of two heavy chains. Not visible in the spectra are the light chains since these are not captured by protein A.

Sample	H	HL	HH	H <sub>2</sub> L <sub>2</sub>
9a	0.03	: 0.58	: 0.03	: 1
9b	1	: 0.43	: 0.63	: 0.02
13a	0.03	: 0.21	: 0.02	: 1
13b	1	: 0.47	: 0.88	: 0.02

**Table 5.3 Compositions of the intra- and extracellular material**

From Figure 5.10, the relative amounts of single heavy chains, HL dimers, heavy chain dimers (HH) and intact mAbs were measured and the ratios of the four were calculated as can be seen in the table above. The first figure represents the single heavy chains, the second represents the HL dimers, the third the HH complexes and the fourth is the intact mAb, i.e. H<sub>2</sub>L<sub>2</sub> tetramers.

## 5.4 Discussion

As previously mentioned, several factors have been shown to affect the glycosylation pattern of mAbs, such as culture method (Cabrera et al, 2005; Kunkel et al, 2000; Maiorella et al, 1993; Schweikart et al, 1999), culture conditions (Kunkel et al, 2000; Maiorella et al, 1993) and media composition (Cabrera et al, 2005; Serrato et al, 2007). However, these studies are all looking at the cultivation step and so far little attempt has been made to investigate the effects of further processing on the detailed molecular structure. The first processing step after culture is most commonly centrifugation. This unit operation is known to exert certain levels of shear on the material, which could have detrimental effects, especially with regards to solids carryover (Hutchinson et al, 2006). In the study by Hutchinson et al. (2006), SDS-PAGE was used to compare the mAbs after treatment with shear. This technique showed a stable product, which has been confirmed here by the Bioanalyzer data. Shearing of either cell broth or supernatant does not seem to have an effect on the glycosylation pattern, as revealed by the mass spectra. Shear rate and time does not impact the molecular structure of the mAb either. This means that with regards to mAb stability and structure, different types of centrifuges, causing different amounts of shear, can be used in mAb production, without concern of impacting the molecular structure of the product. However, from the studies carried out here, it has become obvious that shear does have an effect on the overall conformation of the mAb with respect to the proportion of HL dimers. Shear increases the proportion of dimers to a certain level, above which there seems to be no further increase. The increase seems to be apparent immediately upon shearing and the rate or time that the product stream is exposed to shear does not have an effect once this upper limit has been reached. This phenomenon is connected to IgG4, rather than being a general concern for all mAbs or therapeutic proteins, due to the existence of non-covalently bound H<sub>2</sub>L<sub>2</sub> tetramers caused by the hinge-region of the IgG4 molecule (King et al, 1992). These findings suggest that IgG4 in particular is sensitive to shear with regards to product integrity and that this should be carefully considered when designing the purification process. However, shear in the purification process should be avoided for all mAb subclasses due to

solids carryover, as previously mentioned. Shear during centrifugation does increase solids carryover, so with regards to process economics, where larger filter areas would have to be used after clarification using high-shear centrifuges, a lower shear centrifuge would still be favourable. This study did not include specific activity measurements, but the data still gives a good indication that shear does not affect activity of the mAb, since the glycosylation pattern remained the same upon shearing and glycosylation in turn has been linked to mAb activity (Lund et al, 1996; Mimura et al, 2000). The intracellular material from day 13 contains a larger proportion of non-glycosylated half-mAbs compared to day 9. This could be related to the decrease in glycoform complexity with time of culture, as discussed in chapter 4 and could be due to the glycosylation machinery not being able to cope with the large amount of mAbs being produced. The spectra of the overall composition of the intracellular material shows the presence of single heavy chain as well as HH dimers in addition to the HL dimers that are detected in the extracellular material. Since these two complexes are not present in the extracellular product stream this indicates that the increase in HL dimers is caused by dissociation of  $H_2L_2$  tetramers upon shearing rather than the release of any intracellular material due to cell lysis, or all three complexes would be present in the extracellular material. The intracellular material also shows very low levels of intact mAb. This suggests that the  $H_2L_2$  tetramers are secreted immediately upon assembly. This in turn means that, even if there is a significant amount of intracellular material (in this case ~10%), there is no functional product that is being lost, but instead cell lysis, due to ageing cells or shear, would only increase the levels of unwanted product variants such as single heavy chains, half-mAbs and HH chain complexes. This also speaks in favour of using low-shear centrifuges in order to minimise the load on expensive subsequent chromatography steps.

## 6 Effect of holding time and conditions in between stages

During downstream processing of biopharmaceuticals it is sometimes necessary to add holding stages when unit operations are operated at different flow rates or in a batch mode. This study examines what effects holding time and conditions could have on the molecular structure of mAbs. Samples were taken on day 13 of a fermentation as detailed in Figure 6.1 and held at two different temperatures (+4°C and +37°C) for different lengths of time (2 h, 4 h and 24 h). One sample was processed immediately, before holding, as a control for both temperatures. The samples were then treated as detailed in Figure 6.2, with or without shear. Shear can be experienced for example due to mixing in the holding tank, in pumps, or in the subsequent clarification step and might have a detrimental effect on the process, with increased filtration membrane areas due to increased debris carryover (Hutchinson et al, 2006). The following chapter gives an indication to the effects a holding stage could have on the molecular structure and the overall composition of the IgG studied and how shear experienced in the subsequent centrifugation step could affect the integrity and composition of the mAb. They should also give some insight as to whether the decrease in complexity of the glycoforms with increased cultivation time as reported in chapter 4 could be caused by chemical degradation. This was done by choosing a holding temperature of +37°C mimicking the conditions during the fermentation, while the other temperature, +4°C, was chosen to mimic the effects of keeping the broth in a chilled container.

### ***6.1 Effect of holding on molecular structure and glycosylation***

The effect of holding cell culture broth at +4°C and +37°C after harvest on the molecular structure of a recombinant mAb can be seen in Figure 6.3 and Figure 6.5 respectively. The traces show the structure of the intact mAb as analyzed by time-of-flight mass spectrometry (see section 2.9.1). From both sets of data no trends can be seen by visual inspection, only minor variations occur and are most likely due to the deconvolution process. For all samples studied the G0F/G1F glycoform is the most abundant. In order to get a closer look and determine in

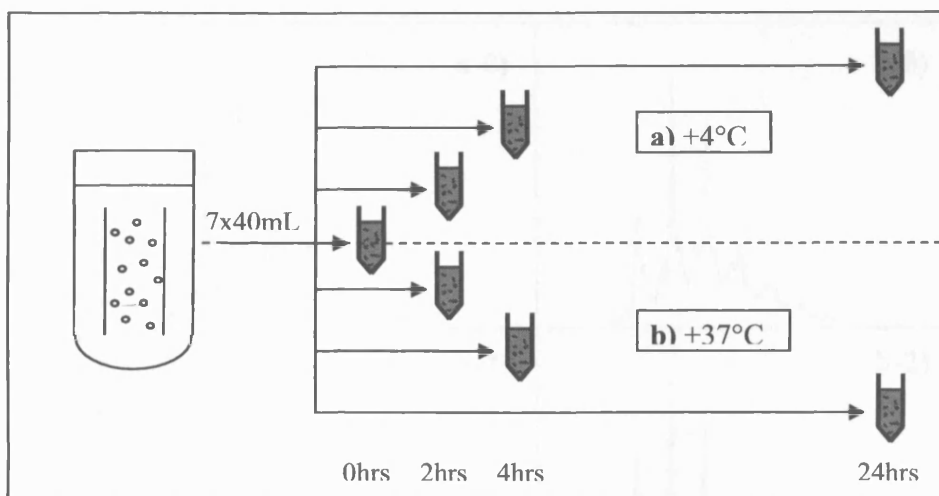


**Figure 6.1** Sampling overview

Seven samples of 40 mL were taken on day 13 of a 10 L fermentation (see section 2.1). One of these samples was treated immediately as detailed in Figure 6.2 as a control. Three of the samples (upper half of Figure 6.1) were kept on hold at +4°C for 2 h, 4 h, or 24 h respectively before treated as detailed in Figure 6.2. The remaining three samples (lower half of Figure 6.1) were kept on hold at +37°C also for 2 h, 4 h and 24 h respectively and then treated as Figure 6.2.

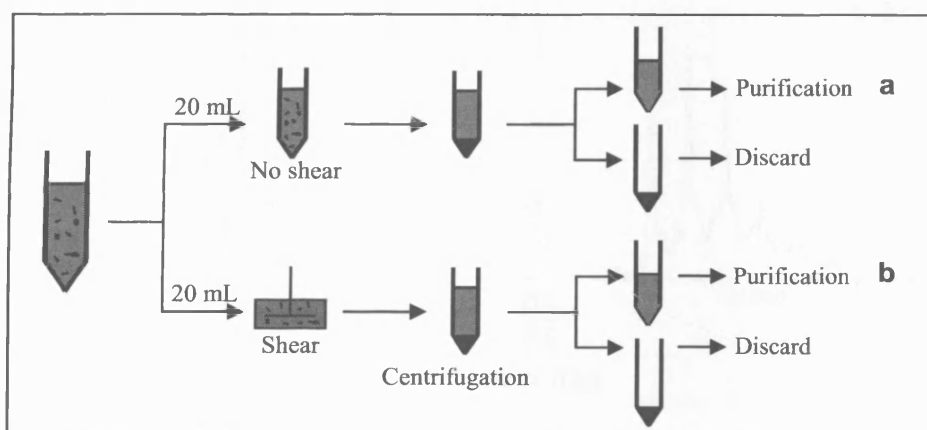


**Figure 6.2** Sample treatment

From Figure 6.1, each 40 mL sample was treated as the above figure shows; 20 mL were centrifuged using a regular benchtop centrifuge (see section 2.2) and the supernatant then purified using protein A chromatography (see section 2.6) before analysis. This sample was used as the base case for looking at the effect of holding. The other 20 mL were first sheared and then clarified, the supernatant then purified and analysed. This sample shows the effect of shear after holding.

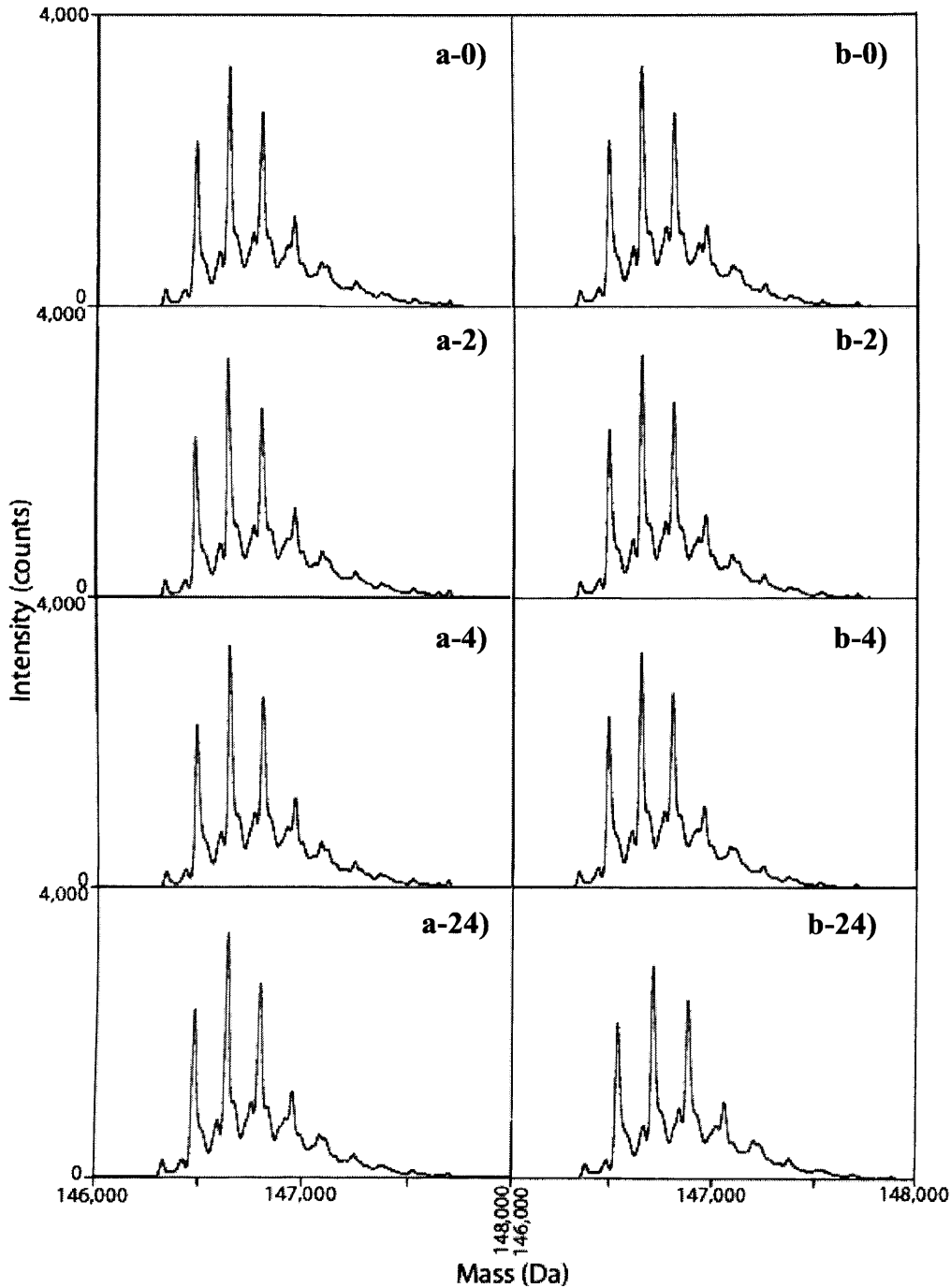


**Figure 6.3** Effect of holding at +4°C on the molecular structure of a mAb

The mass spectra obtained from the samples of the upper half of Figure 6.1, i.e. a sample was taken from the broth and treated as detailed in Figure 6.2 without shear (a) or with shearing (b), after being kept on hold at +4°C for 0 h, 2 h, 4 h and 24 h respectively. The mass spectra have been zoomed in around the intact mAb, from 146,000 Da to 148,000 Da. All data sets are shown to help determine if there are any trends visible. As determined by eye, the spectra all seem

*identical, only with minor variability. These are most likely to be due to the deconvolution software rather than molecular differences.*

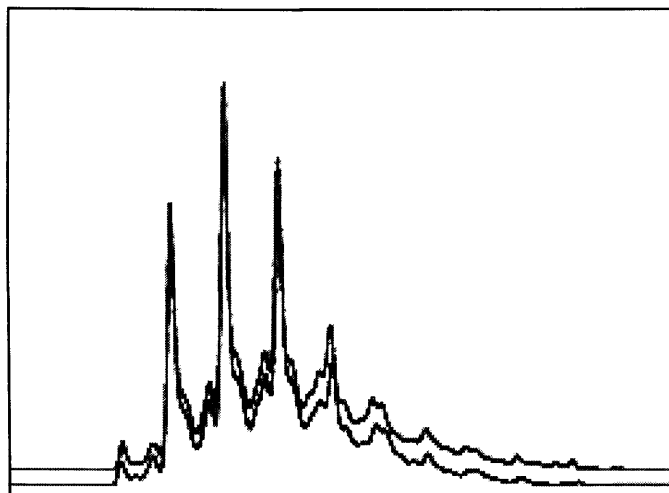


**Figure 6.4 Comparison of the two most extreme samples from Figure 6.3**

*The two most extreme samples, 0 h treated with no shear (a-0) and 24h of holding at +4°C treated with shear (b-24), have been overlaid. No significant differences in the traces can be observed.*

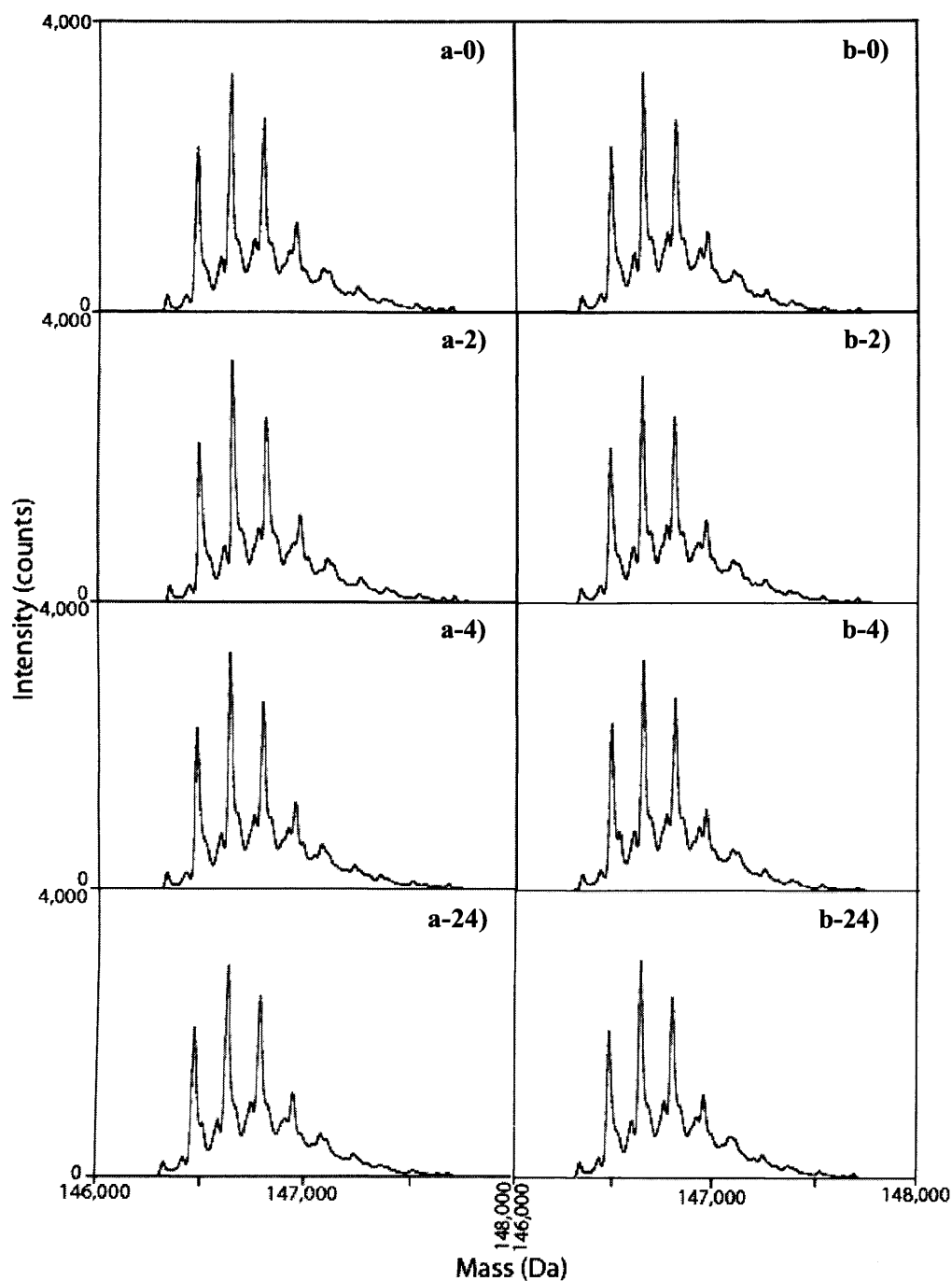


**Figure 6.5 Effect of holding at +37°C on the molecular structure of a mAb**

The mass spectra obtained from the samples of the lower half of Figure 6.1, i.e. a sample was taken from the broth and treated as detailed in Figure 6.2 without shear (a) or with shearing (b), after being kept on hold at +37°C for 0 h, 2 h, 4 h and 24 h respectively. The mass spectra have been zoomed in around the intact mAb, from 146,000 Da to 148,000 Da. As for Figure 6.3, the spectra all seem identical, only with minor variability, due to the deconvolution process.

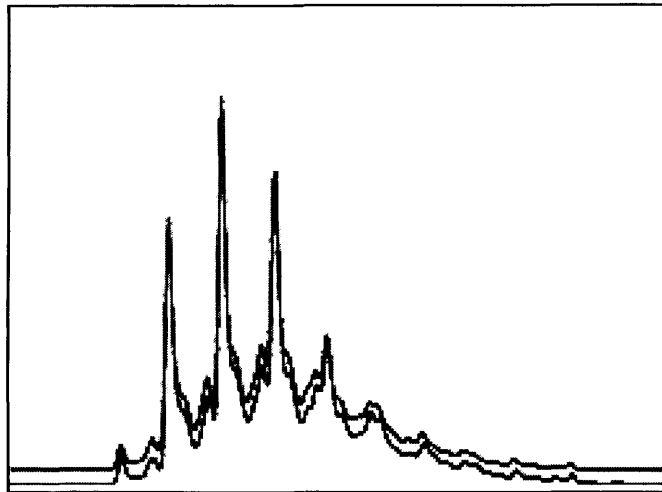


**Figure 6.6 Comparison of the two most extreme samples from Figure 6.5**

*The two most extreme samples, 0 h treated with no shear (a-0) and 24h of holding at +37°C treated with shear (b-24), have been overlaid. No significant differences in the traces can be observed.*

more detail how similar the spectra are, the traces of the two most extreme samples; non-sheared at 0 h and sheared at 24 h, have been overlaid in Figure 6.4 and Figure 6.6 for +4°C and +37°C respectively. Here it becomes more obvious that the traces are close to identical, which confirms the observations made that neither holding nor shear has an effect on the molecular structure and the glycosylation profile of the mAb.

## ***6.2 Effect of holding on mAb conformation***

The integrity of the intact mAb is the main concern during production and purification, since it makes up the final product. However, the composition of the product stream is also of great importance during downstream processing, since any product variants will load up the chromatography columns. If the variants are separated out as non-fully functional, this will also lower the important overall yield. As explained in section 1.6.4, the IgG4 mAb is co-produced with a non-covalently linked version of the mAb, which is prone to disassociation into two HL dimers, “half-mAbs”. Rather than looking at only the effect of holding on the detailed molecular structure of the intact mAb, the impact on the molecular integrity of the molecule can be assessed. Figure 6.7 and Figure 6.8 show the mass spectrometry profiles as an overview of all protein A-positive material in the product stream, for holding at +4°C and +37°C respectively. Three main peaks can be identified; non-glycosylated half-mAb, glycosylated half-mAb and intact mAb (glycosylated). In order to determine whether holding time and conditions, together with harvest method, have any effect on the proportion of half-mAb, the relative amounts of the three structures were measured and the ratios between them were calculated as half-mAb (non-glycosylated) : half-mAb (glycosylated) : intact mAb, as listed in Table 6.1 and Table 6.2 for +4°C and +37°C respectively. These tables show that the proportion of non-glycosylated half-mAb does not appear to be affected by either holding conditions (+4°C or +37°C), holding time (0 h – 24 h) or harvest conditions (no shear or shear), but stays level throughout all treatment conditions. The proportion of glycosylated half-mAb on the other hand, seems to be affected to a certain level. At both +4°C and +37°C the proportion of these HL dimers seems to increase when exposed to shear. Of the total protein A positive material, there is an increase in the proportion of

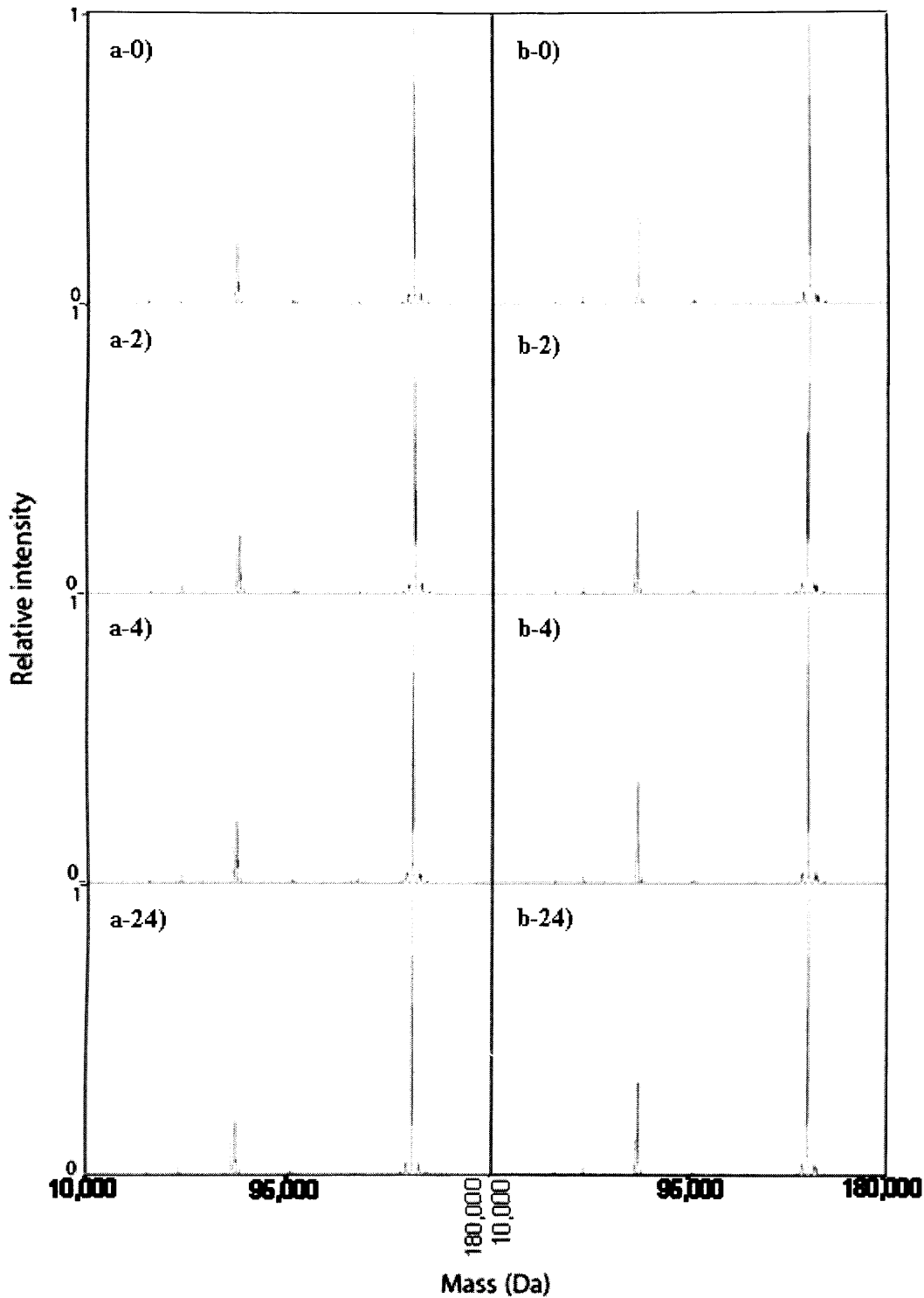


**Figure 6.7** Effect of holding at +4°C on the proportion of HL dimers

The traces correspond to the samples with the same annotation in Figure 6.3, but here the whole range of masses are shown as an overview, from 10,000 Da to 180,000 Da. Three main distinct peaks can be seen that are actually clusters of peaks when looking more closely, corresponding to the different modifications and glycosylation patterns present. There is one group just under 72,000 Da,

which corresponds to non-glycosylated HL dimers, i.e. “half-Abs”. The second one is the glycosylated form of the HL dimer, with masses on 73,000 Da. The third peak cluster is the intact mAb, with the main peak at 146,634 Da, corresponding to the mAb with both C-terminal lysine residues cleaved off (OK), both N-terminal glutamine residues converted to pyroglutamic acid (pE) and with the G0F/G1F glycoform. From determination by eye, looking down each column, i.e. looking at the effect of holding time on the product composition, the proportion of half-mAb (both non-glycosylated and glycosylated) does not seem to change with time (0h, 2h, 4h and 24h), for either non-sheared samples (a) or those treated with shear (b). If instead comparing the two columns at each time point, e.g. a-2 and b-2, there seems to be an increase in the proportion of half mAbs when the sample has been exposed to shear. The increase is not of a major magnitude, but seems consistent and could be of importance. The non-glycosylated proportion does not seem affected by shear.

	<u>No shear</u>			<u>Shear</u>		
	Half-mAb (non-glyc)	Half-mAb	Intact mAb	Half-mAb (non-glyc)	Half-mAb	Intact mAb
<b>0 h</b>	0.14	: 0.22	: 1	0.11	: 0.31	: 1
<b>2 h</b>	0.14	: 0.22	: 1	0.12	: 0.30	: 1
<b>4 h</b>	0.13	: 0.22	: 1	0.13	: 0.37	: 1
<b>24 h</b>	0.13	: 0.21	: 1	0.13	: 0.34	: 1

**Table 6.1 Proportion of HL dimers after holding at +4°C**

From Figure 6.7, the relative amounts of non-glycosylated half-mAbs, glycosylated half-mAbs and intact mAbs were measured and the ratios of the three were calculated as can be seen in the table above. The first figure represents the non-glycosylated HL dimers, the second represents the glycosylated HL dimers and the last is the intact mAb. These calculations confirm the initial observations as detailed under Figure 6.7; the proportion of non-glycosylated mAb stays the same both with holding time and with shear treatment. The proportion of glycosylated half-mAb also stays level with increasing holding time, but from treatment with shear the proportion increases by 5-7 % from 16 % to 21-25 % of total protein A positive material.

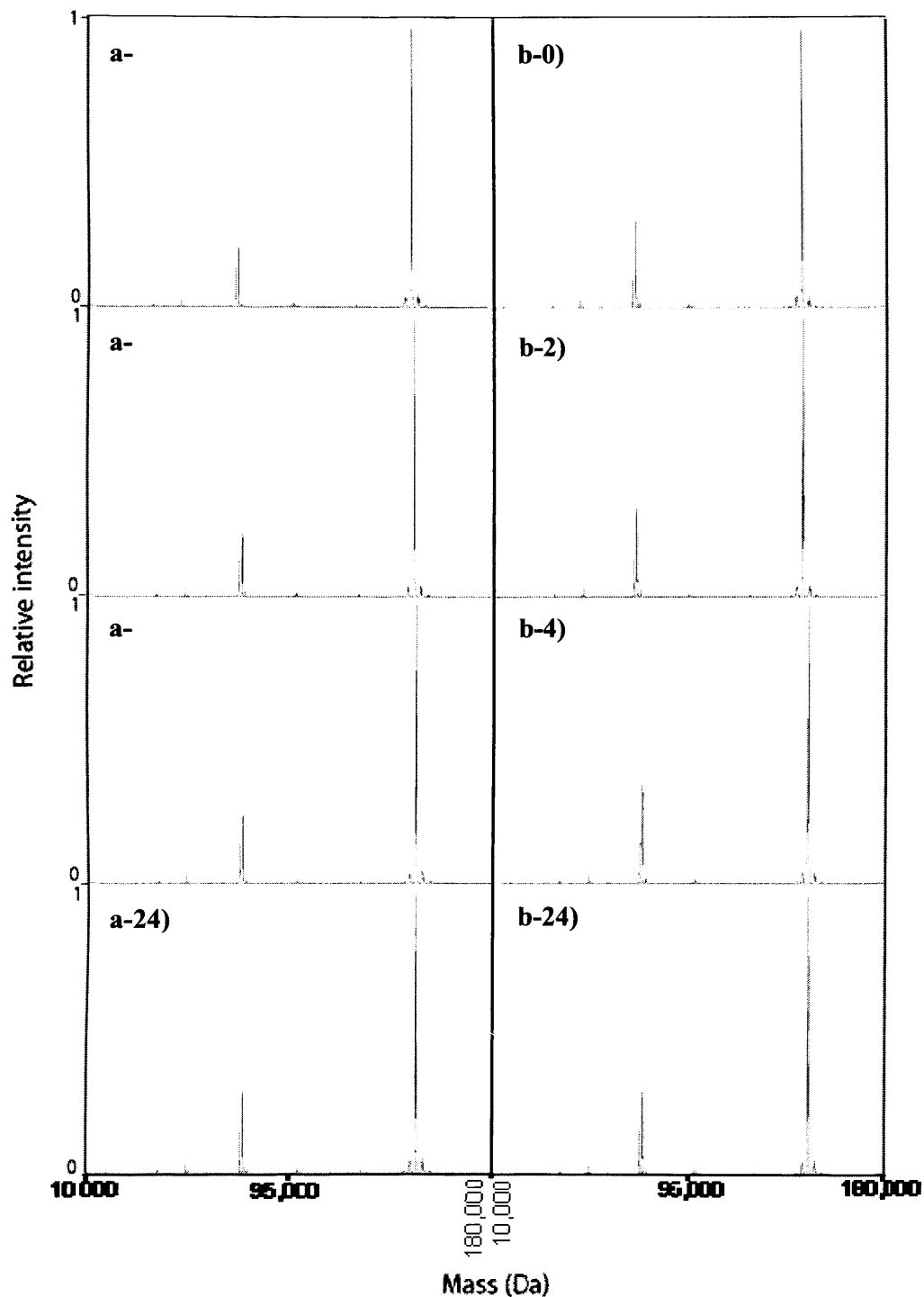


**Figure 6.8** *Effect of holding at +37°C on the proportion of HL dimers*

The traces correspond to the samples with the same annotation in Figure 6.5, but here the whole range of masses are shown as an overview, from 10,000 Da to 180,000 Da. The three main peaks are peak clusters of mAbs with different modifications and glycosylation patterns as in Figure 6.5. The group just under 72,000 Da corresponds to non-glycosylated HL dimers, the second group is the

glycosylated half-mAbs and the third peak is the intact mAb. Looking down the two columns, i.e. looking at the effect of holding time on the product composition, the proportion of non-glycosylated HL dimers does not seem to change with time (0h, 2h, 4h and 24h), for either non-sheared samples (a) or those treated with shear (b). The same is the case for glycosylated HL dimers treated with shear (b). The samples not exposed to shear, on the other hand, (a-0, a-2, a-4 and a-24) the proportion of glycosylated half-mAbs seems to increase slightly. If instead comparing the two columns at each time point, e.g. a-2 and b-2, there seems to be an increase in the proportion of half mAbs when the sample has been exposed to shear. The non-glycosylated proportion does not seem affected by shear.

	<b>No shear</b>			<b>Shear</b>						
	<b>Half-mAb (non-glyc)</b>	<b>Half-mAb</b>	<b>Intact mAb</b>	<b>Half-mAb (non-glyc)</b>	<b>Half-mAb</b>	<b>Intact mAb</b>				
<b>0 h</b>	0.14	:	0.22	:	1	0.11	:	0.31	:	1
<b>2 h</b>	0.13	:	0.23	:	1	0.13	:	0.33	:	1
<b>4 h</b>	0.14	:	0.25	:	1	0.14	:	0.36	:	1
<b>24 h</b>	0.15	:	0.30	:	1	0.16	:	0.30	:	1

**Table 6.2 Proportion of HL dimers after holding at +37°C**

The relative amounts of non-glycosylated half-mAbs, glycosylated half-mAbs and intact mAbs were measured from Figure 6.8 of non-glycosylated half-mAbs, glycosylated half-mAbs and intact mAbs were measured and the ratios of the three were calculated as can be seen in the table above. The first figure represents the non-glycosylated HL dimers, the second represents the glycosylated HL dimers and the last is the intact mAb. These calculations are in accordance with the initial observations as detailed under Figure 6.8. The proportion of non-glycosylated mAb stays the same both with holding time and with shear treatment. The proportion of glycosylated half-mAbs also stays the same for the samples treated with shear. As for holding at +4°C (Table 6.1), the proportion of glycosylated half-mAb increases on exposure to shear, this time by 6% for three of the time points and by 1% for 24 h; from 16-21% to 22-24% of total protein A positive material. For the non-sheared samples, there is an increase of 5% of glycosylated half-mAbs with holding time from 0 to 24 h. The levels of half-mAbs here reach the same levels as when the mAbs are exposed to shear.

glycosylated half-mAbs from approximately 16% to 22% upon shearing, an increase of 6%. If instead looking at the effect of holding time; at +4°C the proportion of glycosylated half-mAbs does not seem affected by holding for 0 h – 24 h. At +37°C on the other hand, there is an increase in these half-mAbs, reaching the same levels after 24 h as is experienced when the mAbs are exposed to shear; the higher temperature causing an increase in HL dimers.

### **6.3 Discussion**

During large-scale production of therapeutic proteins it is often necessary to have holding stages in between unit operations. This can be due to several reasons; the different units have to be run at different flow rates during continuous operation, or a stage has to be run in batch mode and parts of the broth will then have to be kept on hold prior to the subsequent processing step. An example of units being operated at different flow rates is centrifugation, where relatively high flow rates can be expected (170-600 L h<sup>-1</sup>), and chromatography, where the flow rates are much lower (30-200 cm h<sup>-1</sup>). The experiments outlined here were designed to look at the interaction between the fermentation, in this case a fed-batch operation, and the subsequent harvest step. The data presented in this chapter also shows the most abundant glycoform to be the G0F/G1F structure, which fits in well with the profiles reported over time in chapter 4. Exposing the mAb to shear that would be experienced in a large-scale centrifuge after the holding stage does not have an effect on the glycosylation pattern either, causing no concerns about centrifugation conditions in this aspect.

In chapters 4 and 5 the presence of HL dimers, or half-mAbs, was also reported. This chapter gives some insight to how a holding stage could affect the amount of these product variants. It also helps answering some of the questions that were raised in the previous chapters relating to the reasons behind changes in half-mAb proportions. The holding stage used could mimic an actual holding stage in between processes, but could also give some insight as to what would happen upon storage of the mAbs. Formulation would of course put the mAbs in a more suitably protected environment, but this study should still give an indication of the

stability of the H<sub>2</sub>L<sub>2</sub> tetramers. Looking at the overall conformation of the mAb and the proportion of HL dimers in the product stream, the holding stage and further processing seem to have an impact on the product integrity, depending on the holding conditions. Holding at +4°C seems to have a lesser impact than holding at +37°C, with no effect on half-mAb levels with increased holding time. At +37°C there seems to be an increase in glycosylated half-mAb with longer holding times, suggesting that the higher temperature puts the cells in a non-favourable condition. Looking at the effect of shear treatment, the results for the two different temperatures are more similar. The noted levels of glycosylated half-mAbs are fairly constant over the sheared samples at both +4°C and +37°C, with an increase in half-mAbs after shearing for most samples by 5-7%. This is considered a significant increase since four repeat injections gave variations of ±2%. The increase could be either due to cell lysis caused by shear and the subsequent release of incompletely assembled HL dimers or it could be due to the shear forces causing dissociation of the non-covalently bound H<sub>2</sub>L<sub>2</sub> tetramers. The main difference between the two temperatures is that at +37°C, after holding for 24 hrs, there is no increase when comparing the non-sheared and the sheared sample. However, for this sample an increase in glycosylated half-mAbs had already been observed due to holding time and the proportion of these HL dimers was already at the same level observed in all of the sheared samples. The data suggests that both temperature and shear cause an increase in HL dimers, which could be either due to cell lysis and the subsequent release of HL dimers or shear causing the H<sub>2</sub>L<sub>2</sub> tetramers to dissociate. The data also suggests that due to the stronger nature of the bond, the covalently bound tetramers are not affected. The results reported here have to be carefully taken into consideration when designing production and purification processes for IgG4. Even though the glycosylation pattern of the mAb does not seem affected by holding or processing, holding at an elevated temperature as well as treatment with shear has an affect on the overall product composition. When manufacturing IgG4, precautions have to be taken in order not to lose a proportion of the valuable product. As suggested before, this could be done by preventative screening for the most promising clone during cell line development (Deng et al, 2004), or by facilitating the formation of disulphide bonds through media additions, such as copper sulphate (Chaderjian et al, 2005), or alternatively by genetic engineering (Angal et al, 1993; Bloom et al, 1997).

## 7 Overall discussion

A number of important observations have been made and discussed in the chapters detailing the studies that were carried out. In addition to this, the data from the separate experiments can be linked together putting together a bigger picture and more conclusions can be drawn from this. In chapter 6 it was concluded that neither holding time nor temperature has an effect on the glycosylation pattern of the mAb. This can be linked to the studies carried out in chapter 4 and the observation that the glycosylation profile changes with cultivation time. It suggests that the changes in glycosylation profile are not due to the prolonged time the product is being kept in the broth and possible proteolytic degradation. Instead the changes have to be due to one or both of the other two suggested causes: the cells producing incompletely processed material due to stress; release of incompletely processed material due to cell lysis. The data presented in chapter 6 also shows that the most abundant glycoform is the G0F/G1F structure, which fits in well with the profiles reported over time in chapter 4.

In chapters 4 and 5 the presence of HL dimers, or half-mAbs, was also reported. This raised a number of questions regarding processing and its effects on the levels of half-mAbs: What physical conditions affect the proportion of dissociated tetramers? Are there more non-covalently bound mAbs in the final product than the ones that have dissociated into HL dimers? And if there are, will they stay bound or dissociate upon processing, formulation and storage? The studies in chapter 6 were designed to answer some of these questions. The data suggests that both temperature and shear during a potential holding stage cause an increase in HL dimers, which could be either due to cell lysis and the subsequent release of HL dimers or shear causing the H<sub>2</sub>L<sub>2</sub> tetramers to dissociate. Looking back at the findings from chapter 5, it was established that the increase in HL dimers was most likely due to dissociation due to shear rather than cell lysis since no single heavy chains or HH dimers are present in the product stream. This suggests that holding time and temperature should be carefully considered and damaging shear rates should be avoided when designing manufacturing processes for IgG4 and similar therapeutic proteins.

## 8 Conclusions

ESI-TOF analysis of intact mAb has proved to be a very useful technique for monitoring glycosylation as well as the proportion of HL dimers and other contaminating complexes. The technique provides a straightforward way to cut down on time and cost of sample preparation.

The IgG used in this study showed heterogeneity due to glycosylation, C-terminal lysine residues and N-terminal glutamine residues, with two thirds of the mAb having both lysine residues cleaved off and most mAb both glutamine residues converted to pyroglutamic acid. The data presented here also showed that two different glycans can be attached to the heavy chains of the same mAb causing even more heterogeneity.

A decrease in glycan complexity was observed with time of culture, with reduced levels of galactosylation towards the later stages of fermentation, the (G0F)<sub>2</sub> glycoform being the most abundant at time of harvest. Shearing, regardless of rate and time, had no effect on glycosylation and neither does holding time or temperature.

HL dimers were observed in the purified product stream due to the presence of non-covalently bound H<sub>2</sub>L<sub>2</sub> tetramers. Holding time did not affect the proportion of half-mAbs at +4°C, but an increase could be seen after 24 hrs holding at +37°C. Shearing caused a 10% increase in the proportion of HL dimers, regardless of shear rate and time, as compared to a non-sheared control. The increase in half-mAb appeared to be due to shear causing the non-covalently bound tetramers to dissociate rather than due to the release of incompletely processed material from cell lysis.

The ultimate outcome of the work presented is a tool-kit (Figure 8.1) for in-process analysis of complex biopharmaceuticals. This entails sampling from culture broth, product capture and at-line mass spectrometry analysis of the intact protein, without the need for extensive sample preparation.

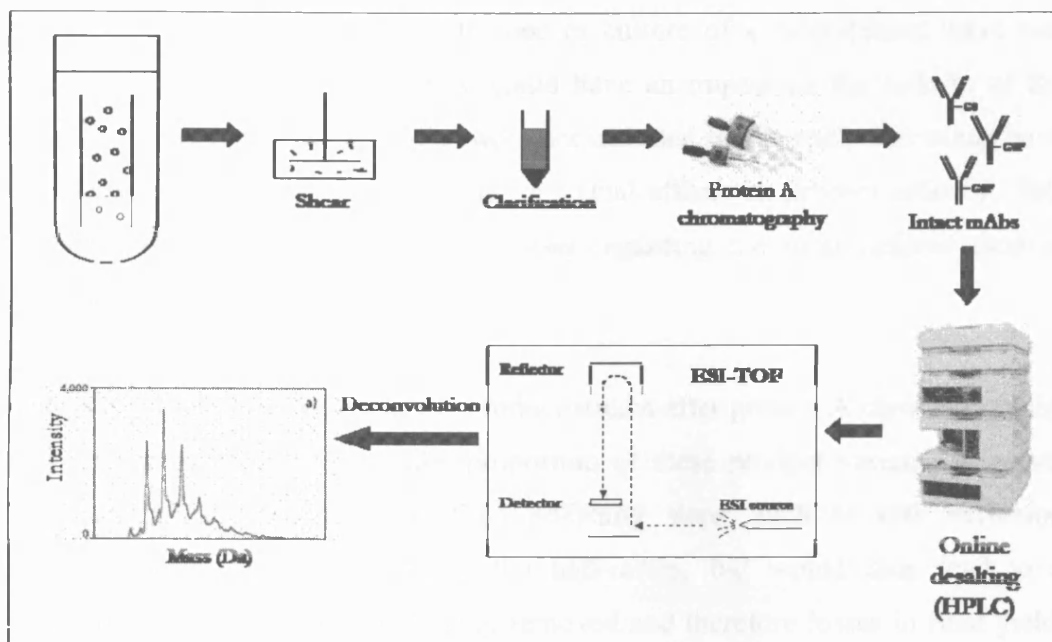


**Figure 8.1 Schematic of the tool-kit**

The ultimate outcome of this work is a tool-kit for in-process determination of the structural and conformational authenticity of complex biopharmaceuticals. This is briefly summarised in the above flow diagramme and entails sampling from fermentation broth and the use of ultra scale-down methodologies, including the shear device, followed by purification, online desalting and at-line analysis of the intact protein, cutting out extensive sample preparations like enzymatic digests.

## 9 Future work

Glycosylation has previously been linked to activity of mAbs, which is why this post-translational modification was the main concern in the work presented here. A decrease in galactosylation with time of culture of a recombinant IgG4 was shown, suggesting time of harvest could have an impact on the activity of the product. However, activity studies were not included in this study and would have to be carried out in order to confirm the actual effects on product efficacy. This would then lead to further investigations regarding the most optimal time to harvest with respect to product activity.

The presence of HL dimers in the product stream after protein A chromatography was also presented and how the proportion of these product variants increases upon exposure to shear. The final polishing steps, such as size exclusion chromatography, would eliminate the half-mAbs, but would then lead to a proportion of the final product being removed and therefore losses in final yield. The size of these losses was outside the scope of this study, but should be investigated further in order to get an estimation of the effect on the overall process economics. Some studies elsewhere have attempted to minimize the presence of the HL dimers, but additional, more efficient ways, would be beneficial to find for the cases where IgG4 is the desirable subclass.

All studies presented here were carried out at small-scale and supported by previous work should give a good representation of the large-scale process. However, it would be beneficial to carry out the same experiments at pilot- or large-scale to confirm this is the case.

The ESI-TOF analysis of intact mAb provided a time-saving technique for protein analysis and glycosylation monitoring. This inspires even further time- and labour-saving thinking around bottlenecks in process evaluation and automation in monitoring protein production. Would online purification and analysis of mAbs and other therapeutic proteins be possible? Could a sample be taken from the culture broth and without extensive sample preparations be analyzed using mass

spectrometry and how long would this take? Would it be possible to cut down analysis time from days to a few hours?

Therapeutic proteins and mAbs in particular have infiltrated the pharmaceutical market very fast over the past decades, offering treatments for diseases that have so far been difficult to treat. During these years a lot of research has gone into studying mAb production and purification and processes have been greatly improved since the beginning. However, there is still a lot of work to be done in order to fully understand what effects production and processing conditions have on structure and efficacy and to improve the processes currently in place.

## Bibliography

Abbas AK, Lichtmann AH, and Pober JS (2000) Antibodies and Antigens **4**: 41 - 62

Angal S, King DJ, Bodmer MW, Turner A, Lawson ADG, Roberts G, Pedley B, and Adair JR (1993) A Single Amino-Acid Substitution Abolishes the Heterogeneity of Chimeric Mouse/Human (Igg4) Antibody *Molecular Immunology* **30**: 105 - 108

Ashford DA and Platt F (1999) Protein Glycosylation 135 - 174

Aybay C (2003) Differential Binding Characteristics of Protein G and Protein A for Fc Fragments of Papain-Digested Mouse IgG *Immunology Letters* **85**: 231 - 235

Bailey MJ, Hooker AD, Adams CS, Zhang SH, and James DC (2005) A Platform for High-Throughput Molecular Characterization of Recombinant Monoclonal Antibodies *Journal of Chromatography B-Analytical Technologies in the Biomedical and Life Sciences* **826**: 177 - 187

Beck A, Bussat MC, Zorn N, Robillard V, Klinguer-Hamour C, Chenu S, Goetsch L, Corvaia N, Van Dorselaer A, and Haeuw JF (2005) Characterization by Liquid Chromatography Combined With Mass Spectrometry of Monoclonal Anti-IGF-1 Receptor Antibodies Produced in CHO and NSO Cells *Journal of Chromatography B-Analytical Technologies in the Biomedical and Life Sciences* **819**: 203 - 218

Birch JR and Racher AJ (2006) Antibody Production *Advanced Drug Delivery Reviews* **58**: 671 - 685

Bjorck L and Kronvall G (1984) Purification and Some Properties of Streptococcal Protein-G, Protein-A Novel Igg-Binding Reagent *Journal of Immunology* **133**: 969 - 974

Bloom JW, Madanat MS, Marriott D, Wong T, and Chan SY (1997) Intrachain Disulfide Bond in the Core Hinge Region of Human IgG4 *Protein Science* **6**: 407 - 415

Boulding N, Yim SSS, Keshavarz-Moore E, Shamlou PA, and Berry M (2002) Ultra Scaledown to Predict Filtering Centrifugation of Secreted Antibody Fragments From Fungal Broth *Biotechnology and Bioengineering* **79**: 381 - 388

Boychyn M, Yim SSS, Bulmer M, More J, Bracewell DG, and Hoare M (2004) Performance Prediction of Industrial Centrifuges Using Scale-Down Models *Bioprocess and Biosystems Engineering* **26**: 385 - 391

Boychyn M, Yim SSS, Shamlou PA, Bulmer M, More J, and Hoare A (2001) Characterization of Flow Intensity in Continuous Centrifuges for the Development of Laboratory Mimics *Chemical Engineering Science* **56**: 4759 - 4770

Broersen K, Voragen AGJ, Hamer RJ, and de Jongh HHJ (2004) Glycoforms of Beta-Lactoglobulin With Improved Thermostability and Preserved Structural Packing *Biotechnology and Bioengineering* **86**: 78 - 87

Busby WH, Quackenbush GE, Humm J, Youngblood WW, and Kizer JS (1987) An Enzyme(S) That Converts Glutaminyl-Peptides Into Pyroglutamyl-Peptides - Presence in Pituitary, Brain, Adrenal-Medulla, and Lymphocytes *Journal of Biological Chemistry* **262**: 8532 - 8536

Cabrera G, Cremata JA, Valdes R, Garcia R, Gonzalez Y, Montesino R, Gomez H, and Gonzalez M (2005) Influence of Culture Conditions on the N-Glycosylation of a Monoclonal Antibody Specific for Recombinant Hepatitis B Surface Antigen *Biotechnology and Applied Biochemistry* **41**: 67 - 76

Carr SA, Huddleston MJ, and Bean MF (1993) Selective Identification and Differentiation of N-Linked and O- Linked Oligosaccharides in Glycoproteins by Liquid- Chromatography Mass-Spectrometry *Protein Science* **2**: 183 - 196

Chaderjian WB, Chin ET, Harris RJ, and Etcheverry TM (2005) Effect of Copper Sulfate on Performance of a Serum-Free CHO Cell Culture Process and the Level of Free Thiol in the Recombinant Antibody Expressed *Biotechnology Progress* **21**: 550 - 553

Coico R, Sunshine G, and Benjamin E (2003) Antibody Structure and Function **5**: 39 - 57

Colangelo J and Orlando R (2001) On-Target Endoglycosidase Digestion Matrix-Assisted Laser Desorption/Ionization Mass Spectrometry of Glycopeptides *Rapid Communications in Mass Spectrometry* **15**: 2284 - 2289

Cromwell MEM, Hilario E, and Jacobson F (2006) Protein Aggregation and Bioprocessing *Aaps Journal* **8**: E572 - E579

Dell A and Morris HR (2001) Glycoprotein Structure Determination by Mass Spectrometry *Science* **291**: 2351 - 2356

Demelbauer UM, Plematl A, Josic D, Allmaier G, and Rizzi A (2005) On the Variation of Glycosylation in Human Plasma Derived Antithrombin *Journal of Chromatography A* **1080**: 15 - 21

Deng L, Wylie D, Tsao YS, Larkin B, Voloch M, and Ling WLW (2004) Detection and Quantification of the Human IgG4 Half-Molecule, HL, From Unpurified Cell-Culture Supernatants *Biotechnology and Applied Biochemistry* **40**: 261 - 269

Dillon TM, Bondarenko PV, and Ricci MS (2004) Development of an Analytical Reversed-Phase High-Performance Liquid Chromatography-Electro Spray Ionization Mass Spectrometry Method for Characterization of Recombinant Antibodies *Journal of Chromatography A* **1053**: 299 - 305

Elliott S, Lorenzini T, Asher S, Aoki K, Brankow D, Buck L, Busse L, Chang D, Fuller J, Grant J, Hernday N, Hokum M, Hu S, Knudten A, Levin N, Komorowski

- R, Martin F, Navarro R, Osslund T, Rogers G, Rogers N, Trail G, and Egrie J (2003) Enhancement of Therapeutic Protein in Vivo Activities Through Glycoengineering *Nature Biotechnology* **21**: 414 - 421
- Fahrner RL, Whitney DH, Vanderlaan M, and Blank GS (1999) Performance Comparison of Protein A Affinity-Chromatography Sorbents for Purifying Recombinant Monoclonal Antibodies *Biotechnology and Applied Biochemistry* **30**: 121 - 128
- Fotinopoulou A, Meyers T, Varley P, and Turner G (2003) Screening for Glycosylation Changes on Recombinant Human IgG Using Lectin Methods *Biotechnology and Applied Biochemistry* **37**: 1 - 7
- Fries S, Glazomitsky K, Woods A, Forrest G, Hsu A, Olewinsky R, Robinson D, and Chartrain M (2005) Evaluation of Disposable Bioreactors - Rapid Production of Recombinant Proteins by Several Animal Cell Lines *Bioprocess International* **3**: 36 - 44
- Fukuda M (1994) Cell Surface Carbohydrates: Cell-Type Specific Expression 1 - 52
- Gadgil HS, Pipes GD, Dillon TM, Treuheit MJ, and Bondarenko PV (2006) Improving Mass Accuracy of High Performance Liquid Chromatography/Electrospray Ionization Time-of-Flight Mass Spectrometry of Intact Antibodies *Journal of the American Society for Mass Spectrometry* **17**: 867 - 872
- Gerlach D, Schlott B, Zahringer U, and Schmidt KH (2005) N-Acetyl-D-Galactosamine/N-Acetyl-D-Glucosamine - Recognizing Lectin From the Snail *Cepaea Hortensis*: Purification, Chemical Characterization, Cloning and Expression in E. Coli *FEMS Immunology and Medical Microbiology* **43**: 223 - 232
- Goldman MH, James DC, Rendall M, Ison AP, Hoare M, and Bull AT (1998) Monitoring Recombinant Human Interferon-Gamma N-Glycosylation During Perfused Fluidized-Bed and Stirred-Tank Batch Culture of CHO Cells *Biotechnology and Bioengineering* **60**: 596 - 607
- Gottschalk U (2005) Downstream Processing of Monoclonal Antibodies: From High Dilution to High Purity *Biopharm International* **18**: 42 - +
- Gottschalk U (2008) Bioseparation in Antibody Manufacturing: The Good, the Bad and the Ugly *Biotechnology Progress* **24**: 496 - 503
- Hagmann ML, Kionka C, Schreiner M, and Schwer C (1998) Characterization of the F(Ab')<sub>2</sub> Fragment of a Murine Monoclonal Antibody Using Capillary Isoelectric Focusing and Electrospray Ionization Mass Spectrometry *Journal of Chromatography A* **816**: 49 - 58
- Hamilton SR and Gerngross TU (2007) Glycosylation Engineering in Yeast: the Advent of Fully Humanized Yeast *Current Opinion in Biotechnology* **18**: 387 - 392

Hanash SM (1998) Two-Dimensional Gel Electrophoresis - A Practical Approach **Third**: 189 - 211

Harris RJ (1995) Processing of C-Terminal Lysine and Arginine Residues of Proteins Isolated From Mammalian-Cell Culture *Journal of Chromatography A* **705**: 129 - 134

Harris RJ, Shire SJ, and Winter C (2004) Commercial Manufacturing Scale Formulation and Analytical Characterization of Therapeutic Recombinant Antibodies *Drug Development Research* **61**: 137 - 154

Harris RJ, Wagner KL, and Spellman MW (1990) Structural Characterization of A Recombinant Cd4-Igg Hybrid Molecule *European Journal of Biochemistry* **194**: 611 - 620

Harrison JS, Gill A, and Hoare M (1998) Stability of a Single-Chain Fv Antibody Fragment When Exposed to a High Shear Environment Combined With Air-Liquid Interfaces *Biotechnology and Bioengineering* **59**: 517 - 519

Hodoniczky J, Zheng YZ, and James DC (2005) Control of Recombinant Monoclonal Antibody Effector Functions by Fc N-Glycan Remodeling in Vitro *Biotechnology Progress* **21**: 1644 - 1652

Hossler P, Goh LT, Lee MM, and Hu WS (2006) GlycoVis: Visualizing Glycan Distribution in the Protein N-Glycosylation Pathway in Mammalian Cells *Biotechnology and Bioengineering* **95**: 946 - 960

Hutchinson N, Bingham N, Murrell N, Farid S, and Hoare M (2006) Shear Stress Analysis of Mammalian Cell Suspensions for Prediction of Industrial Centrifugation and Its Verification *Biotechnology and Bioengineering* **95**: 483 - 491

Jagschies G, Gronberg A, Bjorkman T, Lacki K, and Johansson HJ (2006) Technical and Economical Evaluation of Downstream Processing Options for Monoclonal Antibody (MAb) Production *Biopharm International* 10 - +

Jankovic MM and Kosanovic MM (2005b) Glycosylation of Urinary Prostate-Specific Antigen in Benign Hyperplasia and Cancer: Assessment by Lectin-Binding Patterns *Clinical Biochemistry* **38**: 58 - 65

Jankovic MM and Kosanovic MM (2005a) Glycosylation of Urinary Prostate-Specific Antigen in Benign Hyperplasia and Cancer: Assessment by Lectin-Binding Patterns *Clinical Biochemistry* **38**: 58 - 65

Jung C, Lee YP, Jeong YR, Kim JY, Kim YH, and Kim HS (2005) Characterization of N[Alpha]-Acetyl Methionyl Human Growth Hormone Formed During Expression in *Saccharomyces Cerevisiae* With Liquid Chromatography and Mass Spectrometry *Journal of Chromatography B* **814**: 53 - 59

Karas M, Bachmann D, and Hillenkamp F (1985) Influence of the Wavelength in High-Irradiance Ultraviolet-Laser Desorption Mass-Spectrometry of Organic-Molecules *Analytical Chemistry* **57**: 2935 - 2939

Kawasaki N, Ohta M, Hyuga S, Hyuga M, and Hayakawa T (2000) Application of Liquid Chromatography/Mass Spectrometry and Liquid Chromatography With Tandem Mass Spectrometry to the Analysis of the Site-Specific Carbohydrate Heterogeneity in Erythropoietin *Analytical Biochemistry* **285**: 82 - 91

King DJ, Adair JR, Angal S, Low DC, Proudfoot KA, Lloyd JC, Bodmer MW, and Yarranton GT (1992) Expression, Purification and Characterization of A Mouse Human Chimeric Antibody and Chimeric Fab Fragment *Biochemical Journal* **281**: 317 - 323

Krapp S, Mimura Y, Jefferis R, Huber R, and Sondermann P (2003) Structural Analysis of Human IgG-Fc Glycoforms Reveals a Correlation Between Glycosylation and Structural Integrity *Journal of Molecular Biology* **325**: 979 - 989

Kunkel JP, Jan DCH, Butler M, and Jamieson JC (2000) Comparisons of the Glycosylation of a Monoclonal Antibody Produced Under Nominally Identical Cell Culture Conditions in Two Different Bioreactors *Biotechnology Progress* **16**: 462 - 470

Le JC and Bondarenko PV (2005) Trap for MAbs: Characterization of Intact Monoclonal Antibodies Using Reversed-Phase HPLC on-Line With Ion-Trap Mass Spectrometry *Journal of the American Society for Mass Spectrometry* **16**: 307 - 311

Lee YK, Brewer JW, Hellman R, and Hendershot LM (1999) BiP and Immunoglobulin Light Chain Cooperate to Control the Folding of Heavy Chain and Ensure the Fidelity of Immunoglobulin Assembly *Molecular Biology of the Cell* **10**: 2209 - 2219

Levy MS, Ciccolini LAS, Yim SSS, Tsai JT, Titchener-Hooker N, Ayazi Shamlou P, and Dunnill P (1999) The Effects of Material Properties and Fluid Flow Intensity on Plasmid DNA Recovery During Cell Lysis *Chemical Engineering Science* **54**: 3171 - 3178

Li HJ, Sethuraman N, Stadheim TA, Zha DX, Prinz B, Ballew N, Bobrowicz P, Choi BK, Cook WJ, Cukan M, Houston-Cummings NR, Davidson R, Gong B, Hamilton SR, Hoopes JP, Jiang YW, Kim N, Mansfield R, Nett JH, Rios S, Strawbridge R, Wildt S, and Gerngross TU (2006) Optimization of Humanized IgGs in Glycoengineered *Pichia Pastoris* *Nature Biotechnology* **24**: 210 - 215

Lund J, Takahashi N, Pound JD, Goodall M, and Jefferis R (1996) Multiple Interactions of IgG With Its Core Oligosaccharide Can Modulate Recognition by Complement and Human Fc Gamma Receptor I and Influence the Synthesis of Its Oligosaccharide Chains *Journal of Immunology* **157**: 4963 - 4969

- Maiorella BT, Winkelhake J, Young J, Moyer B, Hora M, Andya J, Thomson J, Patel T, and Parekh R (1993) Effect of Culture Conditions on IgM Antibody Structure, Pharmacokinetics and Activity *Nature Biotechnology* **11**: 387 - 392
- Mannweiler K and Hoare M (1992) The Scale-Down of An Industrial Disk Stack Centrifuge *Bioprocess Engineering* **8**: 19 - 25
- Maybury JP, Hoare M, and Dunnill P (2000) The Use of Laboratory Centrifugation Studies to Predict Performance of Industrial Machines: Studies of Shear-Insensitive and Shear-Sensitive Materials *Biotechnology and Bioengineering* **67**: 265 - 273
- Maybury JP, Mannweiler K, Titchener-Hooker NJ, Hoare M, and Dunnill P (1998) The Performance of a Scaled Down Industrial Disc Stack Centrifuge With a Reduced Feed Material Requirement *Bioprocess Engineering* **18**: 191 - 199
- McCoy R (2009) Allogeneic Cell Therapy: The Impact of the Engineering Environment on Cells During Processing *EngD Thesis*
- Merchant M and Weinberger SR (2000) Recent Advancements in Surface-Enhanced Laser Desorption/Ionization-Time of Flight-Mass Spectrometry *Electrophoresis* **21**: 1164 - 1177
- Merten OW (2006) Introduction to Animal Cell Culture Technology - Past, Present and Future *Cytotechnology* **50**: 1 - 7
- Mimura Y, Church S, Ghirlando R, Ashton PR, Dong S, Goodall M, Lund J, and Jefferis R (2000) The Influence of Glycosylation on the Thermal Stability and Effector Function Expression of Human IgG1-Fc: Properties of a Series of Truncated Glycoforms *Molecular Immunology* **37**: 697 - 706
- Neal G, Christie J, Keshavarz-Moore E, and Shamlou PA (2003) Ultra Scale-Down Approach for the Prediction of Full-Scale Recovery of Ovine Polyclonal Immunoglobulins Used in the Manufacture of Snake Venom-Specific Fab Fragment *Biotechnology and Bioengineering* **81**: 149 - 157
- Nechansky A, Schuster M, Jost W, Siegl P, Gorr G, and Kircheis R (2007) Compensation of Endogenous IgG Mediated Inhibition of Antibody-Dependent Cellular Cytotoxicity by Glyco-Engineering of Therapeutic Antibodies *Molecular Immunology* **44**: 1815 - 1817
- Ohta M, Kawasaki N, Itoh S, and Hayakawa T (2002) Usefulness of Glycopeptide Mapping by Liquid Chromatography/Mass Spectrometry in Comparability Assessment of Glycoprotein Products *Biologicals* **30**: 235 - 244
- Raju TS, Briggs JB, Borge SM, and Jones AJS (2000) Species-Specific Variation in Glycosylation of IgG: Evidence for the Species-Specific Sialylation and Branch-Specific Galactosylation and Importance for Engineering Recombinant Glycoprotein Therapeutics *Glycobiology* **10**: 477 - 486
- Rasmussen LK, Larsen YB, and Hojrup P (2005) Characterization of Different Cell Culture Media for Expression of Recombinant Antibodies in Mammalian

Cells: Presence of Contaminating Bovine Antibodies *Protein Expression and Purification* **41**: 373 - 377

Rehder DS, Dillon TM, Pipes GD, and Bondarenko PV (2006) Reversed-Phase Liquid Chromatography/Mass Spectrometry Analysis of Reduced Monoclonal Antibodies in Pharmaceuticals *Journal of Chromatography A* **1102**: 164 - 175

Robinson DK, Chan CP, Ip CY, Tsai PK, Tung J, Seamans TC, Lenny AB, Lee DK, Irwin J, and Silberklang M (1994) Characterization of A Recombinant Antibody Produced in the Course of A High-Yield Fed-Batch Process *Biotechnology and Bioengineering* **44**: 727 - 735

Rudd PM and Dwek RA (1997) Rapid, Sensitive Sequencing of Oligosaccharides From Glycoproteins *Current Opinion in Biotechnology* **8**: 488 - 497

Saba JA, Kunkel JP, Jan DCH, Ens WE, Standing KG, Butler M, Jamieson JC, and Perreault H (2002) A Study of Immunoglobulin G Glycosylation in Monoclonal and Polyclonal Species by Electrospray and Matrix-Assisted Laser Desorption/Ionization Mass Spectrometry *Analytical Biochemistry* **305**: 16 - 31

Santora LC, Krull IS, and Grant K (1999) Characterization of Recombinant Human Monoclonal Tissue Necrosis Factor-Alpha Antibody Using Cation-Exchange HPLC and Capillary Isoelectric Focusing *Analytical Biochemistry* **275**: 98 - 108

Schlatter S, Stansfield SH, Dinnis DM, Racher AJ, Birch JR, and James DC (2005) On the Optimal Ratio of Heavy to Light Chain Genes for Efficient Recombinant Antibody Production by CHO Cells *Biotechnology Progress* **21**: 122 - 133

Schweikart F, Jones R, Jaton JC, and Hughes GJ (1999) Rapid Structural Characterisation of a Murine Monoclonal IgA Alpha Chain: Heterogeneity in the Oligosaccharide Structures at a Specific Site in Samples Produced in Different Bioreactor Systems *Journal of Biotechnology* **69**: 191 - 201

Serrato JA, Hernandez V, Estrada-Mondaca S, Palomares LA, and Ramirez OT (2007) Differences in the Glycosylation Profile of a Monoclonal Antibody Produced by Hybridomas Cultured in Serum-Supplemented, Serum-Free or Chemically Defined Media *Biotechnology and Applied Biochemistry* **47**: 113 - 124

Sethuraman N and Stadheim TA (2006) Challenges in Therapeutic Glycoprotein Production *Current Opinion in Biotechnology* **17**: 341 - 346

Shields RL, Lai J, Keck R, O'Connell LY, Hong K, Meng YG, Weikert SHA, and Presta LG (2002) Lack of Fucose on Human IgG1 N-Linked Oligosaccharide Improves Binding to Human Fc Gamma RIII and Antibody-Dependent Cellular Toxicity *Journal of Biological Chemistry* **277**: 26733 - 26740

Shukla AA, Hubbard B, Tressel T, Guhan S, and Low D (2007) Downstream Processing of Monoclonal Antibodies - Application of Platform Approaches

Yang Z and Hancock WS (2005) Monitoring Glycosylation Pattern Changes of Glycoproteins Using Multi-Lectin Affinity Chromatography *Journal of Chromatography A* **1070**: 57 - 64

Yim S and Shamlou P (2000) The Engineering Effects of Fluids Flow on Freely Suspended Biological Macro-Materials and Macromolecules 83 - 122

Yu L, Vizel A, Huff MB, Young M, Remmele RL, and He B (2006) Investigation of N-Terminal Glutamate Cyclization of Recombinant Monoclonal Antibody in Formulation Development *Journal of Pharmaceutical and Biomedical Analysis* **42**: 455 - 463

Zhang W and Czupryn MJ (2002) Free Sulfhydryl in Recombinant Monoclonal Antibodies *Biotechnology Progress* **18**: 509 - 513